AD-A158 045 THE DYNAMICS OF THE PHOTOFRAGMENTATION OF KETENE 1/2
3-CYCLOPENTENONE 35-CYCLOHEPTADIENONE AND TROPONE(U)
AIR FORCE INST OF TECH WRIGHT-PATTERSON AFB OH
UNCLASSIFIED B I SONOBE 1985 AFIT/CI/NR-85-90D F/G 7/3 NL

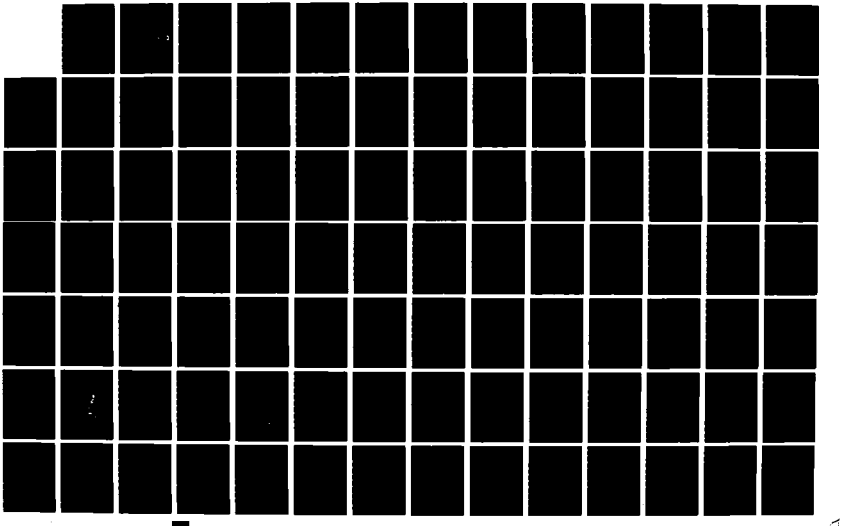

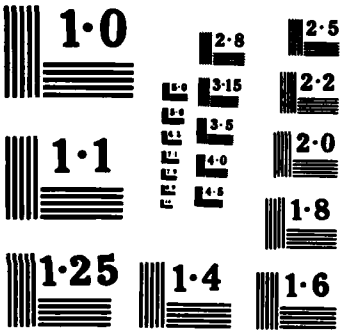

UNCLASS

SECURITY CLASSIFICATION OF THIS PAGE (When Data Entered)

REPORT DOCUMENTATION PAGE

READ INSTRUCTIONS BEFORE COMPLETING FORM

1. REPORT NUMBER: AFIT/CI/NR 85-90D	2. GOVT ACCESSION NO.
3. RECIPIENT'S CATALOG NUMBER	
4. TITLE (and Subtitle): The Dynamics of the Photofragmentation of Ketene 3-Cyclopentenone, 3,5-Cycloheptadienone, and Tropone	5. TYPE OF REPORT & PERIOD COVERED: THESIS/DISSERTATION
	6. PERFORMING ORG. REPORT NUMBER
7. AUTHOR(s): Blake Isamu Sonobe	8. CONTRACT OR GRANT NUMBER(s)
9. PERFORMING ORGANIZATION NAME AND ADDRESS: AFIT STUDENT AT: University of California, Davis	10. PROGRAM ELEMENT, PROJECT, TASK AREA & WORK UNIT NUMBERS
11. CONTROLLING OFFICE NAME AND ADDRESS: AFIT/NR, WPAFB OH 45433	12. REPORT DATE: 1985
	13. NUMBER OF PAGES: 167
14. MONITORING AGENCY NAME & ADDRESS(if different from Controlling Office)	15. SECURITY CLASS. (of this report): UNCLASS
	15a. DECLASSIFICATION/DOWNGRADING SCHEDULE

16. DISTRIBUTION STATEMENT (of this Report)

APPROVED FOR PUBLIC RELEASE; DISTRIBUTION UNLIMITED

DTIC ELECTE S AUG 16 1985 D B

17. DISTRIBUTION STATEMENT (of the abstract entered in Block 20, if different from Report)

18. SUPPLEMENTARY NOTES

APPROVED FOR PUBLIC RELEASE: IAW AFR 190-1

5 AUG 1985

LYNN E. WOLAVER
Dean for Research and
Professional Development
AFIT, Wright-Patterson AFB OH

19. KEY WORDS (Continue on reverse side if necessary and identify by block number)

20. ABSTRACT (Continue on reverse side if necessary and identify by block number)

ATTACHED

DD FORM 1 JAN 73 1473 EDITION OF 1 NOV 65 IS OBSOLETE

UNCLASS

SECURITY CLASSIFICATION OF THIS PAGE (When Data Entered)

The Dynamics of the Photofragmentation of Ketene, 3-Cyclopentenone, 3,5-Cycloheptadienone, and Tropone

Abstract

Photofragment infrared fluorescence methods were used to study energy disposal to the carbon monoxide product of ketene photodissociation. Vibrationally excited CO is formed upon photolysis at 193 nm, but not at 249 and 308 nm. The nascent CO vibrational energy distribution can be characterized by a temperature, T_v=3750 K. The nascent CO rotational energy distribution can be characterized by a temperature, T_r=6700 K. This suggests that ketene undergoes dissociation by a non-linear path following photoexcitation at 193 nm.

Time-resolved laser absorption spectroscopy was used to study the energy partitioning in the photoactivated fragmentation of 3-cyclopentenone, 3,5-cycloheptadienone, and tropone. The CO product vibrational energy distribution was measured at photolysis wavelengths of 193, 249, and 308 nm. The experimental distributions are analyzed by comparing them with distributions calculated by using a statistical model. For 3-cyclopentenone and tropone, only the non-fixed energy of the transition state is available for partitioning among the products' vibrational degrees of freedom, whereas, for 3,5-cycloheptadienone, the full reaction exoergicity is available to be randomly distributed among all the developing products' degrees of freedom. This suggests that the products of the dissociation of 3-cyclopentenone and tropone are vibrationally decoupled from one another in the exit channel. Potential energy is thus released in the exit channel primarily to the relative translational motion of the products. The results of the dissociation of 3,5-cycloheptadienone suggest that the products are strongly coupled well into the exit channel. A mechanistically based model is suggested to account for the observed differences in energy disposal dynamics for these ketones.

Bibliography

Rosenfeld, R.N. and Sonobe, B.I.; J. Amer. Chem. Soc. 1983; 105; 1061-1062.

Sonobe, B.I. and Rosenfeld, R.N.; J. Amer. Chem. Soc. 1983; 105; 7528-7530.

Sonobe, B.I., Fletcher, T.R., and Rosenfeld, R.N.; Chem. Phys. Lett. 1984; 105, 322-326.

Sonobe, B.I., Fletcher, T.R., and Rosenfeld, R.N.; J. Amer. Chem. Soc. 1984; 106; 4352-4356.

Sonobe, B.I., Fletcher, T.R., and Rosenfeld, R.N.; J. Amer. Chem. Soc. 1984; 106; 5800-5805.

AFIT RESEARCH ASSESSMENT

The purpose of this questionnaire is to ascertain the value and/or contribution of research accomplished by students or faculty of the Air Force Institute of Technology (AU). It would be greatly appreciated if you would complete the following questionnaire and return it to:

AFIT/NR
Wright-Patterson AFB OH 45433

RESEARCH TITLE: The Dynamics of the Photogragmentation of Ketene 3-Cyclopentenone, 3,5-Cycloheptadienone, and Tropone

AUTHOR: Blake Isamu Sonobe

RESEARCH ASSESSMENT QUESTIONS:

1. Did this research contribute to a current Air Force project?

( ) a. YES ( ) b. NO

2. Do you believe this research topic is significant enough that it would have been researched (or contracted) by your organization or another agency if AFIT had not?

( ) a. YES ( ) b. NO

3. The benefits of AFIT research can often be expressed by the equivalent value that your agency achieved/received by virtue of AFIT performing the research. Can you estimate what this research would have cost if it had been accomplished under contract or if it had been done in-house in terms of manpower and/or dollars?

( ) a. MAN-YEARS _____ ( ) b. $_____

4. Often it is not possible to attach equivalent dollar values to research, although the results of the research may, in fact, be important. Whether or not you were able to establish an equivalent value for this research (3. above), what is your estimate of its significance?

( ) a. HIGHLY SIGNIFICANT ( ) b. SIGNIFICANT ( ) c. SLIGHTLY SIGNIFICANT ( ) d. OF NO SIGNIFICANCE

5. AFIT welcomes any further comments you may have on the above questions, or any additional details concerning the current application, future potential, or other value of this research. Please use the bottom part of this questionnaire for your statement(s).

NAME GRADE POSITION

ORGANIZATION LOCATION

STATEMENT(s):

The Dynamics of the Photofragmentation of Ketene, 3-Cyclopentenone, 3,5-Cycloheptadienone, and Tropone

By

BLAKE ISAMU SONOBE
B.S. (USAF Academy, CO) 1970
M.S. (Texas A&M University) 1978

DISSERTATION

Submitted in partial satisfaction of the
requirements for the degree of

DOCTOR OF PHILOSOPHY

in

Chemistry

in the

GRADUATE DIVISION

of the

UNIVERSITY OF CALIFORNIA

DAVIS

Approved:

Committee in Charge

Deposited in the University Library _____
Date Librarian

Blake Isamu Sonobe
September 1985
Chemistry

The Dynamics of the Photofragmentation of Ketene, 3-Cyclopentenone, 3,5-Cycloheptadienone, and Tropone

Abstract

Photofragment infrared fluorescence methods were used to study energy disposal to the carbon monoxide product of ketene photodissociation. Vibrationally excited CO is formed upon photolysis at 193 nm, but not at 249 and 308 nm. The nascent CO vibrational energy distribution can be characterized by a temperature, T_v=3750 K. The nascent CO rotational energy distribution can be characterized by a temperature, T_r=6700 K. This suggests that ketene undergoes dissociation by a non-linear path following photoexcitation at 193 nm.

Time-resolved laser absorption spectroscopy was used to study the energy partitioning in the photoactivated fragmentation of 3-cyclopentenone, 3,5-cycloheptadienone, and tropone. The CO product vibrational energy distribution was measured at photolysis wavelengths of 193, 249, and 308 nm. The experimental distributions are analyzed by comparing them with distributions calculated by using a statistical model. For 3-cyclopentenone and tropone, only the non-fixed energy of the transition state is available for partitioning among the products' vibrational degrees of freedom, whereas, for 3,5-cycloheptadienone, the full reaction exoergicity is available to be randomly distributed among all the developing products' degrees of freedom. This suggests that the products of the dissociation of 3-cyclopentenone and tropone are vibrationally decoupled from one another in the exit channel.

Potential energy is thus released in the exit channel primarily to the relative translational motion of the products. The results of the dissociation of 3,5-cycloheptadienone suggest that the products are strongly coupled well into the exit channel. A mechanistically based model is suggested to account for the observed differences in energy disposal dynamics for these ketones.

ACKNOWLEDGEMENTS

It is a pleasure to acknowledge the following persons and organizations whose advice and support made this research possible.

To my research director, Professor Robert N. Rosenfeld, I express my sincere gratitude for his guidance, instruction, friendship, and patience without which this research would not have been possible. His dedication to education and research has been stimulating and motivating. The time spent under his guidance was extremely rewarding.

To the other members of the Rosenfeld Group, Brad Weiner, Rick Fletcher, Bill Peifer, and Eileen McCauley, I gratefully acknowledge their technical assistance and friendship. Their work in the construction and maintenance of the lasers, detectors, amplifiers, etc. is greatly appreciated.

I acknowledge the support of the Petroleum Research Fund and the Air Force Institute of Technology.

Finally, and most importantly, I give thanks to my wife, Janie, and our children, Abigail, Bethany, Rebecca, and Nathanael for their affection, support, and patience throughout this program.

TABLE OF CONTENTS

LIST OF FIGURES

LIST OF TABLES

CHAPTER 1

INTRODUCTION

Mechanistic models in organic chemistry often provide a useful basis for predicting substituent or solvent effects on reactivity and the most likely products of new reactions. Generally, reaction mechanisms are formulated in terms of a series of elementary steps by which reactants are converted to products via one or more intermediates. However, such models may not be useful when products are formed in a single elementary step. In some cases, single step reactions can be described in terms of a set of nuclear motions and/or transition state structure which accounts for the observed stereo- or regiospecificity of the reaction. Mechanistic models formulated in terms of the nuclear degrees of freedom can, in principle, provide detailed models for organic reactivity.

Experimental approaches to characterizing transition state structures have generally involved stereochemical labeling studies or kinetic isotope effect measurements. The conclusions reached in labeling studies are qualitative at best and often ambiguous. The interpretation of kinetic isotope effects may involve assumptions, e.g., linear free energy relationships, whose physical bases are sometimes questionable. A complete mechanistic description of a reaction would result from experiments when the energy in each of the reactant translational, rotational, and vibrational degrees of freedom is specified and the energy distribution in each product degree of

$$\sigma_{t,i} = \sum_{L_i=0}^{L_{i_{max}}} \frac{\pi(2L_i+1)\hbar^2}{2\mu_i E_i} = \frac{\pi\hbar^2(2L_{i_{max}}+1)^2}{2\mu_i E_i} \qquad (2.2)$$

Since the probability of dissociation of the complex to a given state is the same for all states accessible by conservation of total energy and angular momentum, it can be given by one expression,

$$P(n_f,E_f,m_f,L_f;E_T,K,K_z) = 1/N(E_T,K,K_z) \qquad (2.3)$$

The partial cross section to a given state is,

$$\sigma(n_f,E_f,m_f,L_f;n_i,m_i,L_i,E_i) = \frac{\pi\hbar^2(2L_i+1)}{2\mu_i E_i} \times$$

$$\sum_{(L_i-m_i)\leq K\leq (L_i+m_i)} \sum_{K_z=-K}^{+K} \frac{P(n_f,m_f,L_f,E_f;E_T,K,K_z)}{(2L_i+1)(2m_i+1)} \qquad (2.4)$$

$$= \frac{\pi\hbar^2}{2\mu_i E_i(2m_i+1)} \sum_{(L_i-m_i)\leq K\leq (L_i+m_i)} (2K+1)P(n_f,m_f,L_f,E_f;E_T,K,K_z) \qquad (2.5)$$

The total cross section, summed over all the partial sections, is

$$\sigma(n_f,m_f,E_f;n_i,m_i,E_i) = \frac{\pi\hbar^2}{2\mu_i E_i(2m_i+1)} \times$$

$$\sum_{(L_i-m_i)\leq K\leq (L_i+m_i)} (2K+1)\sum_{L_f} P(n_f,m_f,L_f,E_f;E_T,K,K_z) \qquad (2.6)$$

In these equations (2.2-2.6), i is the initial state, f is the final state, $L_{i_{max}}$ is the maximum orbital angular momentum quantum number, n is the vibrational quantum number, m is the rotational angular

partitioning the products of collision among the various product states. Once the system enters this complex, it forgets where it came from. The mode of decomposition is uncorrelated with the mode of formation except through the conservation of energy, total angular momentum and its projection on one axis, and linear momentum. The existence of such a complex has not been established and the lack of correlation is open to question. However, if the coupling between all open channels is strong, statistical behavior should be expected. This is especially probable if the complex exists for a reasonable period of time, periods longer than a rotation.[38] Additionally, even the most sensitive experiments indicate that reaction cross sections are averaged over all possible initial coordinates (phases) and these average cross sections may correlate well with the phase space available even though the cross section for a given initial configuration may correlate poorly.[37]

In the phase space theory of Light,[39,40] the probability that the collision complex dissociates to a given product is proportional to the volume of phase space available to the product under conservation of total energy and angular momentum. The total loss of memory in the strong coupling complex implies that the decomposition is governed by the phase space available. Methods for computing available phase space were given by Light and Lin.[42]

The total cross section for the formation of the collision complex as determined by Light and coworkers[40,41] is,

calculated by averaging the specific dissociation rate over all the possible distributions of energy.

Generally, the decomposing molecule is highly excited and therefore the molecular vibrations are very anharmonic. The model only remotely relates to the behavior of real reacting molecules. All experimental evidence indicates that energy flow does occur freely between the normal modes of molecules. In general, agreement between the Slater theory and experimental data is poor for small molecules having few normal modes of vibration.[35] Reasonable fits of curves calculated using approximate Slater calculations to the experimental data of larger molecules have been obtained.[36] The Slater theory cannot be easily amended by the introduction of anharmonicity as a perturbation since anharmonicity is a large "perturbation" not within the confines of perturbation theory.

D. The Statistical Theory

Statistical approaches[36-41] to chemical kinetics are based on the hopes that complex quantum scattering theory and the uncertainties and labor necessary with classical calculations may be avoided, and qualitative results in good agreement with experiment still obtained. These approaches are especially important in complex situations where other methods cannot be applied. Light[37] suggested that a simple statistical model may give quick but relatively accurate estimates of reaction cross sections for gas phase collisions without activation energies.

The model begins with the assumption that a strong coupling complex is formed and that a statistical prescription can be used for

experimental data was good.

C. The Slater Theory

The Slater theory[30-34] is a dynamical theory providing detailed treatment of molecular vibrations and the behavior of particular molecular coordinates as a function of time. The model uses a collection of harmonic oscillators whose internal configuration is described in terms of normal mode coordinates. The normal modes are strictly harmonic so no energy transfer can occur between them. The amount of energy in each mode is fixed between collisions and only collisions can change them. In the application of the Slater theory, specific interest is in the form of the normal modes and how they affect or influence the behavior of a particular internal coordinate with time. This internal coordinate (or possibly a combination on internal coordinates) is chosen as the critical coordinate. It must be chosen with reference to the motion of the atoms that is believed to accompany reaction. The criterion for reaction is the extension of this coordinate, a bond, to a critical point which is dependent on energy and vibrational phase. Thus, when energy sufficient for reaction is imparted to a molecule and distributerd among the normal modes, reaction is dependent upon the relative chance of the critical coordinate exceeding the critical value (i.e., energy correctly distributed) and the probability of deactivation by collision. The specific dissociation rate for the reaction is determined by the time behavior of all the normal modes and is given by the average frequency with which the critical coordinate exceeds the critical value. The corresponding rate constant for a given total energy may then be

C-I excitation followed immediately by recoil of a semi-rigid alkyl radical. When this dissociation was treated with a simple statistical model, excessive internal excitation was predicted for the alkyl fragment. Failure of this statistical model is expected since most evidence indicate alkyl iodide dissociation is a rapid, direct process.

Application of the impulsive model has also been made to the collision of an excited atom with a molecule. The collision of excited mercury atoms, $Hg^*(^3P_0)$ with CO molecules was studied and a conclusion reached that the work of Holdy, Klotz and Wilson[25] can be easily generalized to any impulsive event.[27] The rapid release of electronic energy during the course of a collision provides an impulse to eject a fragment with high translational energy. The electronic energy is released at the turning point of the Hg*-CO motion and CO is vibrationally excited via the Hg-CO repulsion during the half-collision of the Hg-CO separation. The model used in this study[27] attempts to determine the average vibrational energy transferred to the diatom, the detailed distribution of vibrational states of CO, and the effects of the system parameters (i.e., mass, excitation energy of the atom, and the vibrational spacings of the diatom). The calculated vibrational distribution reproduced the results of Karl, Kruus, and Polanyi.[28] Simple energy sharing models of Hg* + CO could not account for the vibrational distribution or the greater vibrational excitation in corresponding experiments with NO. A similar model was reported for the Hg* + CO collision which allowed a non-linear dissociation of the HgCO complex.[29] Agreement here with

is excited from its ground state to a single excited electronic state and then directly dissociates into fragments on this potential surface. The C-N bond retains its ground state potential curve in the excited state and bending forces are presumed to be negligible in the upper state compared to the C-I repulsion. In the calculations, it is assumed that the molecule arrives on the quasi-diatomic surface from the ground state following a classical Franck-Condon jump which preserves nuclear momentum and position. The average partitioning between vibrational, rotational, and translational motions were calculated by averaging the energy transfer given by classical dissociation trajectories over the phases of the ground state normal modes of the molecule. Finally, the partitioning among the final CN vibrational states is given by a Poisson distribution. The model predicted that most of the available energy goes into translation which appears consistent with flash photolysis studies.

In the photodissociation of alkyl iodides,[26] the impulsive model was used to determine the extent of internal excitation of the alkyl radical. Calculations were made assuming both a "rigid" and a "soft" radical where the alkyl radical would recoil as a rigid body or where the α-carbon is so weakly attached to the rest of the alkyl fragment in relation to the C-I repulsion that it alone absorbs the energy as the fragments repel one another. Experimental results fall between these two calculations with the soft radical model predicting greater internal excitation than the experimental results and the rigid radical model predicting less. These results indicate that a possible model for alkyl iodide photodissociation may involve a quasi-diatomic

having time available for general equilibration of the internal energy. Energy in the excited complex (e.g., from the absorption of a photon) produces forces between separating fragments. The upper (excited state) potential surface may be strongly repulsive and simultaneously produce strong bending torque. The repulsive forces not only push the fragments apart but can also induce vibrational and rotational excitation if one of the fragments is a diatomic or larger.

For a triatomic molecule, ABC, a steep repulsive potential along the A-B bond can lead to recoil; potential energy is released over such a short distance that the B-C bond length and the ABC bond angle will not change significantly in the time that A and B will be effectively separated. The available energy originally in the A-B bond will be partitioned, subject to conservation of linear momentum, between the kinetic energies of A and B. Atom B will then recoil into atom C and the BC fragment will preserve the momentum initially imparted to B alone. If the B-C bond is rigid, movement of B independent of C is not likely and this model will give poor results.

The impulsive model has been used to treat the dissociation of ICN.[25] Here, the model assumes that the molecule will behave as a quasi-diatomic and that only one upper state is involved in the dissociation. Other assumptions in the model include, (1), light absorption affects only the breaking of the I-C bond and (2), the mechanics of the half-collision of the recoiling fragments on this potential surface may be treated classically to predict the average vibrational, rotational, and translational energies, and to predict partitioning between vibrational states. Briefly, then, the molecule

developing product molecules and one fragment is suddenly "removed", the remaining molecule will be formed in a highly excited state. In this reaction, HCl is "dressed" by acetylene. When the acetylene molecule is suddenly stripped away from HCl, the HCl product vibronic distribution is dominated by Franck-Condon factors (corresponding to the "dressed" to "stripped" transition). In this experiment, Golden Rule calculations of HCl photoelimination product vibronic state distributions were made and were found to be in good agreement with experimental data.

Golden Rule-type calculations using an extended treatment of initial and final vibrational degrees of freedom were made for the elimination of CO from CO_2.[9] Previous studies[20-22] ignored the effects of certain degrees of freedom (i.e., the effects of the continuum wavefunction) and were not well suited for CO_2. Vastly different conclusions concerning total dissociation rates, relative rates into specific fragment vibrational states, and isotope effects were obtained when a proper, more detailed description of the normal modes of the molecule before dissociation and the final fragment modes is used. Results of these calculations were found to be in good general agreement with the experimental data of Lee and Judge.[23] However, Berry's conclusion[20-22] that product energy distributions in many dissociation processes are determined primarily by Franck-Condon factors appears to be valid.[23]

B. The Impulsive Model

The impulsive model may be appropriate for reactions where the excited molecule breaks apart in a single vibrational period, without

molecule, W is the constant perturbation Hamiltonian which represents the operation(s) which allows the decay process, and $P(E_n)$ is the number of final states of a given type per unit interval of energy, E_n. The condition, $E_n = E_m$, is imposed upon the process, requiring the conservation of energy during the transition.

The Golden Rule is applicable when transitions are made to an essentially continuous set of final states.[19] This condition may be satisfied by the upper vibrational levels of the ground electronic state (which are quasi-continuous), or by the continuum levels associated with bond cleavage. The molecule may have sufficient energy to dissociate, ionize, or undergo a raditionless transition into a quasi-continuum, but it may not have sufficient energy in a particular (critical) degree of freedom to do so. Within the quasi-continuum, there may exist a degree of freedom which is correlated with the critical coordinate within the molecular system. If sufficient energy flows into this degree of freedom, reaction can occur and the vibrational levels or continuum of the product state will be populated. The flow of energy into the quasi-continuum will effectively entrap the energy in this larger density of states and return to the initial state is minimal. Thus, the reaction is spontaneous and irreversible. The rate given in equation (2.1) can then be construed as the rate of energy flow into the critical degree of freedom.

Application of the Golden Rule has been made to the formation of excited HCl following the photolysis of chloroethylenes.[20] Franck-Condon arguments predict that if there is an interaction between two

CHAPTER 2

THEORIES AND EXPERIMENTS IN PHOTOFRAGMENTATION

Photofragmentation Theories

In the past 50 years, numerous theories have been developed[12-16] to describe the dynamics of photodissociation. These theories have varied from simple statistical to complex dynamical approaches and from classical to quantum mechanical treatments. They have been formulated to treat direct dissociation reactions which occur within 10^{-13} sec following excitation and/or reactions which undergo predissociation (redistribution of energy required for dissociation to occur) with excited state lifetimes generally longer than 10^{-12}-10^{-13} sec. In this section, only the basic features of these theories will be discussed. Modifications have been made to these models to extend their treatment to a broader range of reactions, however, the basic approaches remain the same.

A. The Golden Rule

The rate of the time dependent radiationless transition between molecular levels or states has been approximated using Fermi's Golden Rule. A form of the Golden Rule proposed by Wentzel[17] is shown in equation (2.1) (see ref. 18),

$$\text{Rate} \approx \frac{2\pi}{\hbar}|\langle n|W|m\rangle|^2 P(E_n) \qquad (2.1)$$

where n and m are the initial and final zero order states of the

product energy disposal as a means to develop mechanistic descriptions in the photochemistry of selected ketones. Time-resolved photofragment infrared fluorescence was used in the study of ketene while time-resolved laser absorption spectroscopy was used to study 3-cyclopentenone, 3,5-cycloheptadienone and tropone.

In Chapter 2, the significant theories and experimental methods in photochemistry are briefly described while ketone photochemistry and organic fragmentation mechanisms are summarized in Chapter 3. In Chapter 4, the experimental procedures and results on the photochemistry of ketene are discussed and those of 3-cyclopentenone, 3,5-cycloheptadienone and tropone are discussed in Chapter 5. The Appendix contains a computer listing of the routine used to calculate the vibrational temperature of CO for application to the ketene study.

motion of the $CsSF_6$ complex. Also noted was that for strongly exothermic decay of a loose-coupling complex with many degrees of freedom, the rotational, vibrational, and translational temperatures are nearly equal.

Theoretical and experimental studies indicate that for the photodissociation of some triatomic molecules, measurement of product energy distributions may be useful in differentiating direct and predissociative decay mechanisms.[9] The vibrational distributions of $CO(d^3\Delta)$, $CO(a'^3\Sigma^+)$ and $CO(a^3\pi)$ produced in the photodissociation of CO_2 at various incident photon energies were calculated using an ab initio theory of polyatomic molecule dissociation and compared with experimental data. Agreement between theoretical[9] and experimental[10] distributions was obtained for the $CO(d^3\Delta)$ and $CO(a'^3\Sigma^+)$ states produced via direct photodissociation from CO_2. Similar agreement for the $CO(a^3\pi)$ state[11] could not be obtained and it was proposed that dissociation into this electronic channel proceeded via a metastable predissociative state and not by direct photodissociation as assumed in the calculations. To adequately apply this theory to the predissociative process, the normal modes of the predissociating state must be constructed from the observed vibrational frequencies of that state and the mechanism for predissociation must be known.

The studies of simple molecular systems described above suggest that measurement of product energy distributions can be useful in developing detailed mechanistic descriptions of reactivity. The objective of the work described in this dissertation has been to use

structure of the transition state.

Useful mechanistic information has been obtained from crossed molecular beam experiments by analysis of product velocity distributions, i.e., product translational energy and angular distributions. Differentiation between rebound, stripping, and complex reaction mechanisms is possible on the basis of this information.[4,5] Products of stripping reactions are characteristically forward scattered compared to products of rebound reactions. Other molecular beam experiments employing electric deflection analysis have shown that, for reactions proceeding through a complex, product rotational polarization is related to the nature of the transition state for decay of the complex. In "tight-coupling" complexes, strong polarization with respect to the direction of the final velocity vector of the product (e.g., CsBr from Cs + HBr) is predicted if in the transition state, the effective moment of inertia about the separation axis is small, and weak polarization if that moment of inertia is large. For loose-coupling complexes, where the incipient products rotate freely in the transition state, polarization with respect to the the final velocity vector vanishes (e.g., CsF from Cs + SF_4).[6,7] Finally, in Cs + SF_6 reactions, the symmetry of the angular distribution, symmetrically peaked forward and backward relative to the initial velocity vector, indicates that a collision complex is formed which lives for several rotational and many vibrational periods before the products, CsF and SF_5 emerge. The observed vibrational temperature agrees well with that calculated assuming equipartition of the total energy into all possible modes of

freedom is resolved. In this way, relatively direct information on the dynamical origins of stereochemical selectivity or substituent effects might be obtained.

To date, most experimental studies approaching this level of detail have involved relatively small systems.[1] However, important and provocative results have been obtained which have some relevance to the chemistry of larger polyatomic systems. In their study of metathesis reactions between sodium atoms and halogen gases, mercuric chloride and mercuric bromide, Evans and Polanyi[2] noted that the exoergicity of the reactions was not randomly distributed among the various products' degrees of freedom. They concluded that highly vibrationally excited products were produced in reactions occurring on attractive potential-energy surfaces whereas reactions with repulsive potential-energy surfaces yielded products with translational and rotational excitation. Additionally, the relative amounts of energy in product vibrational and translational degrees of freedom were dependent on the structure of the transition state. Using classical trajectory methods, Polanyi calculated that in these atom-diatomic reactions the relative effectiveness of reactant vibrational or translational energy in promoting reaction was dependent on the structure of the transition state.[3] Translational energy was more effective in reactions with early transition states; and in reactions with late transition states, vibrational energy in the bond under attack was more effective in promoting reaction. For these one-step reactions, detailed mechanistic descriptions were developed by relating the internal energy of the reactants and products to the

momentum quantum number, k is the total angular momentum quantum number, $W(E_T,K,K_z)$ is the number of product states accessible from the reaction complex (E_T,K,K_z), μ_i is the three-body reduced mass, and E_i is the relative energy of the complex. Similar calculations can also be made for the cross sections for vibrational and rotational distributions.

Calculations show that the statistical theory gives reasonable results[40,41] for the magnitude of the reactive cross sections for K + HBr → H + KBr, Na + Cl_2 → NaCl + Cl, and KH + Cl → KCl + H. For ion-molecule reactions[39] such as $O^+ + N_2$ and $N^+ + O_2$, results showed that reaction cross sections always increased with increasing excitation for reactions which are endothermic and slightly decreased for reactions which are exothermic. Good agreement was found between these calculations and experiment in the high energy region above 5 eV, and in some cases, throughout the entire energy range. More pronounced disagreements were noted for the low energies which may indicate that either an attractive energy and/or selection rule restriction is operative.

On the basis of these few molecular beam experiments, it is observed that the statistical theory does not always adequately reproduce experimental data perhaps due to inadequate mixing of the degrees of freedom. Reaction occurs in a time roughly comparable to a vibration frequency and little rotation occurs before decomposition. In energy exchange reactions between translation and vibration, the weak coupling between these modes make phase space theory inapplicable. Ion-molecule reactions are a class of reactions where

the theory should work well. Coupling in these reactions is probably very strong due to large attractive forces.

E. The RRKM Theory

The RRKM theory has been considered the most realistic and successful current theory.[43] It is a statistical theory based on the Lindemann, Hinshelwood, and RRK theories. The principle concepts on which all of these theories are based were established by Lindemann.[44] These concepts are,

(1) Collisions energize a fraction of the molecules in excess of a critical energy, $E_\emptyset$. The rate of energization is dependent on the rate of the bi-molecular collisions.

$$A + M \xrightarrow{k_1} A^* + M \qquad (2.7)$$

where M can be a second reactant molecule or a molecule of inert bath gas. The rate constant, k_1, is energy independent and can be calculated from simple collision theory.

(2) Energized molecules are de-energized by collision. Each collision of A* results in de-energization.

$$A^* + M \xrightarrow{k_2} A + M \qquad (2.8)$$

The de-energization rate constant, k_2, is also energy independent.

(3) A lag time exists between energization and reaction, unimolecular dissociation or isomerization of the molecule,

$$A^* \xrightarrow{k_3} B + C \qquad (2.9)$$

where k_3 is energy independent.

From the Lindemann mechanism, the overall rate of reaction can be given by the expression,

$$v = k_3 A^* = \frac{k_1 k_3 [A][M]}{k_2[M] + k_3} = \frac{(k_1 k_3/k_2)[M]}{1 + k_3/k_2[M]} \qquad (2.10)$$

In general, though the Lindemann theory correctly predicts a fall-off in the first order rate constant with decreasing pressure, a gross discrepancy exists between the calculated and experimental fall-off curves.[45] The principle reason reason for the discrepancy is in the calculation of k_1; the kinetic energy of the molecule is considered but not its internal energy.

To correct for this inadequacy, Hinshelwood[46] modified the Lindemann theory by assuming that part of the required activation could come from the internal energy, thus increasing k_1. Internal energy is stored in the internal degrees of freedom, primarily vibration, of the reactant molecule. An increase in the number of degrees of freedom increases the internal energy of the molecule which in turn increases the rate of energization. Thus, by choosing a suitable number of degrees of freedom, s, one can match the calculated transition pressure where the fall-off begins with experimental data. Unfortunately, the fit over the entire pressure range is generally poor using this method. There is no a priori method for determining s. Contributing to the poor fit is the assumption that k_3 is energy independent when in fact, k_3 increases with increasing energy.

Rice and Ramsperger[47,48] and Kassel[49,50] independently and almost

simultaneously developed theories to consider more realistically the rate of reaction of an energized molecule as a function of its energy content. Both theories require energy accumulation in a certain part of the molecule for reaction to occur. Upon excitation of a molecule to a total energy, E, redistribution of this energy will quickly occur such that for any molecule with E greater than the critical energy, E_c, there is a statistical probability of finding E_c in a relevant part of the molecule. The rate constant is then proportional to this probability. Rice and Ramsperger used a statistical model to calculate that such a concentration would occur in one squared term in the energy expression of the molecule (i.e., $1/2\ m\mu^2$ for kinetic energy or $1/2\ kx^2$ for potential energy of an oscillator). Kassel developed both a classical and a quantum theory and assumed that energy would be concentrated in a single oscillator (both squared terms). Since, in practice, the theories of Rice and Ramsperger and Kassel give similar results, and are very similar in approach, they are generally treated as simply the RRK theory.

In Kassel's classical version, for a system of s classical oscillators with a total energy, E, the probability that a particular oscillator will have an energy greater than E_c is,

$$P = \left(\frac{E - E_c}{E}\right)^{s-1} \tag{2.11}$$

The rate constant, k_3, is proportional to this probability,

$$k_3 = A\left(\frac{E - E_c}{E}\right)^{s-1} \tag{2.12}$$

In his quantum version, the corresponding expression for k_3 is,

$$k_3 = A\frac{n!(n-m+s-1)!}{(n-m)!(n+s-1)!} \qquad (2.13)$$

where A is a proportionality constant which is energy independent, m is the critical number of quanta given by $E_c/h\nu$, n is the total number of quanta given by $E/h\nu$, and ν is the (geometric mean) frequency of the oscillators.

With a suitable choice of parameters, for the first time, the RRK theory yielded results which reproduced experimental results with reasonable accuracy.[43] Unfortunately, the choice of parameters is somewhat arbitrary and empirical. The proportionality constant, A, is not correlated with any observable property of the molecule, both A and E_c must be determined empirically, and even when using a reasonable set of parameters, the number of oscillators, s, required is about one-half the actual number of oscillators in the molecule.

The RRKM theory[51,52] is a more detailed version of the RRK theory and incorporates transition state theory. Transition state theory is based on the application of statistical mechanics to reactants and activated complexes. In the RRKM theory, the Lindemann mechanism is rewritten,

$$A + M \longrightarrow A^* + M \qquad (2.7)$$

$$A^* + M \longrightarrow A + M \qquad (2.8)$$

$$A^* \longrightarrow A^+ \qquad (2.14)$$

$$A^+ \longrightarrow \text{Products} \qquad (2.15)$$

In equation (2.14), the energized molecule containing sufficient energy to react attains a critical configuration (the activated complex, A^+) which is an intermediate between reactant and product. The activated complex, or transition state, then reacts to form products, equation (2.15).

The specific rate constant can be determined by,[53]

$$k_a(E) = L^+ \frac{Z^+}{Z} \frac{\Sigma P(E^+)}{hN^*(E)} \qquad (2.16)$$

where L^+ is a statistical factor for the possibility that a reaction can proceed by several distinct paths which are kinetically equivalent, Z^+ and Z are the products of partition functions for adiabatic rotations in the activated complex and molecule respectively, $\Sigma P(E^+)$ is the total sum of the degeneracies of all possible energy eigenstates of the active degrees of freedom of the activated complex at total energy E^+, h is Planck's constant, and $N^*(E)$ is the number of eigenstates per unit of energy E. Adiabatic degrees of freedom remain in the same quantum state throughout the reaction while active degrees of freedom exchange energy freely. Expressions for $\Sigma P(E^+)$ and $N^*(E)$ have been developed elsewhere.[43]

Like the RRK theory, a redistribution of energy must occur to accumulate sufficient energy in the proper portion of the molecule. Upon accumulation of sufficient energy and attainment of proper configuration, the activated complex is formed. There is usually more than one quantum state of the activated complex A^+ which can be formed from A* because of the different possible distributions of energy between the reaction coordinate and the vibrational and rotational degrees of freedom. This complex is unstable to movement along the reaction coordinate and lies in an arbitrary small range at the top of the potential energy barrier. The rate constant ($k_a(E)$) is evaluated as the sum of contributions from various activated complexes.

The isomerization of cyclopropane is an often used example of the excellent agreement between RRKM calculations and experimental data.[43,54] Calculated values using the Hinshelwood[55] and Slater[56] theories did not fit the experimental data well. RRKM predictions of Weider and Marcus[57] and Lin and Laidler[58] gave very good fits to the dat. . Fair to good agreement have also been obtained for the decomposition of cyclobutene[57,58] and isocyanides,[60] and the pyrolysis of alkyl halides.[61]

The assumption of both RRK and RRKM theories that energy is redistributed rapidly and randomly among the various degrees of freedom of an energized molecule before reaction or de-energization has been shown to be valid for the isomerization of methylcyclopropane.[62] Rynbrandt and Rabinovitch calculated that for hexafluorobicyclopropyl, randomization of energy is 99% complete in 4×10^{-12} s.[63] A bottleneck caused by the single C-C bond between the

two ends of this molecule may however prevent easy transfer of energy from one ring to the other thus allowing non-randomization to be detectable at relatively high pressures. A recent study[64] of infrared multiphoton dissociation of CH_3NC provided considerable evidence that prior to dissociation, the molecule isomerizes to CH_3CN. The CN produced was found to be rotationally and vibrationally hotter than CN produced by direct dissociation of CH_3CN. This may be due to slow vibrational relaxation indicating non-RRKM behavior. Non-RRKM behavior may also be operative in the photodissociation of allyl isocyanide.[65] Observed rate constants differed by up to a factor of 3 implying incomplete randomization of energy at the time of isomerization.

Photofragmentation Experiments

In recent years, the techniques for studying photophysics and photochemistry have vastly improved. Many new methods have been developed which have allowed the experimenter to probe the finer details of photofragment dynamics.[22] The more significant techniques are discussed below.

A. Molecular Dissociation and Photofragment Fluorescence

Molecular dissociation followed by monitoring the fluorescence of the resultant fragments is one of the simplest of experiments. Typical light sources used to initiate fragmentation are excimer lasers, tunable dye lasers, and synchrotron radiation. Detailed information can be obtained on atomic, vibrational, and rotational states of the products. Generally, in these experiments, a gaseous

sample is flowed through a fluorescence cell. The light source is passed through the cell and the resulting fluorescence is detected at right angles to the incident photolysis beam. A recent study using uv dissociation and fluorescence detection measured the infrared fluorescence from NO($X^2\pi$) produced by the photodissociation of NOCl and NOBr at 193 nm.[66] The amount of vibrational excitation in the NO fragment as a function of photolysis wavelength was measured. As the photolysis wavelength decreased, the percentage of available energy partitioned into vibration increased. Grimley and Houston[67] saw no prompt infrared emission from NO during photodissociation of NOCl at wavelengths of 480 nm or longer. At 355 nm, approximately half of the total ir fluorescence amplitude was immediate (detector response time limited), i.e., could be assigned to vibrational excitation of the NO photofragment. Moser and Weitz[66] concluded that for NOCl and NOBr, a direct dissociative process results in the production of "hot" NO.

The dependence of photofragment emission intensity on excitation wavelength in the photochemical decarboxylation of pyruvic acid, in conjunction with a statistical energy disposal model, suggests that the loss of CO_2 occurs via a five-center mechanism and CO_2 is formed in concert with an unstable hydroxycarbene intermediate.[68] The statistical energy partitioning model employed indicated that for fragmentation via a four-center mechanism where acetaldehyde and CO_2 are formed directly, photolysis at 351 nm would generate CO_2, ca. 80% of which would emit at 4.3 μm. Through a five-center process, at 308 nm, 8% of the CO_2 produced would fluoresce. In the above study, no fluorescence was detected at 308 nm.

Time and wavelength-resolved ir fluorescence were used to investigate the photofragmentation dynamics of CH_2I_2 and CH_3I at 248 nm and 308 nm.[69] The vibrational energy distributions, frequencies, and energy transfer kinetics of several vibrationally excited free radicals produced in the photolysis were studied. Observation of vibrationally hot CH_2I fragments from CH_2I_2 photolysis indicated that an extremely high fraction of the total energy goes into vibration and that the photolysis preferentially excited the internal degrees of freedom of the CH_2I radical. Infrared emission results gave direct evidence that the nascent CH_3 radical (from CH_3I) contains a small amount of vibrational excitation localized in the out-of-plane bending mode of the radical.

B. Molecular Beam Photofragmentation

Crossing a light source with a molecular beam and measuring the angular distribution and time-of-flight of the fragments with a mass spectrometer provides information on the lifetime of the excited state and the orientation of the transition moment with respect to the molecular axis. Recent studies of the photodissociation of $CSCl_2$ (248 nm)[70] and OCS (157 nm)[71] measured the translational energy distribution of the fragments from which internal energy distributions were inferred. The impulsive spectator model[72] adequately described the experimental results on $CSCl_2$ where it was assumed that after absorbing the photon, the available energy was partitioned mostly to the relative motion of the C and Cl atoms. As the C atom recoils, the bonds compress converting translational motion into vibrational excitation of the CSCl fragment. In the OCS photodissociation, the

large vibrational excitation of the CO fragment is not predicted by the Franck-Condon theory and the spectator model. The Franck-Condon theory assumes that in the excited state, the repulsive potential acts only to separate the centers of mass of the two fragments. Thus, the spectator model assumes that for this dissociation, the oxygen atom is only a spectator during the initial separation of the C and S atoms. Negligible CO vibrational excitation is predicted by this model, however, strong vibrational excitation is observed. Thus, to explain this strong vibrational excitation, a potential can be selected where the C-O bond length can quasi-oscillate while the C-S bond length gradually increases.

C. Laser Induced Fluorescence

Laser induced fluorescence spectroscopy has been used to probe vibration-rotation levels of ground electronic states. After photodissociation of a parent molecule with a laser or flash lamp, the resultant product fragment is probed with a tunable dye laser which is scanned over the spectral transitions of the fragment to obtain resonance fluorescence spectra. The products of the photodissociation of C_2N_2, ClCN, and BrCN in a pulsed molecular beam were analyzed using laser induced fluorescence.[73] The experimental apparatus consisted of counter propagating dye and excimer laser beams which crossed a molecular beam at right angles in the experimental cell. The induced fluorescence was observed by a filtered and apertured photomultiplier perpendicular to both the laser and molecular beams. The observed CN distributions from ClCN and BrCN were insensitive to the initial internal energy of the parent molecules. The rotational and

vibrational distribution of CN from C_2N_2 varied weakly with changes in the internal energy distribution of the parent. The general shape of the dissociation potential energy surface was deduced from careful analysis of the information obtained.

Laser absorption probing of photofragments has also provided valuable information on the photophysics of reactions. In the photodissociation of formaldehyde, the CO fragments were studied by CO absorption.[74] The CO appearance rates were found to be much slower than corresponding decay rates for $H_2CO(S_1)$. An intermediate state was proposed which yielded CO upon collision. The "intermediate" has since been identified as highly rotationally excited CO.[75] The vibrational energy distributions of CO resulting from the photodissociation of HCNO and CH_2CO were also studied using a CO probe laser.[76] The experimental CO distribution and average vibrational energy compare favorably with statistical predictions based on information theory[76] if $NH(a^1\Delta)$ is formed in the HCNO dissociation. It appears complete randomization of energy among the products' degrees of freedom occurs. The vibrational distribution of CO from ketene also compared well with a statistical model assuming CO and $CH_2(A_1)$ as the primary products.

CO laser absorption spectroscopy has also been used to study the dissociation dynamics of $Cr(CO)_6$.[77] Good evidence was obtained indicating that CO was formed by at least two processes; i.e., serial decarbonylation yielding $Cr(CO)_5$ and $Cr(CO)_4$.

D. Polarized Photofluorescence Spectroscopy

In polarized photofluorescence spectroscopy, the degree of

polarization of the fluorescence of the electronically excited photofragment is measured under collision free environment as a function of the wavelength of the linearly polarized photolysis beam. Excited states of the parent molecules which fragment can be assigned and information related to the lifetime of the excited molecule in any vibronic state initially populated prior to fragmentation obtained. Acquisition of good information is dependent on retention of orientation by the fragments relative to the orientation of the photo-selected parent molecule during the fluorescent lifetime of the fragment.

The degree of polarization of the HgBr($B^2\Sigma^+$) emission was measured following photolysis of $HgBr_2$ by the linearly polarized output of an ArF excimer laser and was found to be in substantial agreement with theory, permitting the identification of the symmetry of the dissociative state.[62] Collisions with Kr atoms resulted in almost a complete loss of polarization.

E. Multiphoton Dissociation

The advent of high intensity excimer and dye lasers has allowed researchers to study new photochemical pathways by accessing states through multiphoton absorption. For example, states which cannot be populated by single photon transitions can, in some cases, be prepared by two photon absorption. Excitation of molecules with CO_2 TEA lasers can result in as many as 30-40 ir photons being absorbed. Measurements of the rovibronic state distributions of nascent CN following the infrared multiphoton dissociation of CF_3CN were recently made.[79] The CN product was monitored by laser induced fluorescence

and the vibrational and rotational distributions measured. Using these measurements and estimating the product's translational distribution, the parent excitation was obtained. The multiphoton dissociation of acetic anhydride leads to $^1CH_2$ (through a ketene intermediate) and OH (through acetic acid formed in the same step as ketene). This was taken as evidence for a sequential up-pumping mechanism.[80] The sequence begins with the dissociation of the anhydride and continues with the absorption of more photons by the intermediates to yield the observed products. Similarly, through fluorescence measurements, the vibrational, rotational, and translational energy distributions of the CF_2 and CFCl products from the dissociation of CF_2CFCl were determined.[81] The carbon-carbon bond cleavage was demonstrated to be the only significant pathway leading to the products. More vibrational energy appeared in the CF_2 fragment than in the CFCl fragment. Multiphoton dissociation of transition metal carbonyl complexes may provide a technique for preparing a wide variety of well-defined gas-phase transition-metal clusters heretofore unavailable in sufficient concentrations for spectroscopic and chemical characterization.[82]

cyclization.[133] The photolysis of 3-cyclopentenone resulted in highly efficient conversion to CO and 1,3-butadiene and though dissociation by biradical formation is possible, no experimental evidence was found to verify a biradical intermediate.[134] Pyrolysis and photolysis of cis- and trans-2,3-dimethyl cyclobutanone and cis- and trans-2,4-dimethyl cyclobutanone have indicated that these processes occur in a concerted manner with a retention of stereochemical configuration.[135]

In an insightful study, Bauer[136] proposed that the mechanisms of fragmentation reactions determine the energy distributions of the nascent products. During the elimination of N_2 from (IX) and CO from (X), the N-N bond length in N_2 and the C-O bond length in CO changes drastically from parent to product (approximately Ø.1Ø-Ø.12 Å). If these processes are concerted, the equilibrium geometries of the separated fragments are quite different than the transition state geometry. The excess energy corresponding to this geometry change may appear as vibrational energy of the fragments and thus N_2 and CO emerge vibrationally excited. The extent of vibrational excitation can be determined in the case of CO by measuring the infrared fluorescence emitted or by laser absorption spectroscopy. If the elimination involves the sequential breaking of two bonds, geometric relaxation of the fragment can occur in the biradical intermediate resulting in little vibrational excitation upon emergence. Additionally, if the fragmentation occurs via a non-linear transition state, rotational, along with vibrational, excitation can perhaps be expected in concerted reactions.

Also, the presence of homoallylic unsaturation facilitates the elimination of CO. The conclusion drawn is that σ-bonds are less polarizable than π-bonds and might be expected to participate less readily in concerted, thermal, electrocyclic reactions where the bonds are extensively delocalized in the transition state. Thus, the degree of concert declines as the π-character of the participating ring bond decreases.[128]

Cheletropic elimination of carbon monoxide from ketones has been observed. Baldwin[132] studied the thermal decomposition of dicyclopentadiene-1,8-dione (VI) at 350 and 240 °C and found the products to be carbon monoxide and cis-bicyclo[4.3.0]nona-2,4,7-trien-9-one (VII) or indone (VIII).

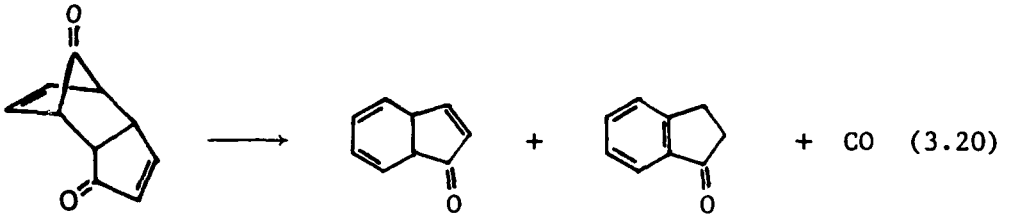

VI VII VIII (3.20)

The decarbonylation was found to be a well-behaved first order processes uncomplicated by side reactions typical of non-concerted processes as in the photolysis of 2-pentanone.[102] Application of the theoretical model of Woodward and Hoffmann indicated that this necessarily disrotatory decarbonylation can be concerted. Highly stereospecific formation of diphenylbenzocyclobutenes from the photolysis of 2,5-diphenyl-3,4-benzocyclopentenones appeared to be the result of a cheletropic fragmentation followed by thermal

2,3-diazabicyclo[4.1.0]hept-2-ene (II), and 2,3-diazabicyclo[4.2.0]-oct-2-ene (III) showed that (I) and (II) were clearly concerted and (III) was probably concerted.[128]

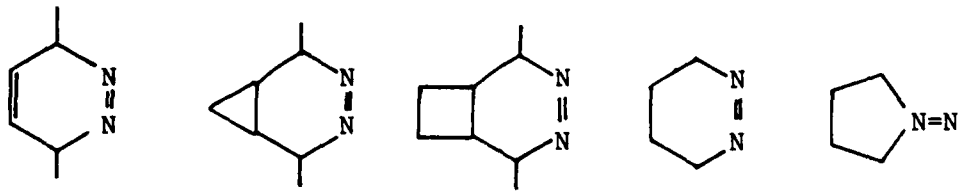

I II III IV V

Thermal decomposition of (IV) and (V) produced a biradical via a non-concerted pathway.[129] Studies of the decomposition of cis- and trans-3,4 and -5,6-dimethyl-3,4,5,6-tetrahydropyridazines indicated that this system represented a point where the 1,4-diradical and the (2+2+2) cycloreversion processes are competitive.[130]

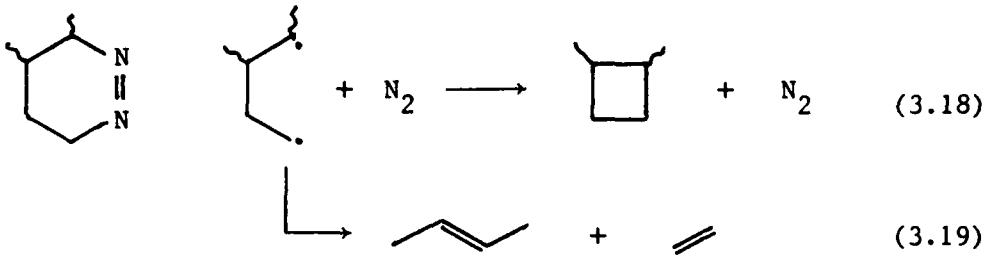

(3.18)

(3.19)

Thus, it appears that traces of concerted reaction can still be found in purely σ-bonded systems as observed in these cyclic azo decompositions. Results indicating similar trends have been observed in the photolysis of cyclic ketones.[131] These results showed that the incorporation of certain structural features into the cyclic ketone including cyclopropane rings, α-alkyl substitutions and β, γ-unsaturation enable such molecules to decarbonylate readily.

sulfones indicated that the extrusion occurred by concerted fragmentation of vibrationally excited ground state molecules.[119] Application of the Woodward-Hoffmann orbital symmetry considerations to the results of the benzene sensitized fragmentation of 2,5-dimethyl sulfones suggested that the concerted reaction should be allowed photochemically and the conrotatory mode should be favored. The data were in accord with this prediction.[120] The thermal extrusion of SO_2 from cis- and trans-dimethyl dihydrothiophene dioxides had been shown to proceed in a disrotatory manner.[121,122]

Investigation of the thermal decomposition of 1-pyrazolines which results in the extrusion of nitrogen showed that both carbon-nitrogen bonds were breaking simultaneously[123] in much the same manner as described by Seltzer in the pyrolysis of azobis-α -phenylethane.[124] In the study of the fragmentation of cis- and trans-3,4-dimethyl-1-pyrazoline, the cis- isomer yielded ethylene, propylene, and only cis-2-butene while the trans- isomer yielded ethylene, propylene, and only trans-2-butene indicating a stereospecific cleavage.[125] Bergman and Carter[126] concluded that sufficient evidence was available to show that an electrocyclic process was occurring in pyrazoline decomposition. Stereochemical and deuterium isotope effects on the thermal decomposition of [N-phenyl(threo-(and erythro)-2-deutero-1-methyl propyl)-amino]-nitrenes shows the reaction occurs via a stereospecific (>98%) syn-elimination.[127] These data are consistent with a concerted elimination reaction via a five-membered cyclic transition state.

The thermal decomposition of 1,2-diazacyclohexa-1,4-diene (I),

The product molecule, N_2, lies along the x-axis upon departure and this process is termed non-linear cheletropic reaction.

It then follows that in the linear cheletropic elimination (equation (3.13)), electrons are transferred from the anti-symmetric orbital to the highest occupied π-orbital. The geometrical displacements occurring at C_1 and C_2 are,

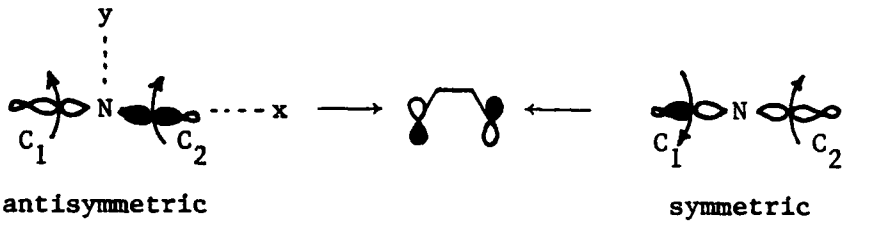

(3.17)

antisymmetric symmetric

Thus, in the linear process, the displacements at C_1 and C_2 must be disrotatory while in the non-linear process, the displacements must be conrotatory. The selection rules can be summarized as follows:

	Allowed Ground State Reactions	
m	Linear	Non-Linear
4n	Disrotatory	Conrotatory
4n+2	Conrotatory	Disrotatory

where m is the number of electrons involved in the process and n is an integer.

Cheletropic elimination processes have been observed in sulfones, pyrazolines, and ketones. The first observation of SO_2 formation from

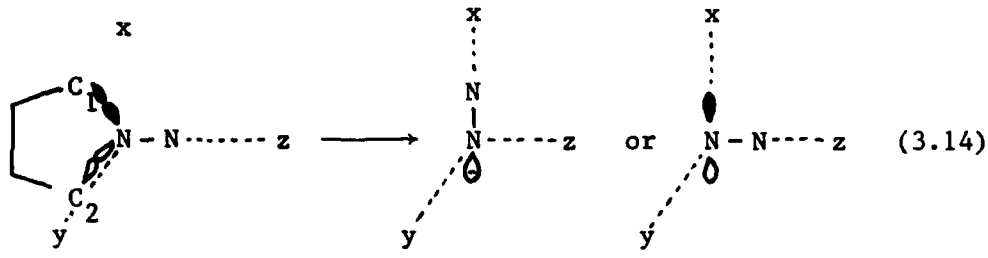

(3.14)

N_2 molecule remains in the yz plane along the z-axis (equation (3.15)). This process is designated as a linear cheletropic reaction.

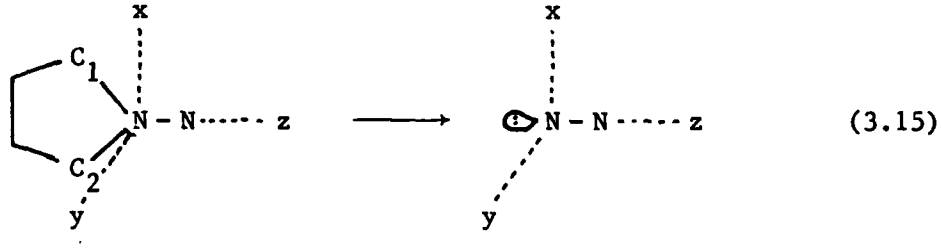

(3.15)

In equation (3.14), the ring nitrogen obtains its electrons from the anti-symmetric orbital as N_2 departs co-linearly. The ring nitrogen remains in the yz plane while the exocyclic nitrogen is displaced in both the x and z directions (equation (3.16)).

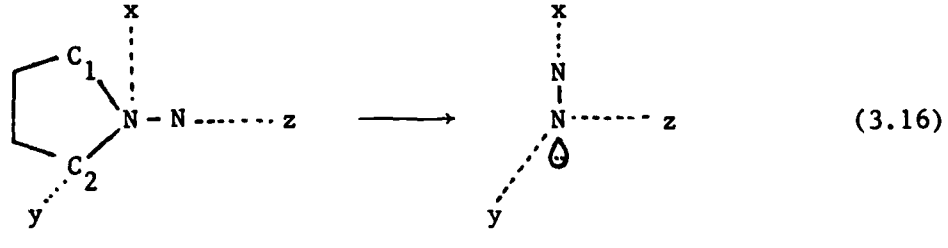

(3.16)

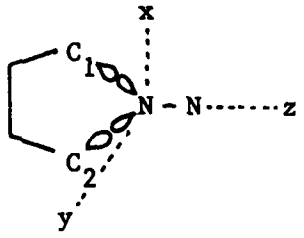

(3.12)

During the reaction, two electrons from these orbitals are donated to each of the developing products with the conservation of orbital symmetry. The delivery of electrons to the nitrogen molecule can occur in two distinct ways:

(a) Two electrons from the symmetric orbital may be delivered to a z-symmetric lone-pair orbital of N_2 or enter a π-system anti-symmetric with respect to the xy plane.

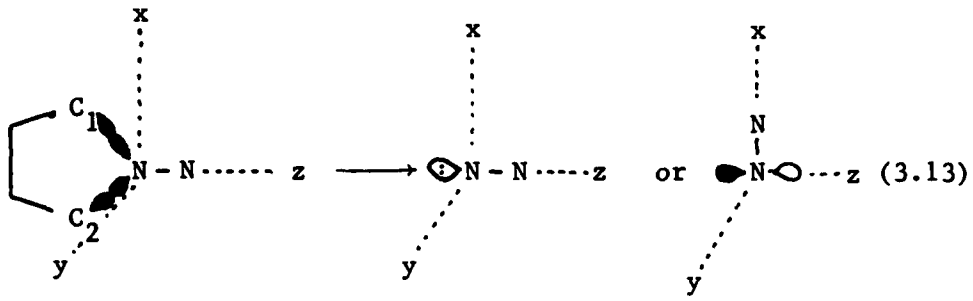

(3.13)

(b) Two electrons from the anti-symmetric orbital may be delivered to an x-symmetric lone pair orbital of N_2 or enter a π-system anti-symmetric with respect to the yz plane. For a co-linear departure of N_2 in equation (3.13), the nitrogen atom in the ring obtains its electrons from the symmetric σ orbital and the

Woodward and Hoffmann have suggested that the rates and stereochemistry of these reactions are controlled by the symmetry properties of the reactant and product molecular orbitals. In any concerted process, the orbitals of the starting materials must be transformed into orbitals of the product that have the same symmetry, hence, conservation of orbital symmetry. If, during the concerted process, bonding orbitals of the starting material are transformed into bonding orbitals of the product of the same symmetry, the reaction proceeds with low activation energy and is allowed. If, however, bonding orbitals of the starting material are transformed into or correlate with anti-bonding orbitals of the product, the reaction has a relatively large activation barrier and is forbidden.

In the cheletropic elimination of nitrogen from diazenes (equation (3.11)), the geometrical displacements of the terminal carbon atoms are dependent on the detailed geometry of the departure of the nitrogen molecule. If upon colinear departure, the nitrogen molecule and the two terminal carbon atoms remain in the same plane, the process is termed a linear cheletropic reaction. If the nitrogen molecule departs co-linearly in an orientation such that the nitrogen atoms and the terminal carbon atoms are no longer in the same plane, these processes are designated non-linear cheletropic reactions.

The geometrical aspects of the reaction can be illustrated[118] with a coordinate system whose origin is located at the nitrogen atom in the ring and whose z-axis bisects the angle between the carbon atoms bonded to the nitrogen atom. The σ bonds being broken lie in the xz plane and their electrons are distributed among two orbitals.

at 400-500 °C with the formation of an alkene and a carboxylic acid. Homoallyl alcohols decompose upon heating to form a carbonyl compound and an alkene. At high temperatures, amides undergo pyrolytic eliminations forming alkenes and unstable tautomers. Fragmentation and elimination reactions can also be initiated by the absorption of a photon resulting in the cleavage of a sigma bond(s). The photolysis of cyclic esters at 77 K produces CO_2 and an alkene. Carbenes are formed by the photoelimination of N_2 from diazo compounds.

Of particular interest to this study are elimination reactions which appear to be concerted. Concerted reactions give no evidence of intermediates such as free radicals and are processes where both bond-making and bond-breaking contribute to the transition state. For a time, these processes were referred to as "no mechanism thermal reorganizations".[117] Significant insight into these processes has since been provided by Woodward and Hoffmann[118] suggesting that the pathways for reactions are governed by the symmetry properties of the reactant and product states or the orbitals involved. When two bonds which terminate at a single atom are made or broken in concert, the process is defined as a cheletropic elimination. The net result is the extrusion of a single atom or a small molecule from a ring. The elimination of nitrogen from diazenes appears to be a cheletropic process.

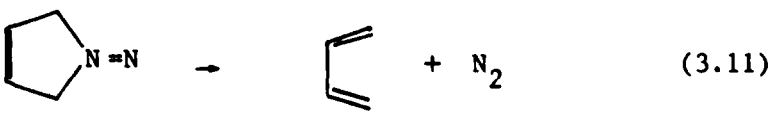

(3.11)

(3) Norrish Type III - the Type III process, equation (3.8), has been postulated to account for the formation of olefinic products in the photolysis of compounds where the fission of the α-β bond cannot yield them.[115]

$$\rightarrow \quad CH_3CHO + CH_2{=}CH_2 \qquad (3.8)$$

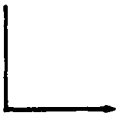

$$CH_3CO + C_2H_5 \rightarrow CH_3CHO + C_2H_4 \qquad (3.9)$$

$$CH_3 + CO \qquad (3.10)$$

The Type III process occurs by the formation of a 4-membered ring formed by hydrogen bonding between the carbonyl carbon and a hydrogen atom on the β-carbon of the alkyl chain.[116] Hydrogen abstraction (equation (3.9)) by CH_3CO from the Type I cleavage of the reactant ketone does not compete favorably with dissociation (equation (3.10)).[116] Type III reactions have only been observed in molecules such as methyl ethyl ketone[115] and methyl isopropyl ketone[116] which do not have γ-carbon atoms and hence cannot proceed through Type II intermediates.

Fragmentation Mechanisms in Organic Molecules

A large number of organic molecules including esters, amine oxides, ketones, and some hydrocarbons undergo thermal unimolecular decompositions. Esters containing β-hydrogen atoms readily decompose

bond β to the carbonyl group, equation (3.6). Methyl n-butyl ketone[88] undergoes Type II cleavage, but, the process is general for ketones with hydrogen atoms on gamma carbons. Intramolecular hydrogen abstraction is observed in these Type II processes.[100,101]
In the reaction,

$$CD_3COCD_2CH_2CH_3 \xrightarrow{h\nu} CD_3COCD_2H + C_2H_4 \qquad (3.7)$$

Ausloos and Murad[102] observed that Type II reactions consist of a transfer of a γ-hydrogen followed by β-bond cleavage to yield an enol-ketone and olefin. Similar observations were made on the photolysis of 2-hexanone-5,5'-d_2-[103] and 2-pentanone.[104]

Davis and Noyes[105] proposed that the intramolecular Type II process proceeds via a 6-member ring, formed by internal hydrogen bonding, which can dissociate directly into an olefin and a lower ketone. Photolysis studies on cyclic (cyclopentanone)[103] and acyclic (2-pentanone)[106] molecular systems have confirmed this proposal. In the mercury-sensitized photolysis of a number of ketones, no Type II products were observed.[107] Since the reactants were generated in the triplet state, it was concluded that Type II reactions must result from reactants in the singlet state. However, later studies[108-113] provided strong evidence for Type II reactions from both the excited singlet and triplet states of 2-pentanone, 2-hexanone, and 2-octanone. Kinetic analysis of Type II photoelimination reactions of 2-hexanone indicate that the chemical reactivities of the S_1 and T_1 states toward intramolecular hydrogen abstraction are comparable.[114]

comprehensive review of Type I reactions. The photolysis of methyl ethyl ketone occurs via a Type I process.[87,88] Simple cyclic ketones such as cyclopentanone, cyclohexanone, and cycloheptanone were also found to undergo Type I cleavages.[96]

The reactivity of the S_1 and T_1 states of cyclic alkanones toward Type I cleavage were compared directly.[97,98] The T_1 state of 2,2,5,5-tetramethyl cyclopentanone is at least two orders of magnitude more reactive than the S_1 state. A biradical intermediate had been postulated for a long time and in 1969, Baltrop and Coyle[99] demonstrated that the photorearrangement of cis- and trans-2,3-dimethyl cyclohexanone to aldehydes and ketones proceeded via a common and discrete biradical intermediate.

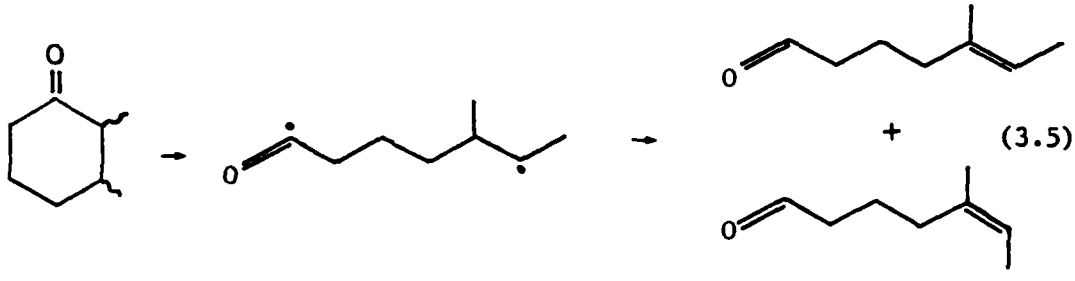

(3.5)

(2) Norrish Type II process - cleavage of a carbon-carbon

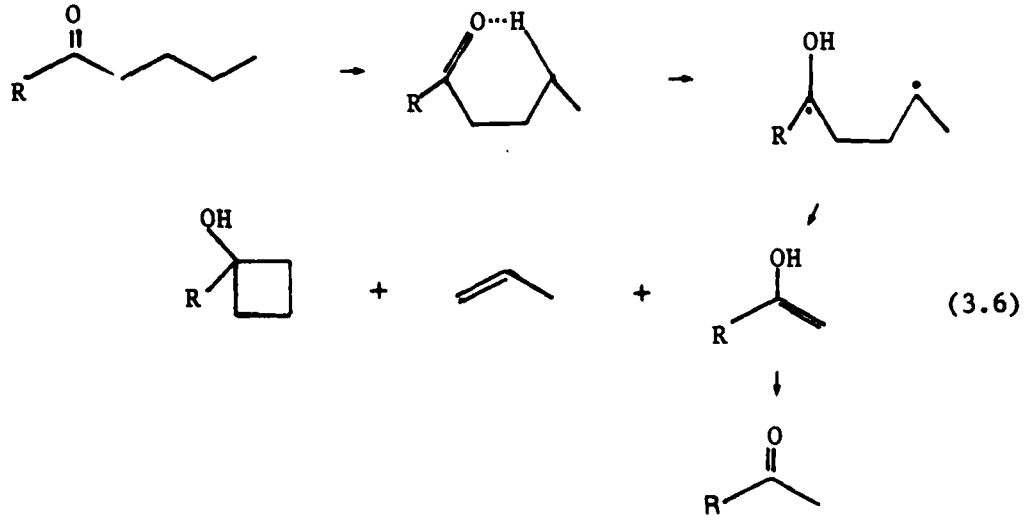

(3.6)

visible and ultraviolet regions of the spectrum, 200-700 nm. In simple ketones, an absorption band in the 260-380 nm region is observed which corresponds to an $n-\pi^*$ transition. An absorption band is also generally observed in the region less than 220 nm and corresponds to a $\pi-\pi^*$ transition.

The general features of the important processes in the gas-phase photochemistry of carbonyl compounds have been described in detail.[89,94] In brief, when a molecular system absorbs a quantum of electromagnetic radiation and becomes electronically excited, usually to an excited singlet state, the system tends to decay by one of several routes; (1) decay directly to the ground state of the same multiplicity as the excited state by radiative emission (fluorescence), (2) decay by radiationless transition to a lower state of the same multiplicity (internal conversion), (3) decay by radiationless transition to an isoenergetic triplet state (intersystem crossing), or (4) reaction to form products, e.g., isomers or fragments, directly from the excited state. Further radiative, non-radiative, and photochemical processes can occur from intermediate excited states.

Typical photochemical reactions observed in simple ketones in the gas phase are:

(1) Norrish Type I process - cleavage of a carbon-carbon bond to the carbonyl group, equation (3.4). Weiss[95] has provided a

$$R - \overset{\overset{O}{\|}}{C} - R \xrightarrow{h\nu} RCO + R \qquad (3.4)$$

CHAPTER 3

PHOTOCHEMISTRY OF KETONES AND FRAGMENTATION MECHANISMS OF ORGANIC MOLECULES

Photochemistry of Ketones

In the first of a long series of papers studying the photochemistry carbonyl compounds, Norrish and Griffiths[83] noted that glyoxal undergoes complicated reaction and discussed the possible behavior of the CHO radical. A study of formaldehyde[84,85] showed that reaction (3.1) rather than (3.2) to be the primary process.

$$HCHO \xrightarrow{h\nu} H + HCO \qquad (3.1)$$

$$HCHO \xrightarrow{h\nu} H_2 + CO \qquad (3.2)$$

Acetone, the simplest of the ketones, received much early attention.[86,88] Norrish and Appleyard[87,88] proposed that acetone dissociates via free radicals by the reaction,

$$CH_3COCH_3 \xrightarrow{h\nu} COCH_3 + CH_3 \qquad (3.3)$$

The study of methyl ethyl ketone confirmed that the primary dissociation of simple ketones is into radicals by the detection of ethane, propane, and butane as products of the photolysis.

Since these early investigations, the photochemistry and photophysics of carbonyl compounds have been widely studied.[89-93] In general, photochemical processes in carbonyl compounds are initiated by the absorption of electromagnetic radiation (photons) in the

IX

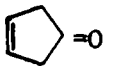

X

The results of the pyrolysis of pyrazolines (XI) and (XII) have been correlated with Bauer's hypothesis.[137] Pyrazoline (XII) yields vibrationally excited spiropentane while pyrazoline (XI) does not.

XI

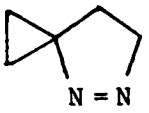

XII

The symmetrical pyrazoline (XI) most likely decomposes by simultaneous cleavage of both C-N bonds proceeding through a symmetrical transition state where the coupling of the N-N vibration with the vibrational modes of the organic fragment is poor. The N_2 would thus be formed with a highly stretched bond and vibrationally excited, carrying off much of the excess energy, and leaving the spiropentane thermalized. Pyrazoline (XII), however, has one relatively strong and one weak C-N bond and probably fragments via a sequential cleavage of the C-N bonds generating a biradical intermediate. If the lifetime of the intermediate is sufficient, efficient coupling of the N-N vibration and the vibrational modes of the organic fragment in the diradicals may occur, according to Bauer. Thus, the N_2 will be extruded cold. The available energy will be statistically distributed among both

fragments.

It has been shown that mechanistic descriptions of fragmentation processes may be formulated on the basis of the energy distribution to the nascent products. For example, Bauer's hypothesis suggests that a concerted decomposition mechanism should result in a vibrationally excited diatomic fragment. Similar reasoning suggests that a non-linear cheletropic reaction should result in a rotationally excited diatomic fragment. Thus, the energy content of the fragment may depend on the structure of the transition state and experimental studies where the channels for energy disposal into product modes can be directly monitored can provide detailed information on the dynamics or mechanism for these types of reactions. The object of this work has been to study the dynamics of the photodecarbonylation of ketene, 3-cyclopentenone, 3,5-cycloheptadienone and tropone by determining the energy content of the nascent carbon monoxide product.

CHAPTER 4

KETENE PHOTODISSOCIATION

Introduction

The photochemistry of ketene has been extensively studied largely because it is a relatively simple molecule conducive to theoretical calculations and also a convenient source of methylene radicals. Two distinct absorption regions are observed in the spectrum of ketene, one in the near-ultraviolet region which is attributed to a weak $\pi^* \leftarrow n$ transition with an absorption coefficient below 10 l/mol-cm, and the other below 240 nm, a strong absorption (approximately 3×10^3 l/mol-cm) assigned to the $\pi^* \leftarrow \pi$ transition.[138] There is general agreement that the transition in the 370-240 nm region is $^1A_2 \leftarrow {}^1A_1$ if the upper state remains in a linear molecular configuration and maintains C_{2v} symmetry, or $^1A'' \leftarrow {}^1A_1$ if the upper state of ketene is nonlinear, in-plane bent, described in C_s symmetry.[139] Other computations have shown[140,141] that the excited state of ketene accessible with these wavelengths are nonlinear. Also, rapid electronic relaxation from the $^1A''$ state prior to dissociation has been suggested.[139] Basch[142] and Pendergast and Fink[143] have shown that photodissociation of ketene does not occur from the electronically excited $^1A_2$ state in the 200 nm region. Del Bene[144] found that at 337 nm, the $^1A_2$ state of ketene correlated with states of the separated fragments with much higher energy than the $CH_2(\tilde{a}^1A_1)$

state which would not allow the $^1A_2$ state to directly decay into the products observed by Feldmann et al.[145] Lin and coworkers[146] have concluded that since fluorescence has not been observed from ketene, internal conversion from the excited to the ground electronic state must occur very rapidly and dissociation takes place from a highly vibrationally excited state.

Since the initial photodissociation study of ketene by Norrish, Crone, and Saltmarsh[147], many other experiments have been conducted. Kistiakowsky[138] determined that the quantum yield for CO at 214 nm was 2 and that singlet ($^1CH_2$) and triplet ($^3CH_2$) methylene were produced in a 7:3 ratio. A mechanism was proposed whereby upon absorption of a photon, ketene dissociates directly to singlet or triplet methylene. Zabransky and Carr[139] observed that at 313 nm, the relative singlet and triplet yields were independent of the pressure of a buffer gas and that the quantum yield for dissociation was approximately unity. However, at 366 nm, the quantum yield was less than unity. They concluded that the state which was collisionally deactivated at 366 nm was not $^1A''$ but another state reached by rapid electronic relaxation. A mechanism was proposed for ketene dissociation at 313 nm:[2]

$$^1A_1 \longrightarrow {}^1A'' \qquad (4.1)$$

$$^1A'' \longrightarrow {}^1A_1^* \qquad (IC) \qquad (4.2)$$

$$^1A_1^* \longrightarrow CH_2(^1A_1) + CO \qquad (4.3)$$

$$^1A_1^* \longrightarrow {}^3A' \longrightarrow CH_3(^3B_1) + CO \qquad (ISC) \qquad (4.4)$$

$$^1A_1^* + M \longrightarrow {}^1A_1 + M \qquad (4.5)$$

This mechanism is essentially identical to that proposed by Strachan and Thornton[148] who noted that $^1CH_2$ and $^3CH_2$ were formed at all wavelengths with the relative yield of $^3CH_2$ increasing with increasing wavelength. More recently, Lengel and Zare[149] have found that between 340 and 290 nm, $CH_2(\tilde{a}^1A_1)$ is formed upon photolysis of ketene, and Lee and coworkers[150] have found that at 308 nm, methylene is formed exclusively in its $\tilde{a}^1A_1$ state while at 351 nm, only methylene in its $\tilde{X}^3B_1$ state is observed. Correlation diagrams[143] indicate that the $\tilde{a}^1A_1$ product state of methylene from ketene irradiation in the 200 nm region can be readily accessed only from ketene's ground state.

Comparison of experimental data with theoretical predictions show that the rate of dissociation for a vibrationally and electronically excited molecule of ketene is consistent with unimolecular rate theory.[151-153] Bowers[153] applied RRKM theory to the photodissociation of ketene in the gas phase and found the relative rate of dissociation as a function of temperature and dissociation wavelength to be consistent with a mechanism where the radiationless conversion from the first excited singlet state was the rate controlling step.

An oxirene intermediate has been suggested[154] in the photolysis of $^{14}CH_2CO$,

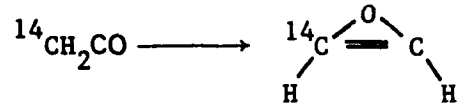

(4.6)

An appreciable, pressure-dependent yield of ^{14}CO was detected which strongly suggests the formation of this oxirene intermediate which is

capable of rearrangement and decomposition or de-excitation without decomposition. Theoretical calculations[155,156] on the oxirene intermediate shows that the molecule lies in a shallow potential well with the barrier for rearrangement to ketene very small. Rearrangement should occur readily under experimental conditions. Also, scrambling of ^{14}C takes place on the ground state of the CH_2CO system.

The methylene singlet-triplet energy difference has been the focus of much attention. Since ketene is a convenient source of methylene radicals, it has been thoroughly scrutinized in order to provide the singlet-triplet splitting. Halberstadt and McNesby[157] were the first to attempt to determine this value and found the splitting to be 2.5 kcal/mol. Carr et al.[158] later determined the value to be between 1-2 kcal/mol. Since then, the concensus of investigators is that the singlet-triplet splitting of methylene is between 8-10 kcal/mol.[149,150] Recently, controversy arose when a value of 19.5 kcal/mol was reported[159] from the photoelectron spectrum of CH_2^-, conceivably the most direct measurement of the singlet-triplet splitting. This erroneous result was due to problems in correctly identifying the origin of the triplet band system[160]. Elimination of the hot band activity which led to the error yielded a splitting of approximately 9 kcal/mol.[160]

The studies described above have begun to provide a useful picture of the photofragmentation dynamics of ketene. Though much is known, still, many important questions remain. For example, the nature of the relevant potential surface over which dissociation

occurs has not been conclusively established. The role of nonradiative relaxation processes prior to fragmentation has not been directly addressed. Attempts to address these problems have been limited by lack of development of ab initio theoretical approaches for estimating the rates of radiationless transitions in polyatomics to the point where quantitative predictive accuracy can be expected. By studying polyatomic reactivity on an increasingly microscopic level, we can begin to develop useful points of comparison for new theoretical methods in dynamics. The simple time-resolved photofragment infrared fluorescence method in this study permitted us to characterize the ro-vibrational energy disposal to the nascent CO product in the photolysis of ketene. This method is described below.

Preparation of Ketene

Ketene was prepared by the pyrolysis of acetic anhydride vapor in an evacuated (20 mm Hg) quartz tube heated to approximately 780 K.[161] The vapors were passed through a trap at 197 K where unreacted acetic anhydride and acetic acid from the pyrolysis were removed, and through a second trap at 77 K where ketene was collected. A third trap at 77 K was used to prevent back diffusion of pump vapors from the mechanical pump into the ketene. The ketene was purified by trap-to-trap distillation and purity was checked by infrared spectrophotometry of ketene in the gas phase.

Experimental Procedure

A schematic diagram of the experimental configuration is shown in Figure 1. Ketene was flowed through the aluminum fluorescence cell either neat or diluted with helium or argon gas. The cell was equipped with a quartz window through which the uv beam was propagated. The interior of the cell was painted black to minimize scattered light. The uv source employed was a rare-gas halide excimer laser (Lambda Physik EMG 101) whose pulse width is approximately 15 ns. The pulse rate was maintained at approximately 2 Hz to permit maximum exchange of gases within the cell between pulses. The beam was passed through a circular aperture 10 mm in diameter and observed on a fluorescing target to ensure homogeneity.

The photofragment infrared fluorescence was observed at 90° relative to the excimer beam through a 35 mm CaF_2 window. A gold mirror opposite the CaF_2 window was used to reflect fragment ir fluorescence toward the viewing window. The infrared fluorescence was measured with a 77 K InSb detector (50 mm^2 and 7 μm cut-off) through a 10 mm evacuable cold gas filter cell, a silicon window which serves as a 1.2 μm long-pass filter, and a 4.7 μm wide bandpass filter (1.0 μm FWHM). The detector output was preamplified and then averaged with a Princeton Applied Research Corporation Model 162 Boxcar Averager with a Model 164 Integrator. The processed signal was recorded on an X-Y recorder. The rise time of the detection system was less than 1 μs.

Neat ketene was flowed into the fluorescence cell from a 197 K bath. Ketene diluted with helium or argon was premixed in 5-liter

Figure 1. Schematic diagram of the experimental configuration used for photofragment infrared studies.

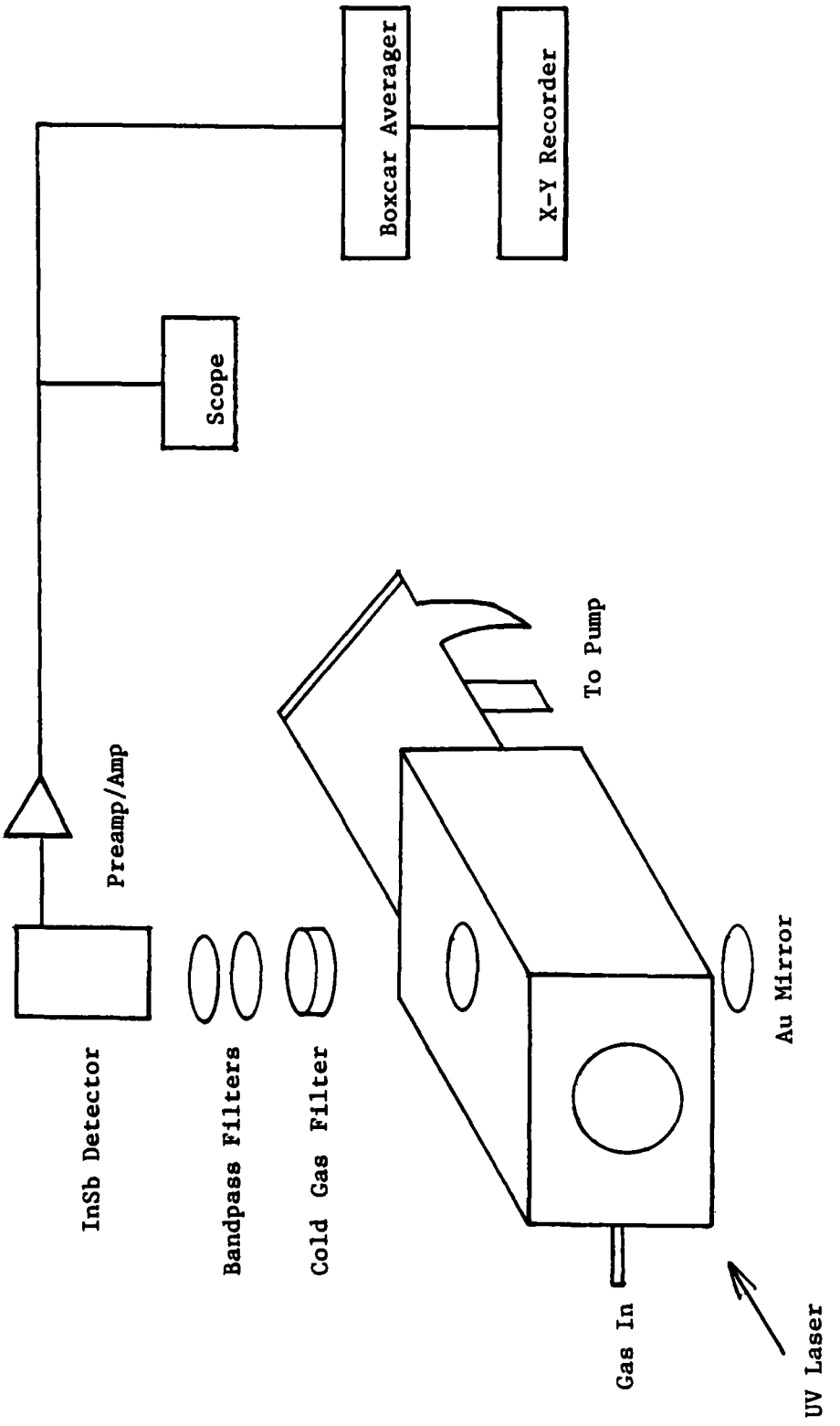
Boxcar Averager
X-Y Recorder
Scope
Preamp/Amp
To Pump
InSb Detector
Bandpass Filters
Cold Gas Filter
Au Mirror
Gas In
UV Laser

Figure 1

glass bulbs and allowed to stand for a minimum of two hours prior to use. The pressure in the fluorescence cell was regulated by adjusting the pumping speed and rate of sample injection. The cell pressures were measured using calibrated thermocouple gauges, a dibutyl phthalate manometer, or a mercury manometer. Pressure in the cold gas filter was measured using a calibrated Bourdon gauge. The laser intensity was maintained at approximately 4 mJ/cm^2 and measured using a Scientech power meter at the start and conclusion of each spectrum. Visible condensation of polymers on the quartz and CaF_2 windows required periodic cleaning or replacement of windows. The scan time per spectrum was 1000 s. Extreme care was taken to ensure that the detection configuration remained constant throughout all the experiments. The CGF cell was filled or evacuated in place, without disturbing the experimental configuration.

Results[162]

Intense infrared fluorescence at 4.7 μm from the CO fragment was observed upon irradiation of ketene at 193 nm (ArF^*). This fluorescence was found to vary linearly with the uv laser intensity between 2 and 9 mJ/cm^2 suggesting that the production of vibrationally excited CO follows a single photon absorption process. A typical CO fluorescence decay curve is shown in Figure 2. Upon irradiation of up to 2 torr of ketene at 249 nm (KrF^*) at uv laser intensities from 10 to 25 mJ/cm^2 or 308 nm ($XeCl^*$) at intensities between 2 and 6 mJ/cm^2, no CO fluorescence was detected. Acetylene, ethylene, and CO were found in detectable quantities by ir analysis of the products at all

Figure 2. Typical 4.7 μm fluorescence decay for CO formed by the irradiation of 0.34 torr of ketene at 193 nm (4 mJ/cm^2).

Figure 3. 4.7 μm fluorescence decay for CO formed by the irradiation of 0.34 torr of ketene at 193 nm (4 mJ/cm^2) attenuated when approximately 20 torr of CO is introduced into the CGF.

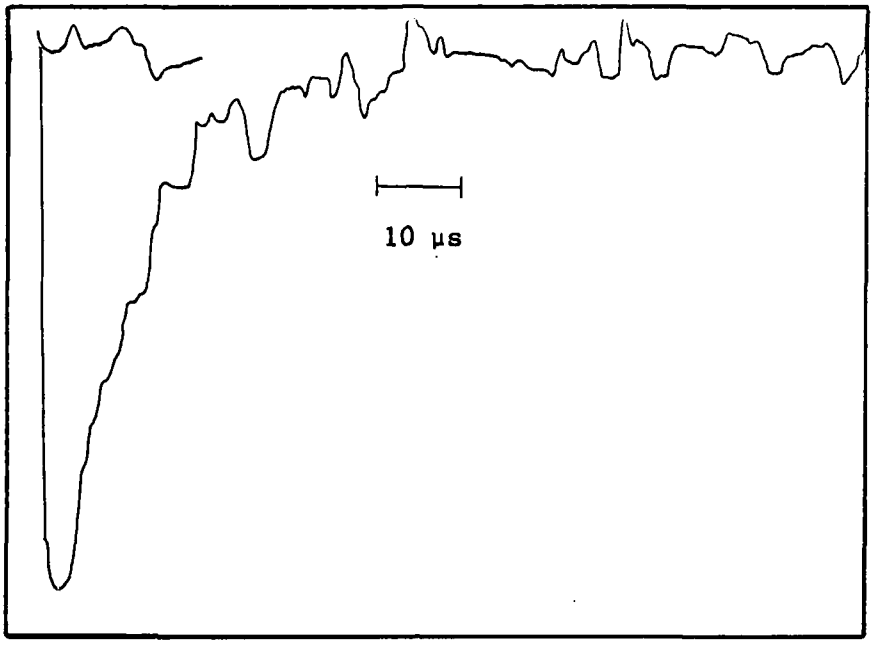

Figure 2

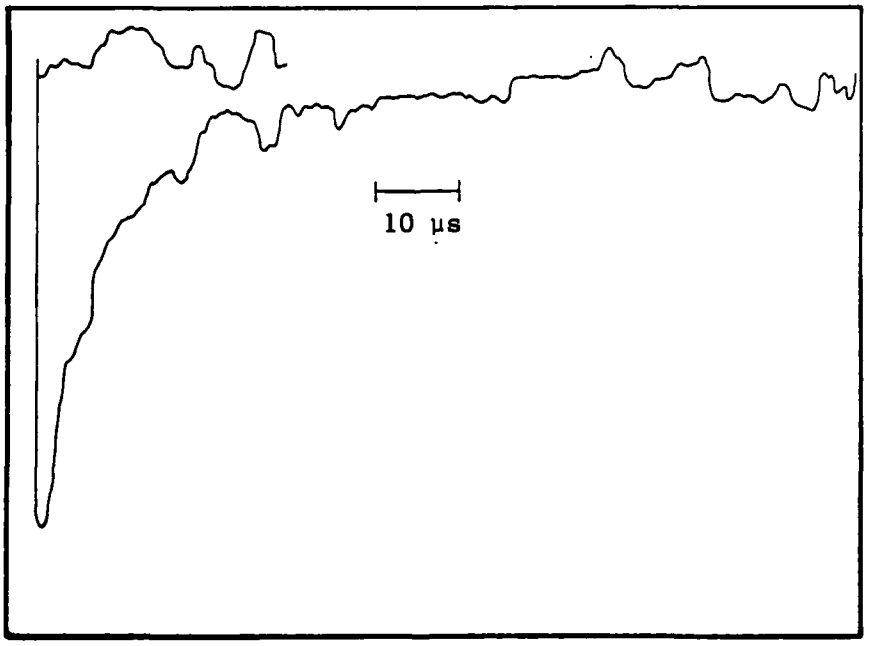

Figure 3

three wavelengths.

The origin of the infrared fluorescence was determined using the cold gas filter cell. When the fluorescence was viewed through the cell filled with approximately 25 torr of ketene or ethylene, there was no observable effect on the fluorescence amplitude or decay time. When viewed through a 3.3 μm bandpass filter, the fluorescence signal is completely attenuated. These results indicate that the ir fluorescence observed is not due to ketene, ethylene, or the asymmetric stretching mode of CH_2. However, when approximately 20 torr of CO is introduced into the CGF cell, the transmitted (integrated) fluorescence intensity is attenuated relative to the intensity observed through the evacuated cell (see Figure 3 relative to Figure 2) suggesting strongly that this fluorescence at 4.7 μm results from vibrationally excited CO.

When viewed through the CaF_2 window, faint visible fluorescence was present following photodissociation at 193 nm (4 mJ/cm^2). The emission was dispersed with a 0.6 m monochromator, detected with a photomultiplier tube, and recorded on a strip chart recorder. This emission (Figure 4) occurred in the 4315-4295 Å region corresponding to the $CH(\tilde{X}^2\pi \leftarrow \tilde{A}^2\Delta)$ fluorescence with a (0,0) transition near 4315 Å[163]. No emission in the 5000-7000 Å region corresponding to $CH_2(\tilde{a}^1A_1 \leftarrow \tilde{b}^1B_1)$ fluorescence was observed indicating that no $CH_2(\tilde{b}^1B_1)$ was produced in the photolysis of ketene at 193 nm. Thus, photodissociation of ketene at 193 nm yields vibrationally excited CO and $CH_2(\tilde{a}^1A_1)$ which may undergo subsequent uv multiphoton absorption to yield $CH(\tilde{A}^2\Delta)$.

with product rotational excitation along with translational excitation. Thus, nonlinear decay provides a means for efficiently coupling available energy to the products' rotational degrees of freedom that is not available via the linear path. Though we can conclude that the photofragmentation of ketene occurs via a nonlinear process, from our studies, we cannot determine whether the CCO bond angle bends in or out of the molecular plane as the reaction occurs.

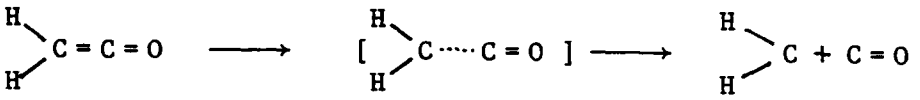

(4.12)

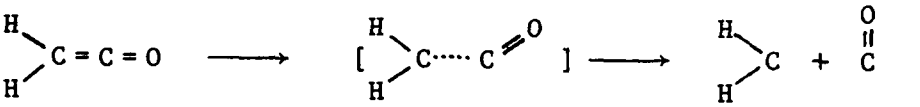

(4.13)

photoproduct rotational population by a single parameter, T_r, it is certainly possible that the nascent state distribution is non-Boltzmann. Nevertheless, our data clearly suggests that extensive rotational energy release is a dominant feature of the photofragmentation dynamics of ketene at 193 nm.

Rotational energy release to the photoproducts is highly probable if the ketene molecule undergoes dissociation from an excited state where the CCO bond angle is less than 180°. It has been shown that all excited states accessible via 193 nm photon absorption are nonlinear[141,144]. However, as discussed earlier, ketene dissociation occurs on the ground electronic state surface. In their ab initio calculations, Pendergast and Fink[143] found that both linear (least-motion) and nonlinear decay were possible having comparable energetic requirements. Yamabe and Morokuma[173] have shown that the least-motion pathway, one that maintains the C_{2v} symmetry of the ketene molecule in the ground electronic state of ketene, will have a high barrier to dissociation and is forbidden. They predict that the photodissociation leading to $CH_2(^1A_1)$ will proceed via a bent out-of-plane configuration where the oxygen atom no longer remains in the same plane as the hydrogen atoms. Equations (4.12) and (4.13) illustrate the linear and nonlinear decay channels, respectively. Computational studies do not as yet provide a sufficient basis for conclusively predicting which of the two types of fragmentation occurs. For a linear decay, motion along the reaction coordinate correlates primarily with product translational excitation whereas for the nonlinear decay, motion along the reaction coordinate correlates

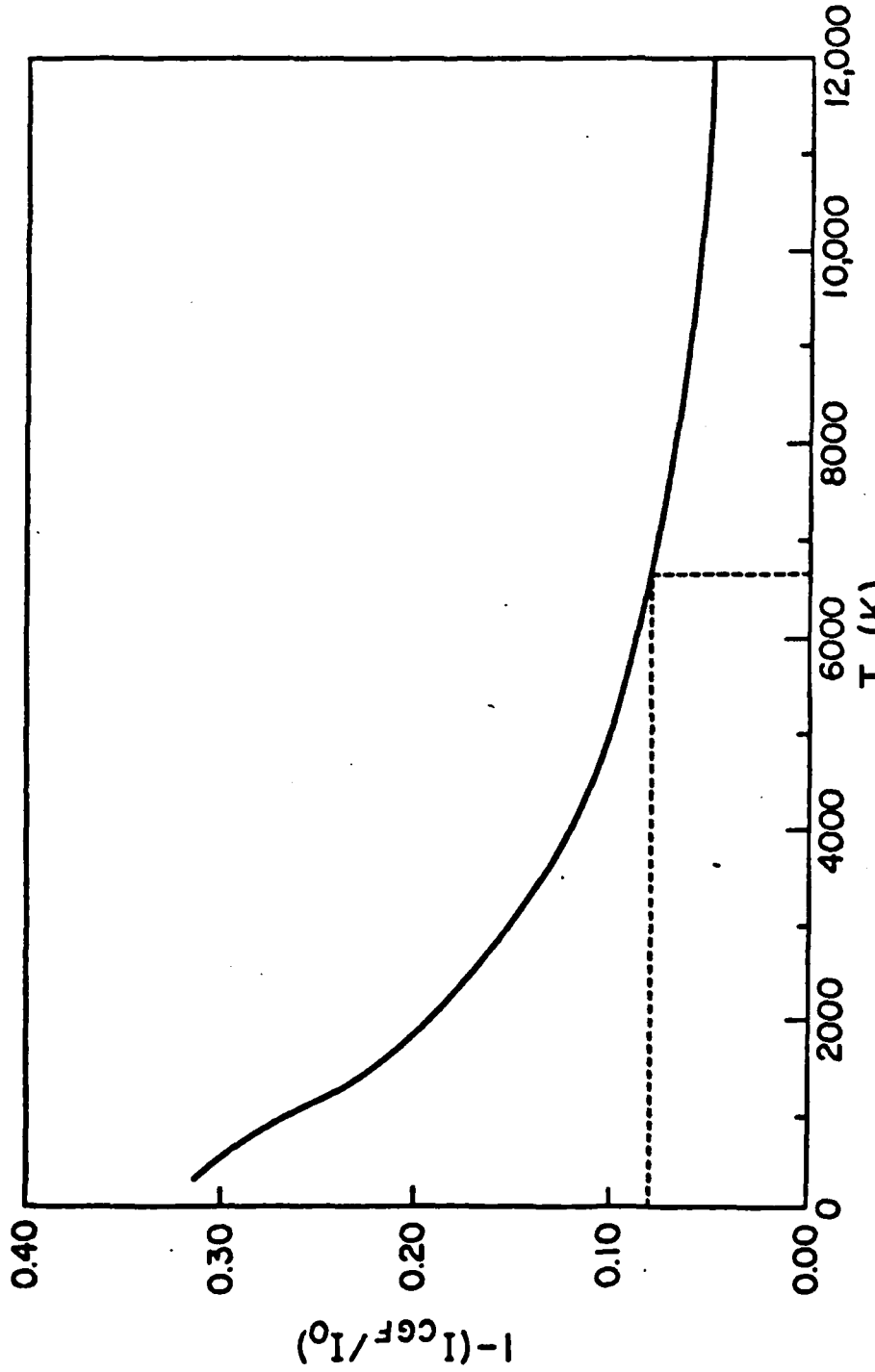
0.40
0.30
0.20
0.10
0.00
0
2000
4000
6000
8000
10,000
12,000
T_r (K)
$1-(I_{CGF}/I_O)$

Figure 6

Figure 6. Calculated attenuation of 4.7 μm fluorescence by a CGF containing 20 torr of CO as a function of the rotational temperature, T_r, of the emitting CO. A vibrational temperature of 3750K is assumed for the emitting CO. A dashed line is drawn at the experimentally determined zero pressure attenuation and the corresponding T_r (see text).

originate and terminate on the thermally populated rotational levels of CO. If the CO photoproduct is formed with little or no rotational excitation, reducing the fluorescence cell pressure should result in little or no change in the observed CGF attenuation of the 4.7 μm fluorescence intensity. However, significantly less attenuation ($1-(I_{CFG}/I_o) \cong 0.10$) is observed at low pressures suggesting that a larger component of the ir fluorescence intensity must consist of transitions that terminate on CO states not populated at 300 K, i.e., highly excited rotational states.

A linear extrapolation of the data shown in Figure 5 suggests that in the limit of zero pressure, which corresponds to a near nascent CO rotational state distribution, $1-(I_{CGF}/I_o) \cong 0.08$. Thus, the CGF data indicate that the CO photoproduct from the photolysis of ketene at 193 nm is rotationally excited. The degree of rotational excitation expressed in terms of a rotational temperature, T_r, can be calculated in much the same manner as T_v was calculated above. Using equations (4.7)-(4.10), and assuming that the CO rotational state distribution can also be represented by a Boltzmann function, $D_r(T_v=3750\ K)$ in equation (4.7), the rotational temperature can be obtained by iteratively computing $1-(I_{CGF}/I_o)$ as a function of T_r until the simulated value agrees with the value determined by the extrapolation of the data in Figure 5 ($1-(I_{CGF}/I_o)=0.08$) to zero pressure. The results of these computations are shown in Figure 6. The extrapolated CGF attenuation corresponds to a rotational temperature of $T_r=6700\pm1500$ K. Though we have assumed a Boltzmann rotational state distribution for CO in order to characterize the CO

heights were found to be directly proportional to the integrated intensities within the first 5 μs and were a more easily measured value. By fitting the experimentally determined, high pressure attenuation, $1 - (I_{CGF}/I_o) = 0.31$, to that calculated[172] by equations (4.9) and (4.10), the vibrational temperature, T_v, was determined to be 3750 ± 400 K. Using time resolved laser absorption spectroscopy, Lin and coworkers[146] found T_v=4000 K. We used a method similar to Lin's and found T_v=3720 K (see Chapter 5 for procedure). This agreement, in conjunction with the CO vibrational relaxation time we observe via fluorescence decay ($p\tau \cong 48$ torr-μs for CO-argon collisions), provide strong evidence that the vibrational temperature determined in these experiments corresponds to the nascent vibrational population. The method described by Flynn[164] for estimating vibrational temperatures gives a result in good agreement with the value obtained here. Values for T_v using this method can be obtained by,

$$1 - (I_{CGF}/I_o) = [1 - \exp(-h\nu/kT_v)]^2 \qquad (4.11)$$

where $h\nu$ is the CO($0 \leftarrow 1$) vibrational quantum. Using $1-(I_{CGF}/I_o)=0.31$, T_v obtained by this method is approximately 4000 K.

The degree of rotational excitation in the CO photofragment was determined from experiments where low pressures of ketene (approximately 0.10 torr ketene only) were photolyzed. At high fluorescence cell pressures, rotational thermalization occurs within the detector rise time, and the filled CGF cell selectively removes the resulting $v=1 \rightarrow 0$ emission. In this case, the fluorescence must

is the Herman-Wallis factor[168-170] for the $(v,J' \rightarrow v-1,J'')$ transition. The emission intensity transmitted through the CGF of length, l, containing CO gas at 300 K and pressure, p, can be expressed by,

$$I_{CGF}(v,J') = I_o(v,J')10^{-kpl} \qquad (4.8)$$

where k is the population weighted absorption coefficient for the indicated ro-vibrational transition. Values for k were determined by scaling low-resolution absorption coefficients[171] to an empirically determined $P_{1,0}(9)$ high resolution absorption coefficient at 300 K. This high resolution absorption coefficient was determined by using a grating tuned, continuous wave CO laser assembled in our laboratory (see Chapter 5). The intensity of the $P_{1,0}(9)$ line from the CO laser was measured through the CGF cell evacuated and filled with 20 torr of CO gas. The absorption coefficient was then determined for this line and used to scale the low resolution absorption coefficients.

The ratio of the simulated fluorescence intensities (as a function of T_v) detected through a filled and evacuated CGF cell, I_{CGF} and I_o, can be determined by summing equations (4.7) and (4.8) over the appropriate values of v and J',

$$I_{CGF}/I_o = \sum_v \sum_{J'} I_{CGF}(v,J') / \sum_v \sum_{J'} I_o(v,J') \qquad (4.9)$$

The degree of attenuation of the fluorescence signal is then,

$$1 - (I_{CGF}/I_o) \qquad (4.10)$$

In our experiments, the fluorescence intensities were determined from the peak heights in the first 5 μs after the laser pulse. The peak

Table 1. Summary of Observations on CO Photofragment Fluorescence Intensity vs. Ketene Excitation Wavelength

Excitation Wavelength nm	Photon Energy kcal/mol	Absorption Cross Section cm^2	Available Energy kcal/mol	4.7 μm Fluorescence Observed
193	148	5×10^{-19}	63	Yes
249	115	2×10^{-21}	30	No
308	93	3×10^{-20}	8	No

product's vibration to yield any fluorescence (for CO(v=1)=6.1 kcal/mol) at 4.7 μm. Thus no CO fluorescence is anticipated from ketene photolysis at 308 nm. The high upper limit for CO fluorescence at 249 nm is due to the low absorption coefficient of ketene at this wavelength. Table 1 contains a summary of the relevant data.

The cold gas filter studies described above[164] provide a means by which the vibrational distribution of the CO photoproduct can be characterized in terms of a vibrational temperature, T_v, assuming a Boltzmann distribution of the vibrational states and a rotational distribution of 300 K. The CGF functions by selectively quenching the emissions from transitions which terminate on ro-vibrational states that are thermally populated. At 300 K, only the ground vibrational state of the CO in the CGF cell is appreciably populated. Essentially, then, it is an ideal filter for the removal of $v=1 \rightarrow 0$ fluorescence of rotationally thermalized molecules since the absorption band matches line for line with the emission frequencies.

To determine T_v, the CO fluorescence spectral distribution as a function of T_v is expressed as,

$$I_o(v,J') = I_0 D_v(T_v) D_r(T_v,T_r) A_v F_v(J',J'') \qquad (4.7)$$

where $I_o(v,J')$ is the fluorescence intensity originating from the indicated ro-vibrational state, I_o is the total fluorescence intensity, $D_v(T_v)$ is the Boltzmann distribution at vibrational temperature, T_v, $D_r(T_v,T_r)$ is the corresponding Boltzmann rotational state distribution (here, we assume T_r=300 K), A_v is the Einstein coefficient for spontaneous emission[167] from state, v, and $F_v(J',J'')$

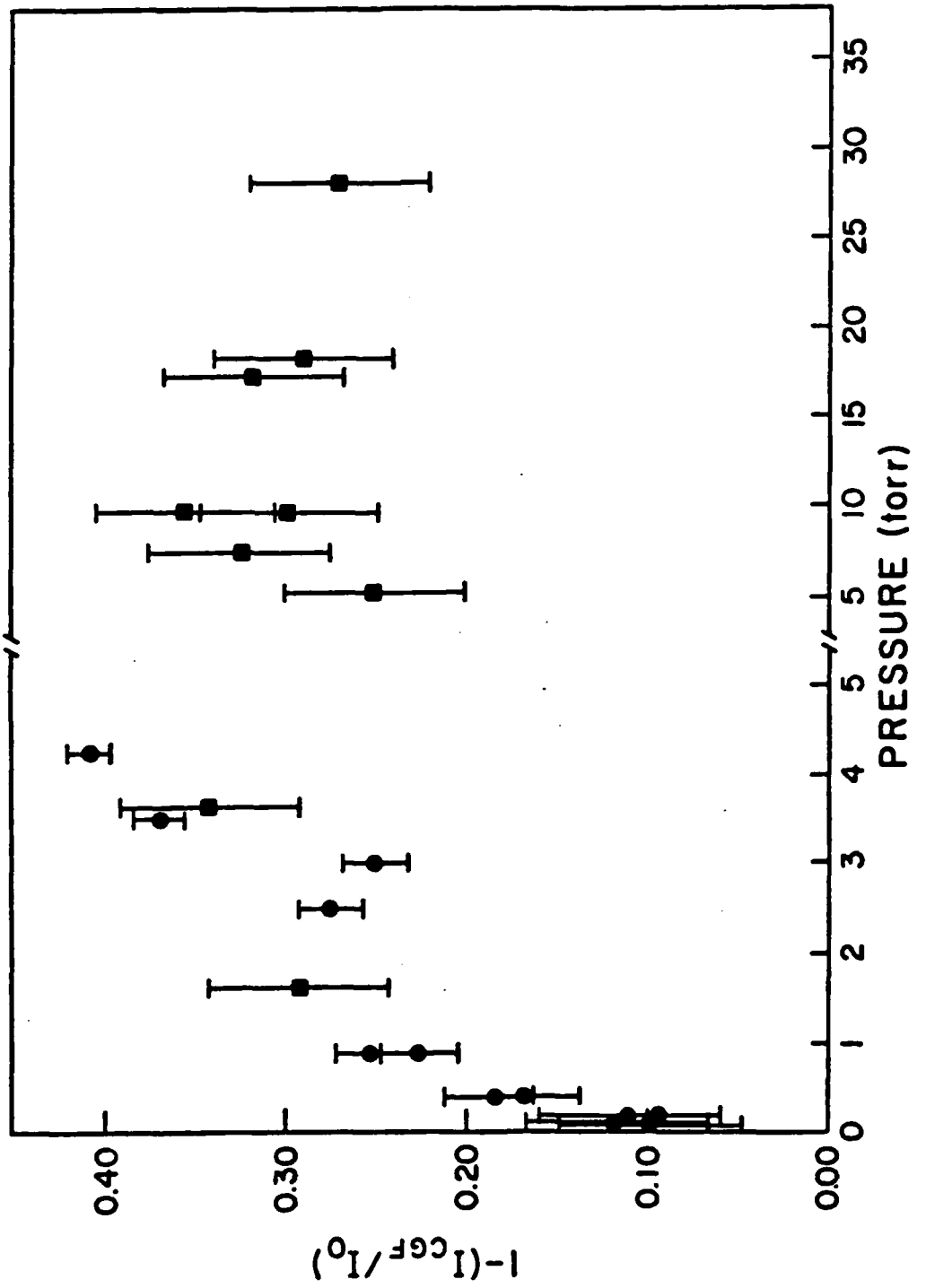
0.40
0.30
0.20
0.10
0.00
1-(I_CGF/I_O)
0
1
2
3
4
5
10
15
20
25
30
35
PRESSURE (torr)

Figure 5

Figure 5. Attenuation of 4.7 μm fluorescence by a CGF containing approximately 20 torr of CO as a function of total pressure: (●) pure ketene; (□) 0.16 torr ketene in argon.

Flynn et al.[164] have described a procedure by which the extent of vibrational excitation, i.e., the vibrational temperature (assuming a Boltzmann distribution of the vibrational states), can be estimated. To use this procedure, the degree of attenuation of the fluorescence resulting from the CGF evacuated and filled with CO must be known. When relatively high sample pressures are used in the fluorescence cell, e.g., 0.16 torr ketene in 20 torr of argon, the ir fluorescence intensity (intensity within the first 5 μs following the laser pulse) was attenuated by approximately 31% when 20 torr of CO was introduced into the CGF cell. When low pressures were used, e.g., 0.1 torr ketene neat, the filled CGF attenuated the fluorescence only approximately 10%. Figure 5 shows the relative attenuation with varying sample pressures.

Discussion

The lack of detectable CO photofragment fluorescence at 249 and 308 nm suggests that at 249 nm, less that 30% of the CO product fluoresces at 4.7 μm while at 308 nm, less that 6% of the CO product fluoresces at 4.7 μm. These values were determined based on the detection sensitivity of our system, ketene pressure, laser fluence, the volume subtended by the detector field-of-view, absorption coefficient of ketene at each irradiation wavelength[165], and the CO quantum yields at each wavelength[138,139]. Assuming that methylene is formed in its $\tilde{a}^1A_1$ state, the threshold for dissociation has been determined to be approximately 85 kcal/mol[145,149,150,166]. At 308 nm, almost all of the available energy must be partitioned to the CO

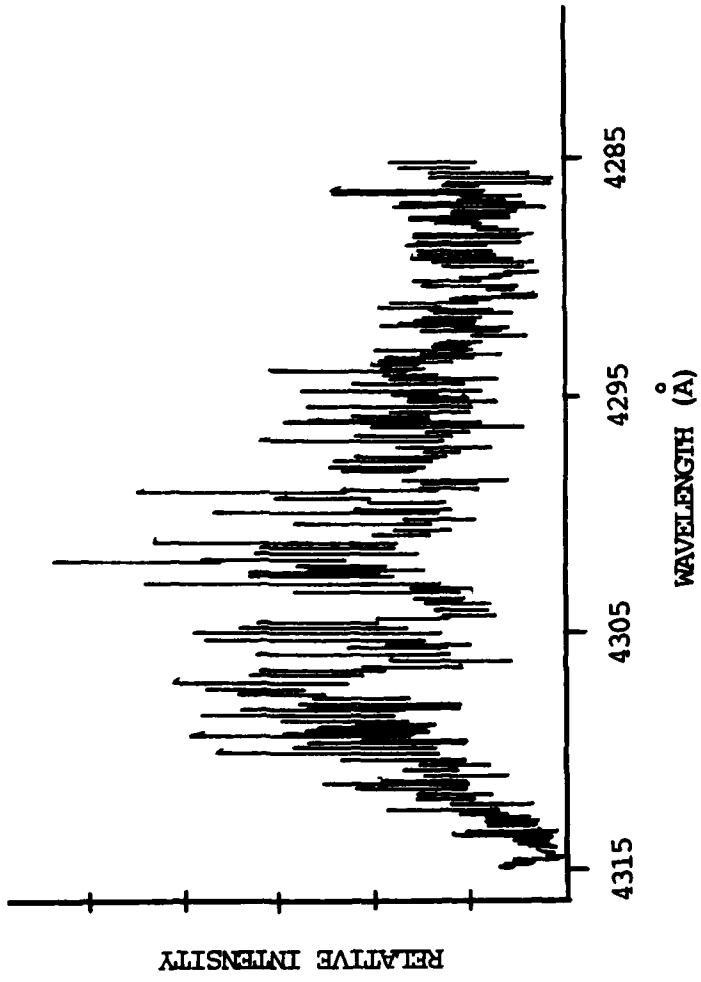

Figure 4

Figure 4. Spectrum of the visible emission in the 4315-4295 Å region corresponding to the $CH(\tilde{X}^2\pi \leftarrow \tilde{A}^2\Delta)$ from the photodissociation of ketene at 193 nm (4 mJ/cm^2).

CHAPTER 5

THE PHOTOCHEMISTRY OF 3-CYCLOPENTENONE, 3,5-CYCLOHEPTADIENONE, AND TROPONE

Introduction

Photodecarbonylation studies by Eastman et al.[131,174] showed that the photolysis rate of thujone (XIII) was 15-30 fold greater than cyclopentanone (XIV) and cyclohexanone (XV). The greater rate was ascribed to the presence of the cyclopropane ring in thujone.

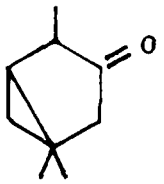

XIII

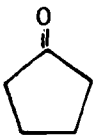

XIV

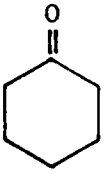

XV

As noted in Chapter 3, structural features facilitating decarbonylation were found to be a suitably located cyclopropane ring, β,γ-unsaturation, and α-alkyl substitution.[128,131] The facilitation of decarbonylation of 3-cyclopentenone was thus predicted.[174] An early study[134] of the photochemistry of 3-cyclopentenone in the gas phase indicated that at 313 nm, the molecule decomposes to yield only CO and 1,3-butadiene (equation (5.1)),

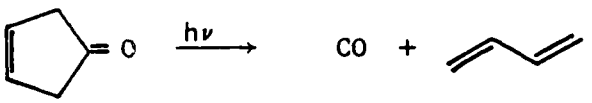

(5.1)

The quantum efficiency for the formation of these products was near unity, and was constant over the temperature range 60-190 °C. No evidence was obtained indicating the formation of a biradical intermediate and the possibility of a concerted process was suggested. Similar products were obtained from the triplet sensitized photolysis[175] and the pyrolysis[176] of 3-cyclopentenone in the gas phase. The reaction was found to be first order with an Arrhenius activation energy of 51.2 kcal/mol[176]. A biradical mechanism (equation (5.2)) should have an activation energy of approximately 60.5 kcal/mol, resulting from the initial cleavage of the C-C bond.

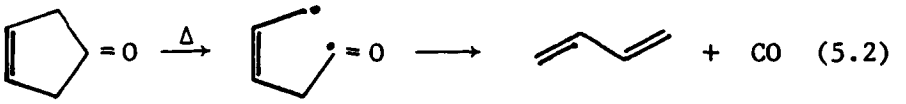

(5.2)

The authors concluded that the reaction must be concerted.[176] The observed entropy of activation obtained from the A-factor for the decomposition also supports a concerted process.[176] Similar conclusions have been reached in photodecarbonylation studies of stereochemically labeled 3-cyclopentenones.[177]

In the triplet sensitized ($Hg(^3P_1)$) photodecomposition of 3-cyclopentenone,[175] addition of NO did not change the ratio of the quantum yield of CO to butadiene. It was concluded that CO and butadiene were produced via a common intermediate and no radical species contributed to their production. In the reaction of atomic oxygen with cyclopentadiene,[178] a vibrationally excited ground state 3-cyclopentenone was assumed to be formed which decomposed to CO and

butadiene. Comparison of this data with the results of Hess and Pitts[134] led the authors to conclude that decomposition following these two excitation processes was not collisionally quenched under the stated experimental conditions.

In their study of dienes generated from 3-pyrrolines by treatment with nitrohydroxyl amine (equation (5.3)), Lemal and McGregor[179] noted that the reactions occurred with complete stereospecificity. These fragmentations were found to occur in a sigmasymmetric fashion. The decomposition of XVI was expected to

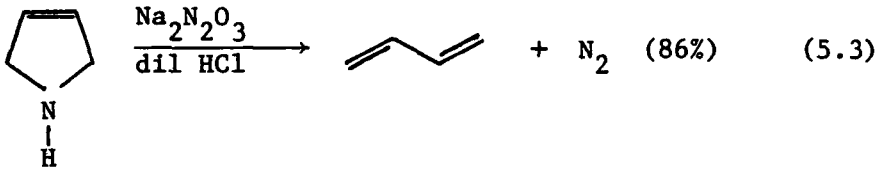

(5.3)

occur axisymmetrically. 3,5-Cycloheptadienone (XVII) was predicted to decarbonylate in the same manner as XVI.[179]

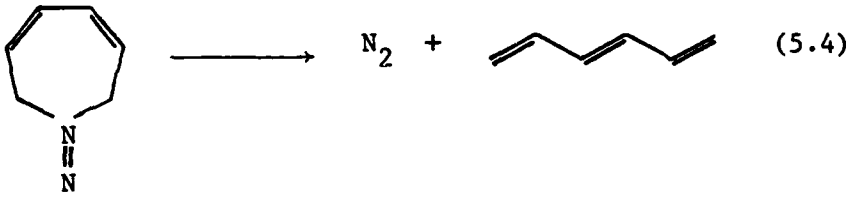

XVI

(5.4)

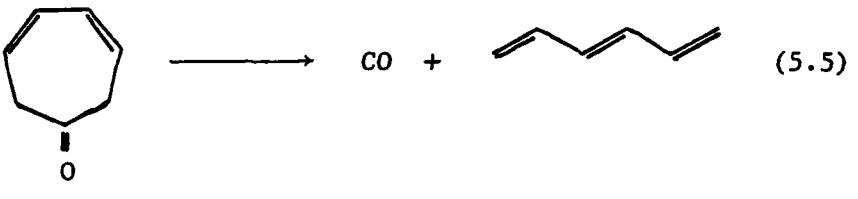

XVII

(5.5)

Irradiation of 3,5-cycloheptadienone in ether at 246, 256, and 266 nm gave carbon monoxide and an isomeric mixture of 1,3,5-hexatrienes

while in a similar fashion, the irradiation of 2-methyl-3,5-cyclo-heptadienone in ether at 252, 261, and 271 nm gave CO and a mixture of isomeric 1,3,5-heptatrienes.[180,181] Triplet sensitized photolysis of 3,5-cycloheptadienone did not yield the same products as in the direct photolysis, but instead XVIII.[182,183] If the decarbonylation can be rationalized in terms of a concerted expulsion of CO from a singlet state, then in the production of XVIII, the 2-fold axis of symmetry is lost when the spin unpaired triplet state is generated. Concerted fragmentation is forbidden by orbital symmetry considerations and the alternate pathway leading to XVIII is followed.[182] Triplet states do not play a significant role in the chemistry of 3,5-cycloheptadienone induced by direct photoexcitation.

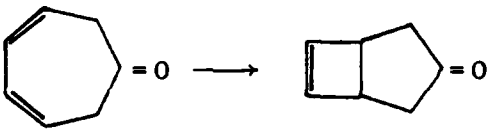

XVIII

The decarbonylation of cis- and trans-2,7-dimethyl-3,5-cyclo-heptadienone at 313 nm showed that the stereospecific reaction occurs with conrotation.[184] A linear thermal cheletropic elimination is predicted to occur by an axisymmetric conrotation[179] while a non-linear cheletropic fragmentation with disrotation is also thermally allowed. Extrusion of SO_2 from stereoisomeric sulfones analogous to these ketones was shown to occur by the axisymmetric conrotatory path.[185] Though diradical formation by α-cleavage,

followed by loss of CO in the second step, may be operative in molecules similar to 3,5-cycloheptadienone, concerted elimination pathways are still favored.[186] The photofragmentation of 3,5-cycloheptadienone in solution was found by Schuster and co-workers[183] to occur via the lowest excited singlet state. If a higher excited singlet state, S_2, was prepared by irradiation with $\lambda < 300$ nm, rapid radiationless transition occurred prior to dissociation. Using semiempirical electronic structures methods, the nature of the excited states were investigated.[183] All excited singlet states accessible by uv photoexcitation were characterized by varying degrees of interactions between the diene and carbonyl chromophores, i.e., zeroth order (n, π^*) and (π, π^*) states are mixed.

Thermochemical considerations dictate that the products from the photofragmentation of 3,5-cycloheptadienone for $\lambda \geq 240$ nm must be formed in their ground electronic states. If it is assumed that at 193 nm, ground electronic state products are formed from 3,5-cycloheptadienone, then the photoactive singlet, S_1, must undergo radiationless transition to the ground electronic state prior to dissociation. These transitions are facilitated when the vertical energy difference between the two coupled potential surfaces is minimized.[187] The favored geometry under these conditions is most likely at an energy maximum on the ground state surface, i.e., the transition state.

Photolysis and pyrolysis studies of the decarbonylation of tropone and detailed analysis of the transformation of tropone and tropolones leading to benzenoid compounds have been made.[188-190]

Irradiation of ethereal solutions of tropone through Pyrex by a mercury lamp yielded photodimers.[191] Tropone photodimerization has been suggested to occur through a triplet intermediate.[192,193] Different dimers have been observed in acidic versus neutral media.[194] Mukai has suggested that the pyrolytic decarbonylation of tropone proceeds via a norcaradienone intermediate rather than a biradical resulting from α-cleavage (path G below).[188]

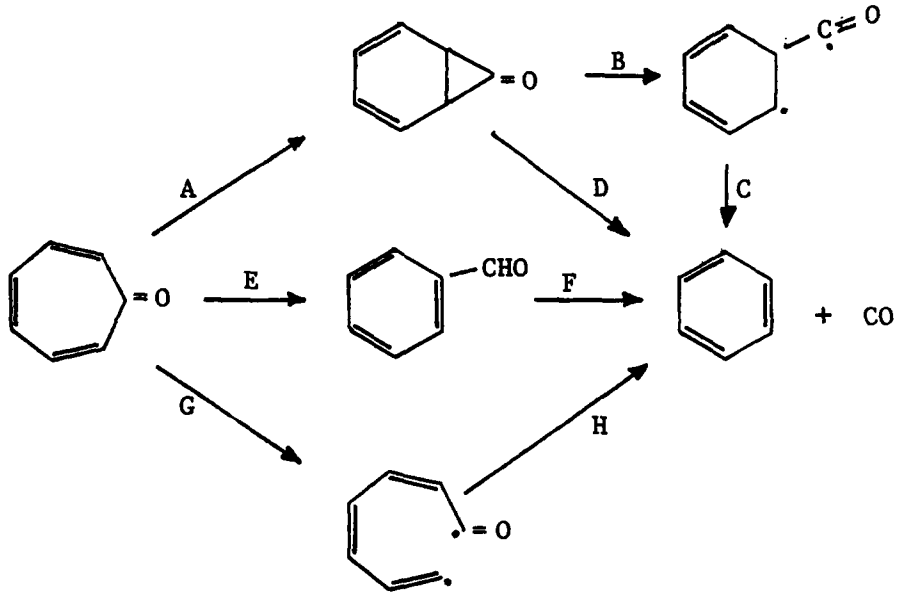

The low activation energy (54.1 kcal/mol) for this reaction relative to the total energy necessary for C-C bond fission and the small entropy of activation (1.2 e.u.) for the reaction suggests that path G is not likely to be followed.[188] Decarbonylation can occur via paths B, C, D, or F. Path F can be ruled out since benzene was not observed as a pyrolysis product of benzaldehyde[188] though the photolysis of benzaldehyde at 276 nm has yielded benzene.[196] Also, benzaldehyde has

not been observed as a pyrolysis product of tropone.[190] Failure to detect bibenzyl as a product indicates that path D is preferred over path B, though path B cannot be excluded if decarbonylation occurs rapidly from the biradical.

The results of the photolysis of tropone in the gas phase also suggest that decarbonylation occurs via the norcaradienone intermediate.[189] The decarbonylation yield was found to be 30% as compared to the 1% found from photolysis in solution. The addition of CO resulted in a decrease in the decarbonylation yield. The authors[189] concluded that the photoexcited tropone molecule converts via internal conversion to the vibrationally excited ground state which then decarbonylates through the norcaradienone intermediate.

Though norcaradienone has never been observed, sufficient evidence exists to give its formation serious consideration. In addition to the activation energy and entropy arguments above, studies of cycloheptatriene suggest the formation of the metastable intermediate in equilibrium with cycloheptatriene.[196] Norcaradiene derivatives were found to exist at room temperature[197] and Diels-Alder reaction of cycloheptatriene yielded products which could only be derived from a norcaradiene intermediate.[198]

For each of these three molecules (3-cyclopentenone, 3,5-cycloheptadienone, and tropone), it has been suggested that dissociation proceeds without intervention of any biradical intermediate. Since, during the course of these reactions, the C-O bond length changes appreciably, the CO product vibrational energy distribution may serve as a useful probe of the dissociation dynamics.[136] The distribution

of available energy among the products' various degrees of freedom can yield information on transition state structure and the interaction of separating products.[3] In the following study, energy partitioning to the carbon monoxide product is probed using time-resolved laser absorption spectroscopy for several photoactivation wavelengths. The CO laser absorption method used here has been employed by other workers in studies of photodissociation dynamics.[74,76]

Preparation of 3-Cyclopentenone

The starting material for the preparation of 3-cyclopentenone, cyclopentadiene, was obtained by doubly distilling dicyclopentadiene at 40 °C through a 45 cm Vigreux column. Cyclopentadiene was trapped and stored at 197 K until use. Using the method described by Korach, et al.,[199] 3,4-epoxycyclopentene was prepared by the reaction of cyclopentadiene (45 ml) with peracetic acid (40%, 70 ml) in methylene chloride (400 ml) and sodium carbonate (85 g). The peracetic acid was initially treated with sodium acetate (1 g) to neutralize the sulfuric acid, and the peracetic acid was then filtered. Maintaining the mixture of cyclopentadiene, sodium carbonate, and methylene chloride at 20 °C, the peracetic acid was added dropwise over a 30 min period while vigorously stirring. Upon completion of the peracetic acid addition, the mixture was stirred for an additional hour at 20 °C. The mixture was filtered and the solids in the filter washed three times with 40 ml portions of methylene chloride. The bulk of the methylene chloride was removed by atmospheric distillation at 40 °C. 3,4-epoxycyclopentene was collected at 93 mm Hg and 56-59 °C. NMR and

IR spectra of the product matched those found in literature for 3,4-epoxycyclopentene. Slight contamination from the isomerization[200] of the epoxide to the aldehyde was detected.

3-Cyclopentenone was prepared from 3,4-epoxycyclopentene using tetrakis(triphenylphosphine)palladium(0), $Pd(PPh_3)_4$.[201] The reactivity of $Pd(PPh_3)_4$ required handling under an inert atmosphere (Ar). The epoxide (12 g) was added dropwise over a 12 min period to a stirred mixture of methylene chloride (75 ml) and $Pd(PPh_3)_4$ (20 µg) immersed in an ice bath. The mixture was stirred for two hours until heat evolution had ceased. Methylene chloride was removed by flash distillation and the 3-cyclopentenone product collected at 100 mm Hg and 61-63 °C. NMR and IR results indicated that the 3-cyclopentenone was prepared with only minute impurities.

Preparation of 3,5-Cycloheptadienone

Reduction of tropone by lithium aluminum hydride gives 3,5-cycloheptadienone in good yield.[202] To a rapidly stirred mixture of 2.7 g of lithium aluminum hydride and 380 ml of anhydrous ether was added 16 ml of tropone dropwise over 40 min. The mixture was stirred at room temperature for 30 min after the tropone addition. While stirring continued, 46 ml of ethyl formate in 275 ml of anhydrous ether was added dropwise to the reaction flask cooled in an ice bath. The mixture was stirred for an additional 30 min. Water (5.4 ml) and 10% sodium hydroxide (4.3 ml) were added successively at a 10 min interval until the precipitate became granular. The mixture was filtered and the residue washed three times with 50 ml portions of

ether. The solution was dried over anhydrous magnesium sulfate overnight. After filtering, the ether was removed by vacuum distillation and the 3,5-cycloheptadienone product obtained at 1 mm Hg and 68-73 °C. The NMR and IR spectra showed trace contamination by 3,5-cycloheptadienol.

Preparation of Tropone

Tropone was prepared using the procedure of Radlick[203] with the modifications suggested by Takakis and Agosta.[204] To a 1 l flask containing a stirred mixture of potassium dihydrogen phosphate (13.5 g), water (33 ml), cycloheptatriene (49 ml), and spectral grade 1,4-dioxane (360 ml) was added selenium dioxide (47.6 g). The mixture was refluxed for 21 hr at 90 °C using a Vigreux column. After cooling, 300 ml of water was added and the products extracted with four 150 ml portions of methylene chloride. The organic layer was washed three times with 150 ml portions of 10% sodium bicarbonate and dried overnight over anhydrous magnesium sulfate. After filtering, the methylene chloride was removed by flash distillation and tropone was distilled at 5 mm Hg and 80-85 °C. NMR analysis indicated only slight contamination by dioxane.

Experimental Procedure

The instrumentation employed for the CO laser absorption spectroscopy is illustrated in Figure 7. 3-Cyclopentenone, 3,5-cycloheptadienone, and tropone were flowed slowly through a 13 or 100 cm cell either neat at 0.05-.5 torr or diluted in argon. Reactant

Figure 7. Diagram of experimental apparatus for the CO laser absorption studies. G, diffraction grating; I, iris; PZT, output coupler mounted on piezoelectric translator; D_1, PbSe detector; A, amplifiers and preamplifier; ND, neutral density filters; M, mirrors; DBS, dichroic beam splitter; PD, fast photodiode; F, infrared filters; D_2, InSb detector.

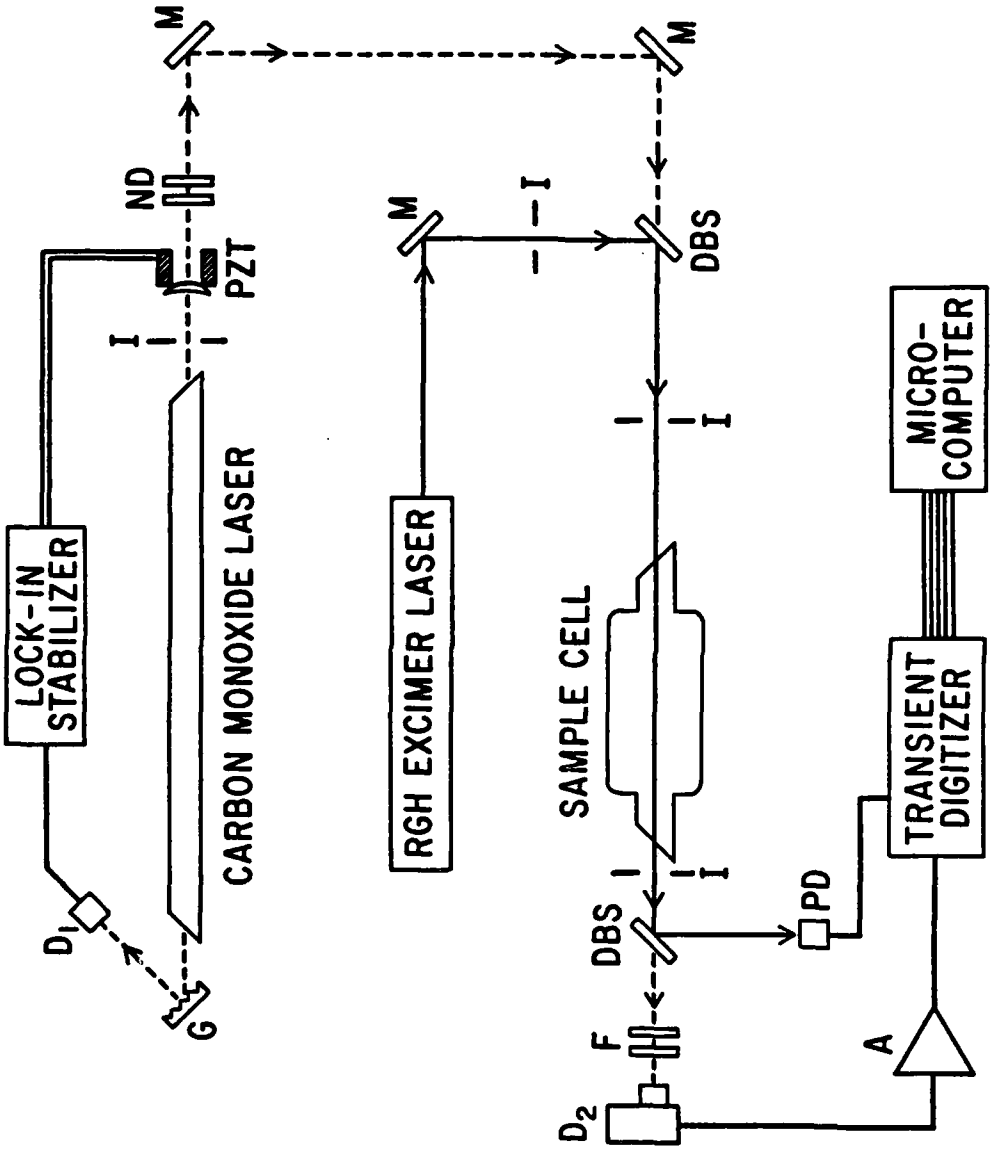
M
ND
PZT
I
I
I
LOCK-IN STABILIZER
CARBON MONOXIDE LASER
D1
G
M
I
DBS
RGH EXCIMER LASER
SAMPLE CELL
I
I
I
DBS
PD
F
D2
A
TRANSIENT DIGITIZER
MICRO-COMPUTER

Figure 7

pressure and cell length were selected to ensure that a "thin target" approximation was valid. The reactant flow rate was regulated such that the signal intensity did not change with increasing flow rates. The absorption cells were equipped with calcium fluoride windows mounted at Brewster's angels. The ketones were photoactivated with the excimer laser (Lambda Physik Model EMG 101) described in Chapter 4. The excimer pulse rate was maintained at approximately 2 Hz at fluences typically 1-5 mJ/cm^2.

The TEM_{00} output of a grating tuned, continuous wave (cw) CO laser was coprogagated through the absorption cell coaxially with respect to the excimer laser. Care was taken to ensure that the CO laser beam was well within the excimer pulse diameter. The CO laser was designed to optimize output on the $1 \rightarrow 0$ vibrational transition where 5-8 mW could be routinely obtained. Djeu[205] has previously described the construction and operation of a similar laser. Appreciably more power (up to 40 mW) was obtained when the laser was tuned to other vibrational transitions. The CO laser intensity transmitted through the cell was monitored with a 2-mm diameter InSb detector. CO formed in the absorption cell via the photodissociation of one of the cyclic ketones produces a transient decrease in the CO laser intensity reaching the detector. The corresponding detector signal was amplified and then digitized using a Biomation 8100 Signal Digitizer. The digitized signal was accumulated in a Commodore 8032 microcomputer for signal averaging. Typically, 300-500 transient signals were averaged. The detection system rise time was approximately 80 ns. CO laser power and excimer laser energy were

measured with a Scientech 36-0000l power/energy meter, and sample pressure in the cell was measured with a Baratron capacitance manometer. The CO product vibrational distributions were determined by recording absorption curves with successive CO laser vibrational transitions until no further absorption could be detected. Initial CO laser intensities ($I_{\emptyset}$) were measured under the same conditions as the absorption curves with the exception that the excimer laser beam was totally blocked. A beam chopper was used to obtain the full, unattenuated amplitude of the $I_{\emptyset}$ signal, from which the degree of signal absorption was determined. The absorption curves were normalized and the relative population at each vibrational state determined. Calibration of the CO laser grating drive was made using a 0.6 m monochromator to determine the laser wavelengths.

The ketones at pressures, between 0.5-2.0 torr, were photolyzed with several thousand laser pulses at 193,249, and 308 nm. In each case, the products were collected and analyzed by NMR and IR spectroscopic methods.

Analysis of Data

The photodissociation of 3-cyclopentenone, 3,5-cycloheptadienone, and tropone results in the formation of carbon monoxide in some distribution of ro-vibrational states, {CO(v,J)}. Detection by CO laser absorption spectroscopy occurs when CO in state (v,J) resonantly absorbs the laser $P_{v+1,v}(J)$ line. Transient absorption curves were obtained by using laser lines corresponding to v=0 to v=v_m where $v_m \leq 4$ for 3-cyclopentenone, v_m=3 for 3,5-cycloheptadienone, and v_m=1 for

AD-A158 845 THE DYNAMICS OF THE PHOTOFRAGMENTATION OF KETENE 2/2
3-CYCLOPENTENONE 35-CYCLOHEPTADIENONE AND TROPONE(U)
AIR FORCE INST OF TECH WRIGHT-PATTERSON AFB OH
UNCLASSIFIED B I SONOBE 1985 AFIT/CI/NR-85-90D F/G 7/3 NL

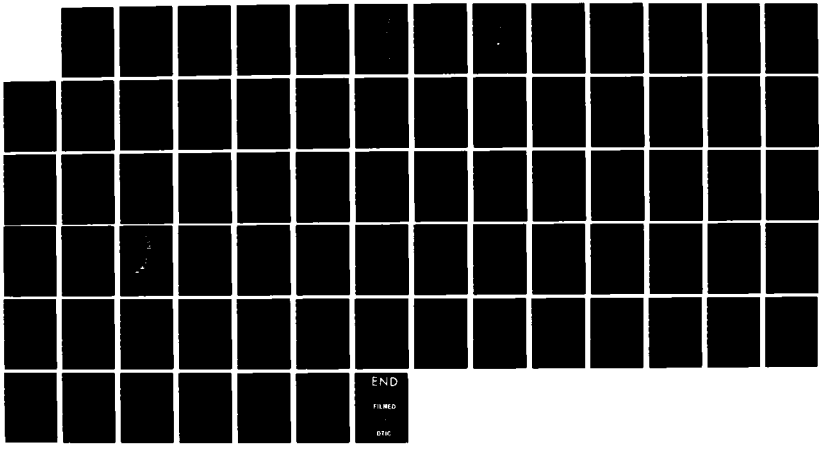

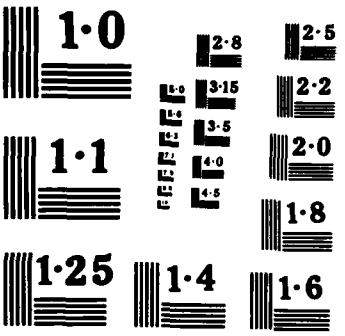

NATIONAL BUREAU OF STANDARDS
MICROCOPY RESOLUTION TEST CHART

tropone. No absorption was observed for $v > v_m$ for each reactant molecule. Typical absorption curves are shown in Figures 8-1Ø. The initial or rising portion of the curve provides information on the net rate of formation of CO(v,J), while the decaying portion of the curve is determined by the net relaxation rate of CO(v,J). The relative population of CO(v), N_v, can be determined from the maximum absorption amplitude as long as neglible relaxation has occurred at the time measurement is made of the maximum amplitude. In all of the cases discussed here, the absorption rise times were at least ten times faster than the corresponding decay times. Under these conditions, the maximum absorption amplitudes provide a good measure of the nascent CO population in vibrational state v, N_v, from the absorption of the $P_{v+1,v}(J)$ laser line. The relationship derived by Houston and Moore[74],

$$N_v \propto \sum_{i=v}^{v_m} \left(\frac{2J+1}{2J-1}\right)^i \frac{S_{i+1}}{i+1} \qquad (5.8)$$

is used to find N_v. Here, S_{i+1} is the signal amplitude. In our experiments, v_m is determined by the signal-to-noise ratio (rather than thermochemistry) which in turn is determined primarily by the amplitude stability of the CO and excimer lasers.

Results[206]

At all photolysis wavelengths, the effect of a buffer gas, argon, was investigated and with 3-cyclopentenone and 3,5-cycloheptadienone,

Figure 8. CO transient absorption curve obtained upon the photolysis of 0.5 torr of 3-cyclopentenone at 249 nm. The $P_{1,0}(9)$ CO laser transition was used as a probe. The reported curve was obtained by averaging 300 KrF* pulses.

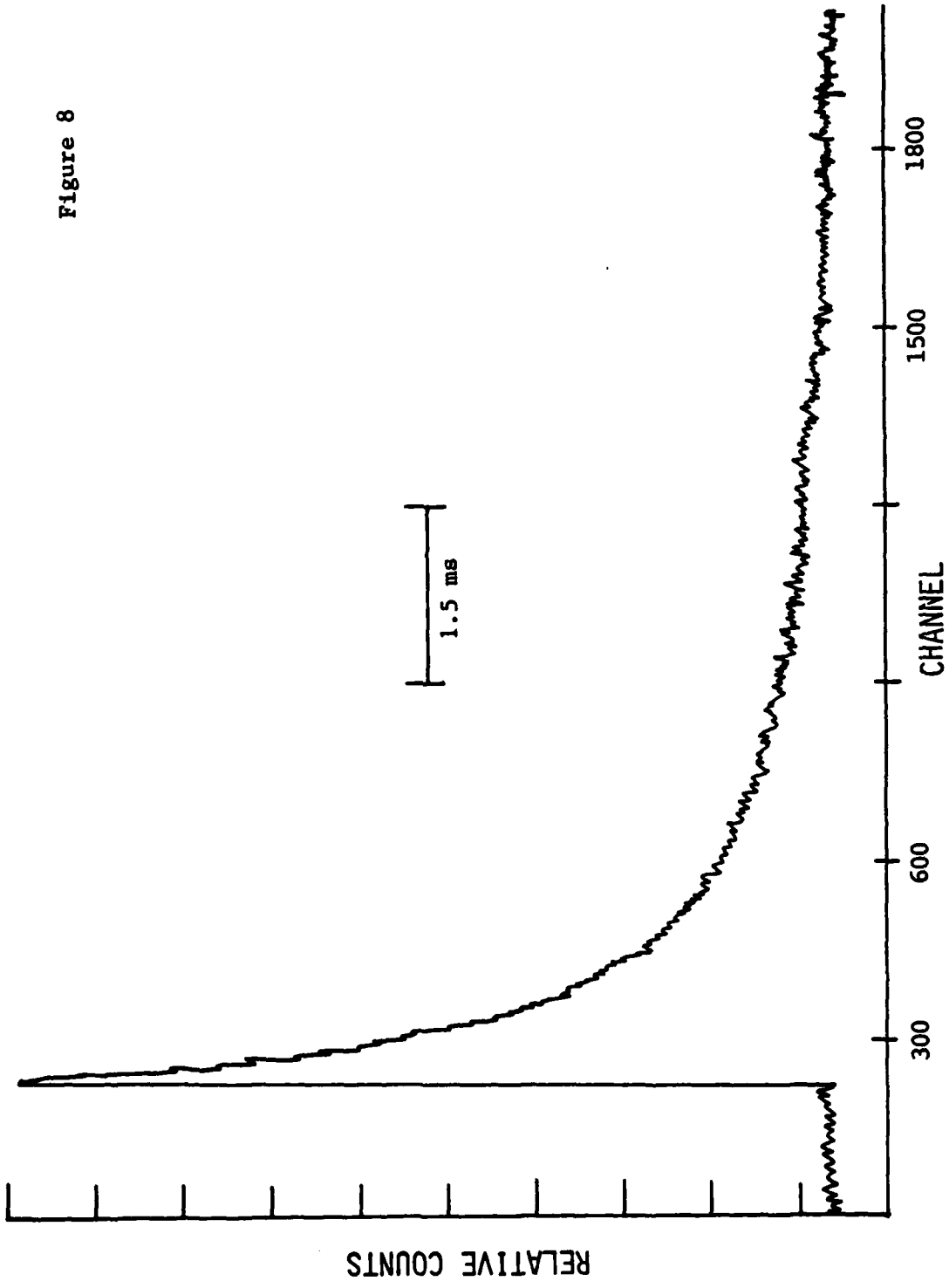

Figure 8

Figure 9. CO transient absorption curve obtained upon the photolysis of 0.5 torr of 3-cyclopentenone at 249 nm. The $P_{2,1}(9)$ CO laser transition was used as a probe. The reported curve was obtained by averaging 500 KrF* pulses.

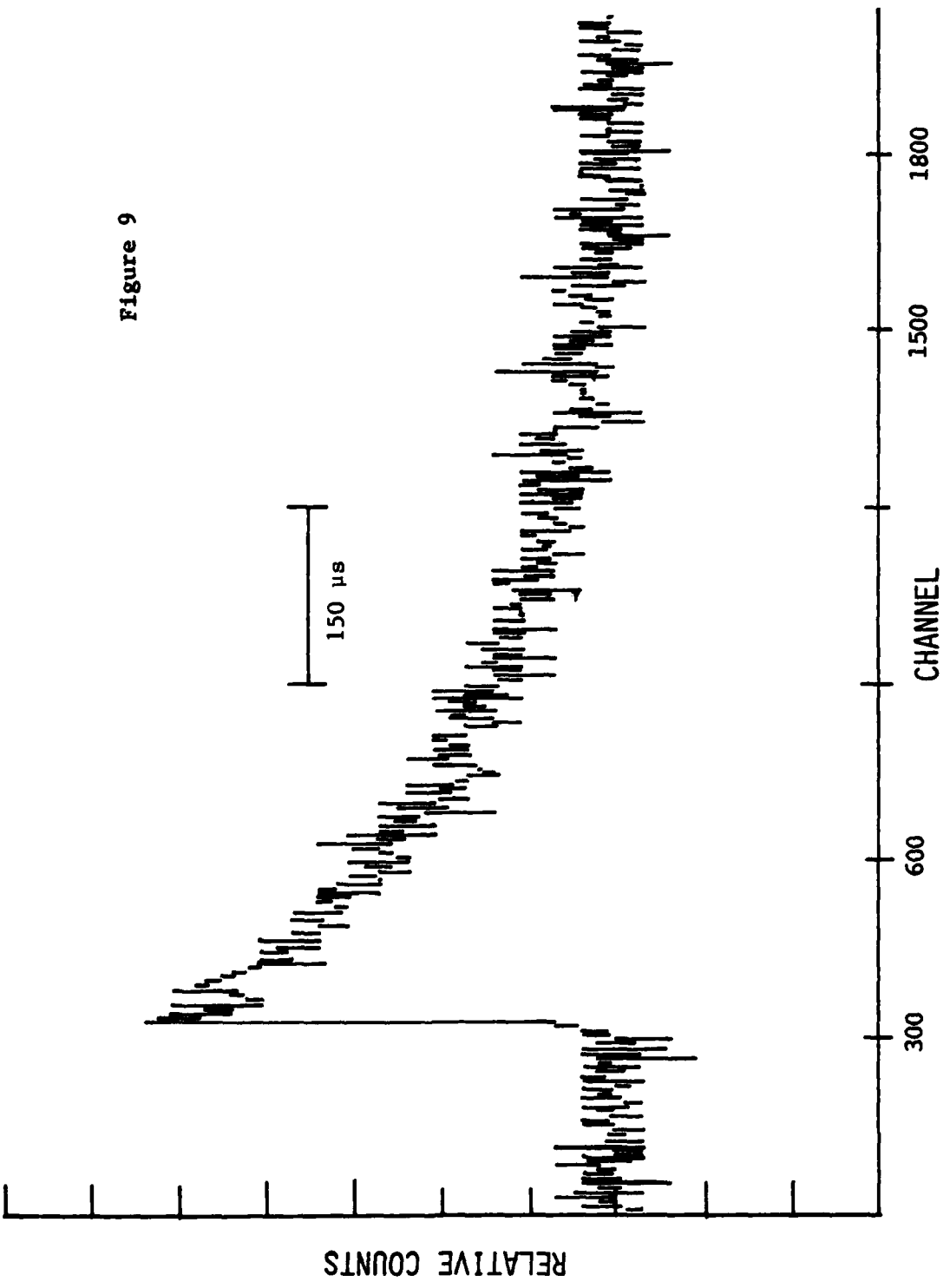

Figure 9

Figure 10. CO transient absorption curve obtained upon the photolysis of 0.5 torr of 3-cyclopentenone at 249 nm. The $P_{3,2}(10)$ CO laser transition was used as a probe. The reported curve was obtained by averaging 500 KrF* pulses.

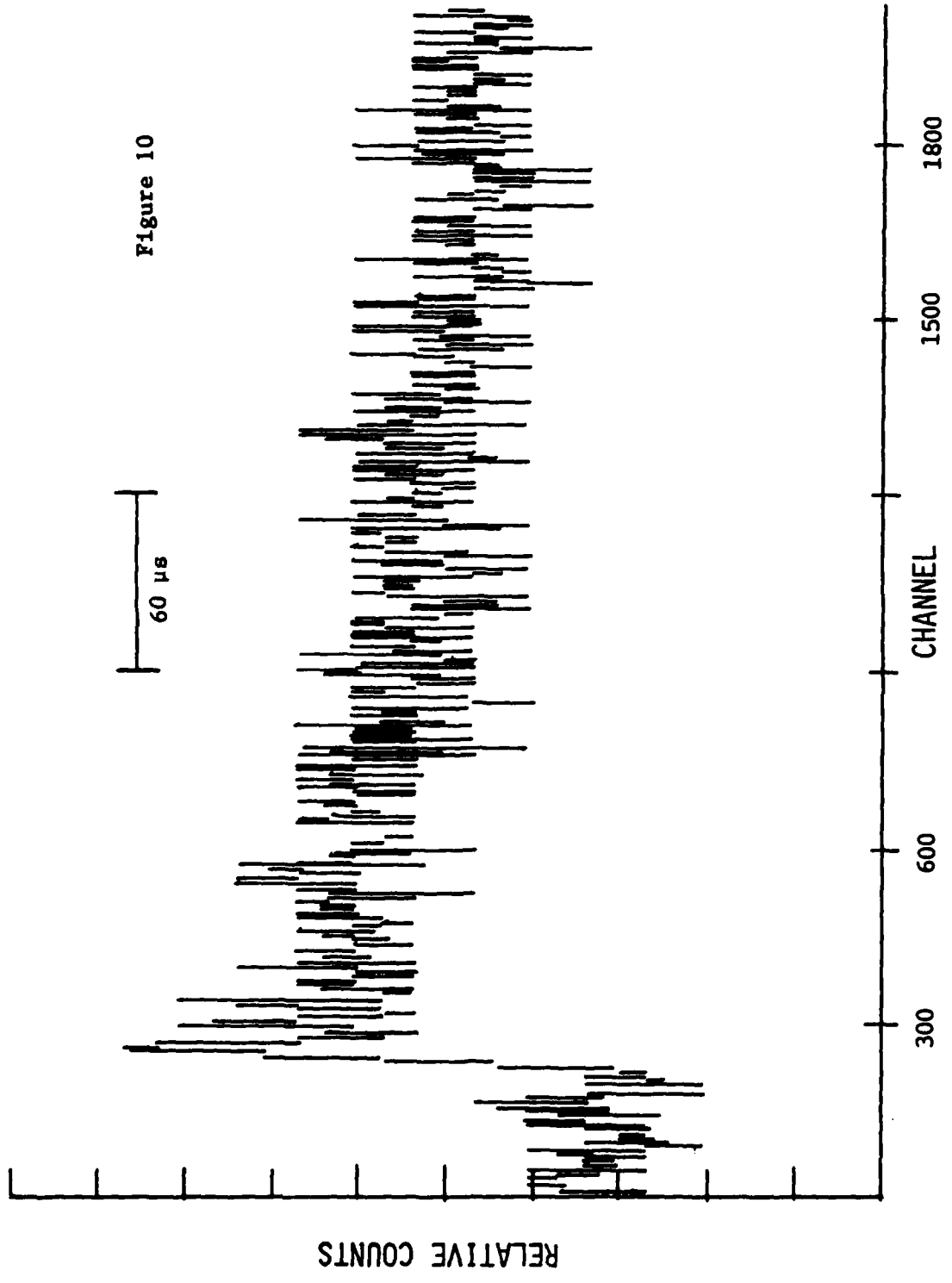

Figure 10

argon was found to decrease the absorption rise times and absorption decay times. The effect of uv laser intensity on CO laser absorption amplitude was also investigated at each photolysis wavelength. With the exception of tropone at 193 nm, the absorption amplitude was found to vary linearly with uv laser intensity indicating that CO is formed via a single photon absorption in our experiments. The nascent vibrational distributions of CO for each compound at the various wavelengths are presented in Table 2 and the corresponding vibrational temperatures are listed in Table 3.

Thermal lensing effects were observed in these experiments on an approximately 100 μs time scale at higher sample pressures. These lensing signals were easily differentiated from true absorption signals by their temporal behavior and by the observation that their amplitudes were independent of the CO laser line used. Thermal lensing could be observed by using CO laser lines, $P_{v+1,v}(J)$, for which $v > v_m$. These effects were neglible at low sample pressures, and all quantitative work was done under low-pressure conditions.

The collected products from the irradiation of 3-cyclopentenone at 193, 249, and 308 nm were identified by gas phase ir spectroscopy. The only products observed were carbon monoxide and 1,3-butadiene. Similarly, the products from the irradiation of 3,5-cycloheptadienone and tropone at these three wavelengths were found by conventional nmr and ir methods to be carbon monoxide and 1,3,5-hexatriene and carbon monoxide and benzene, respectively.

Table 2. Nascent CO Vibrational Distributions.

Wavelength	Nascent Vibrational Distributions		
	3-Cyclopentenone	3,5-Cycloheptadienone	Tropone
193 nm	$N_0 = 1.00$ $N_1 = 0.30$ $N_2 = 0.11$ $N_3 = 0.04$ $N_4 = 0.01$	$N_0 = 1.00$ $N_1 = 0.33$ $N_2 = 0.09$	Two Photon Process
249 nm	$N_0 = 1.00$ $N_1 = 0.24$ $N_2 = 0.03$	$N_0 = 1.00$ $N_1 = 0.24$ $N_2 = 0.04$	$N_0 = 1.00$ $N_1 = 0.19$
308 nm	$N_0 = 1.00$ $N_1 = 0.02$	$N_0 = 1.00$ $N_1 = 0.14$ $N_2 = 0.02$	$N_0 = 1.00$ $N_1 = 0.10$

Table 3. Vibrational Temperatures from Vibrational Distributions.

	Vibrational Temperatures		
Wavelength	3-Cyclopentenone	3,5-Cycloheptadienone	Tropone
193 nm	2900 K	2600 K	-
249 nm	1800 K	2000 K	1850 K
308 nm	640 K	1600 K	1360 K

Discussion

If the photofragmentation of 3-cyclopentenone occurs with spin conservation, insufficient energy is available for formation of electronically excited products (CO and butadiene) for $\lambda \geq$ 200 nm. Correlation diagrams indicate that ground electronic state products can only be formed adiabatically from the ground electronic state of 3-cyclopentenone. Thus, it can be concluded that nonradiative decay to the ground state potential surface occurs prior to product formation in our experiments where $\lambda \geq$ 193 nm. From our data, the geometry at which radiationless transition occurs cannot be determined. Nonradiative processes may be particularly facile in polyatomic molecules where low-frequency torsional and/or bending modes can serve to dramatically increase ro-vibrational state densities.[208] Thus, it is reasonable to regard the dissociation of 3-cyclopentenone in analogy to a chemically activated unimolecular process. In this context, variation of the photoexcitation wavelength is equivalent to a concomitant variation in reactant internal energy.

The pressure dependent rise times of the transient absorption curves, e.g., Figures 8-10, indicate that the nascent CO formed by the photodissociation of 3-cyclopentenone is rotationally excited to some extent, i.e., its rotational temperature is greater than 300 K. A qualitative indication of the extent of rotational excitation can be determined. For all excitation wavelengths, the absorption rise times are pressure dependent with $p\tau$ of approximately 3×10^{-7} torr-s. If the CO product was formed in a thermalized (300 K) distribution of

rotational states, the absorption rise time would be detector limited $\leq 1 \times 10^{-7}$ s, independent of pressure. Assuming a Boltzmann distribution of product rotational states, the CO formed by the photofragmentation of 3-cyclopentenone has a rotational temperature, T_r, greater than 300 K. From the ketene work at 193 nm discussed earlier, we found that for $T_r \geq 6700$ K by fluorescence spectroscopy, the corresponding absorption rise time is approximately 3×10^{-6} torr-s. From these data, the degree of rotational excitation cannot be determined, however, it is apparent that the photolysis of 3-cyclopentenone yields CO which is substantially colder than that obtained from ketene. Though these absorption studies do not provide the degree of rotational excitation (the CO laser employed oscillates only on a few low J transitions in a given vibrational band, typically P(9)-P(14)), they do provide a direct measure of the nascent distribution of the vibrational energy. The nascent vibrational distributions are shown in Figures 11-13 and each can be characterized by a vibrational temperature, T_v. This temperature is obtained from the slope of the best straight line through the data points of a log N_v vs. G_v plot, where G_v is the CO vibrational term. For the excitation wavelengths of 193, 249, and 308 nm, $T_v \cong 2900$, 1800, and 640 K respectively. This indicates that the extent of CO product vibrational excitation increases with photon energy or available energy.

Somewhat more insight regarding the physical significance of the experimentally determined vibrational distributions can be obtained by comparing these distributions to that predicted by a limiting case

Figure 15. Nascent CO vibrational distribution from the 193 nm photolysis of 3,5-cycloheptadienone: (●) experimental data; (□,○) calculated using equation (5.9) with an available energy, E_{av} = 140 and 130 kcal/mol, respectively.

excited in both cases. Further measurements are required to accurately characterize the degree of rotational excitation.

The plots of the experimentally determined vibrational distributions in Figures 15-17 show that the nascent CO photoproduct obtained via the uv excitation of 3,5-cycloheptadienone is vibrationally excited. As with 3-cyclopentenone, the information-theoretic model (equation (5.9)) was used to determine the CO vibrational distributions for several choices of available energy and when compared with the experimentally determined distributions (Figures 15-17), they indicate that 130-140, 100, and 70-80 kcal/mol is required at 193, 249, and 308 nm, respectively, to reproduce the experimental data. Using standard thermochemical estimation methods,[211] the reaction exoergicity is found to be 132.5, 99.3, and 77.5 kcal/mol at 193, 249, and 308 nm, respectively. Thus, the full reaction exoergicity ($E_{av} = h\nu - \Delta H_1^\circ$) appears to be available for statistical partitioning among all product modes. This result is significantly different from that obtained for 3-cyclopentenone where the energy available for statistical partitioning was substantially less than the full reaction exoergicity. A comparison of the results (Table 4) shows that a greater portion of the reaction exoergicity is partitioned into the product vibrational modes in the photodissociation of 3,5-cycloheptadienone than 3-cyclopentenone implying that there are fundamental differences in the fragmentation dynamics for the two reactions.

It is inconceivable that this difference results from a photophysical basis. For both 3-cyclopentenone and 3,5-cyclohepta-

Since little product rotational excitation was observed (relative to ketene photodissociation), the potential energy released in the exit channel, $E_a - \Delta H_1^\circ$, must be partitioned primarily to the relative translational motion of the products. This is in accord with the recent results of molecular beam experiments where product translational energies were directly determined. The infrared multiphoton dissociation of ethyl vinyl ether was found[212] to occur by two paths, one of which has a large barrier. Extensive translational energy release was observed only for the dissociation channel with the large barrier suggesting that a large fraction of the exit barrier is converted to translational excitation. Dissociation studies of chemically activated haloalkanes also suggest the validity of this model. For dissociation reactions with a low or negligible activation barrier, such as ketene (ab initio calculations[173] indicate that ketene fragmentation has a negligible activation barrier), the product vibrational energy distributions should be statistical assuming availability of the full reaction exoergicity. A statistical distribution of the CO product vibrational energy was observed in the ketene photodissociation at 193 nm.[143]

The pressure-dependent rise times of the transient laser absorptions by the nascent CO product indicate that the CO produced by the photofragmentation of 3,5-cycloheptadienone is rotationally excited to some extent. The absorption rise times observed for 3,5-cycloheptadienone are comparable to those observed for 3-cyclopentenone suggesting, but not necessarily requiring, that the CO product rotational distributions are likely to be comparably

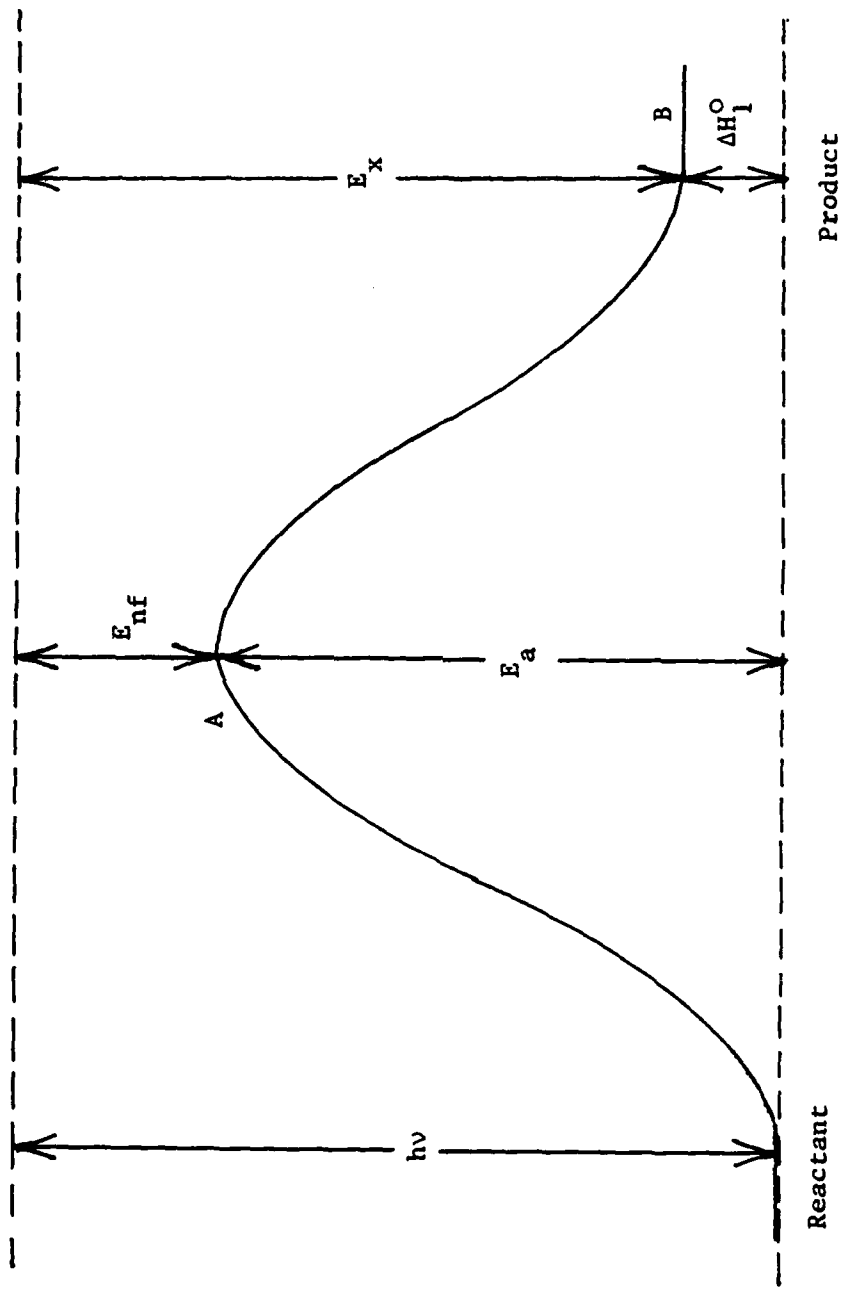

Figure 14

Figure 14. Schematic potential energy diagram for the dissociation of 3-cyclopentenone. E_a is the reaction activation energy, E_{nf} is the transition state's non-fixed energy, and E_x is the reaction exoergicity. This diagram represents a type 2 surface (see ref. 14).

energy disposal to the CO fragment may be determined at a point on the potential surface where the product fragements are vibrationally decoupled from one another and the available energy is less than the reaction exoergicity. If vibrational energy partitioning occurs near the transition state for dissociation, the available energy is $E_{av} \cong h\nu - E_a$, where E_a is the Arrhenius activation energy. This corresponds in the RRKM terminology[43] to the "non-fixed" energy of the transition state. Figure 14 illustrates the schematic energy diagram for the reaction. Following photoexcitation, if internal conversion occurs when the molecule is at a geometry similar to the reactants or transition state, the exit channel for the fragmentation is on the ground-state potential surface. If the fragments remain vibrationally coupled, i.e., interfragment vibration to vibration energy transfer occurs readily, until point B in Figure 14, then the reaction exoergicity is available for partitioning among the products' degrees of freedom. If, however, the vibration to vibration coupling becomes inefficient at point A, then the energy available to be statistically distributed is less than the reaction exoergicity, $E_{av} \cong h\nu - E_a$. Using the reported[176] Arrhenius activation energy of 51 kcal/mol, the non-fixed energy available is 97, 64, and 30 kcal/mol at 193, 249, and 308 nm, respectively, which with the exception at 308 nm, are very similar to the available energies required to obtain qualitative agreement between theory and experimental results. The discrepancy at 308 nm results from the semiclassical state counting algorithm used in equation (5.9) which becomes a relatively poor approximation to direct count results at low energies.

translational energy, E_t. The denominator in equation (5.9) normalizes the distribution function and equation (5.9) can be evaluated numerically for a given E_{av}. The CO vibrational-state densities are computed from the harmonic oscillator approximation and the Whitten-Rabinovitch semiclassical algorithm[209] is used for approximating rotation-vibration energy level densities ($P_r(E_{av})$). This statistical model allows computation of CO product vibrational energy distributions under conditions where all product (CO and butadiene) modes are strongly coupled with an available energy, E_{av}.

For several choices of available energy, the model (equation (5.9)) was used to calculate CO vibrational distributions from the photofragmentation of 3-cyclopentenone. The CO vibrational distributions are plotted in Figures 11-13. An a priori estimation of the available energy may be determined by $E_{av} = h\nu - \Delta H_1^\circ$, i.e., the reaction exoergicity, where $h\nu$ is the photon energy and ΔH_1° is the enthalpy change for the reaction. Thermochemical estimation methods[211] indicate that ΔH_1° at 298 K is 15 kcal/mol. Thus, the reaction exoergicity at 193, 249, and 308 nm is 130, 100, and 80 kcal/mol, respectively. From the plots in Figures 11-13, it is apparent that the experimental distributions are, in each case, significantly colder than that calculated with $E_{av} = h\nu - \Delta H_1^\circ$. When the available energy used in the calculations is reduced, colder vibrational distributions are subsequently obtained. Thus, if energy is statistically distributed among the products' vibrational degrees of freedom, the energy is less than the reaction exoergicity.

A possible explanation for these results is that vibrational

statistical model for energy partitioning among the products of a fragmentation reaction.[68,208] In this model, a surprisal analysis was developed[208] to analyze vibrational distributions which require the specification of a prior expectation for the distribution of the energetically accessible product vibrational states. Equal probability for all product quantum states is assumed and the problem can then be reduced to calculating the densities of states for each energetically accessible level. Thus, the expected probability of observing a given v in CO at a fixed total energy is simply the densities of states for the expected product (CO(v)) divided by the sum of the total densities of all accessible states. This value is the fraction of the total phase space available to this product state. In the context of this model, the probability for forming CO with vibrational energy ϵ when the available energy is E_{av} is given by,

$$f(\epsilon,E_{av}) = \frac{N_{CO}(\epsilon)\int_{E_t=0}^{E_{av}-\epsilon} P_r(E_{av}-\epsilon-E_t)E_t^{\frac{1}{2}}dE_t}{\sum_{E=0}^{E} N_{CO}(\epsilon)\int_{E_t=0}^{E_{av}-\epsilon} P_r(E_{av}-\epsilon-E_t)E_t^{\frac{1}{2}}dE_t} \qquad (5.9)$$

where $f(\epsilon,E_{av})$ is the CO vibrational energy distribution for any specified available energy, E_{av}; $N_{CO}(\epsilon)$ is the CO vibrational density of states at energy, ϵ ; $P_r(E)$ is the degeneracy of butadiene vibrational states and all relative rotational states at energy, E, and $E_t^{1/2}$ is the one-dimensional translational-state density[208] at

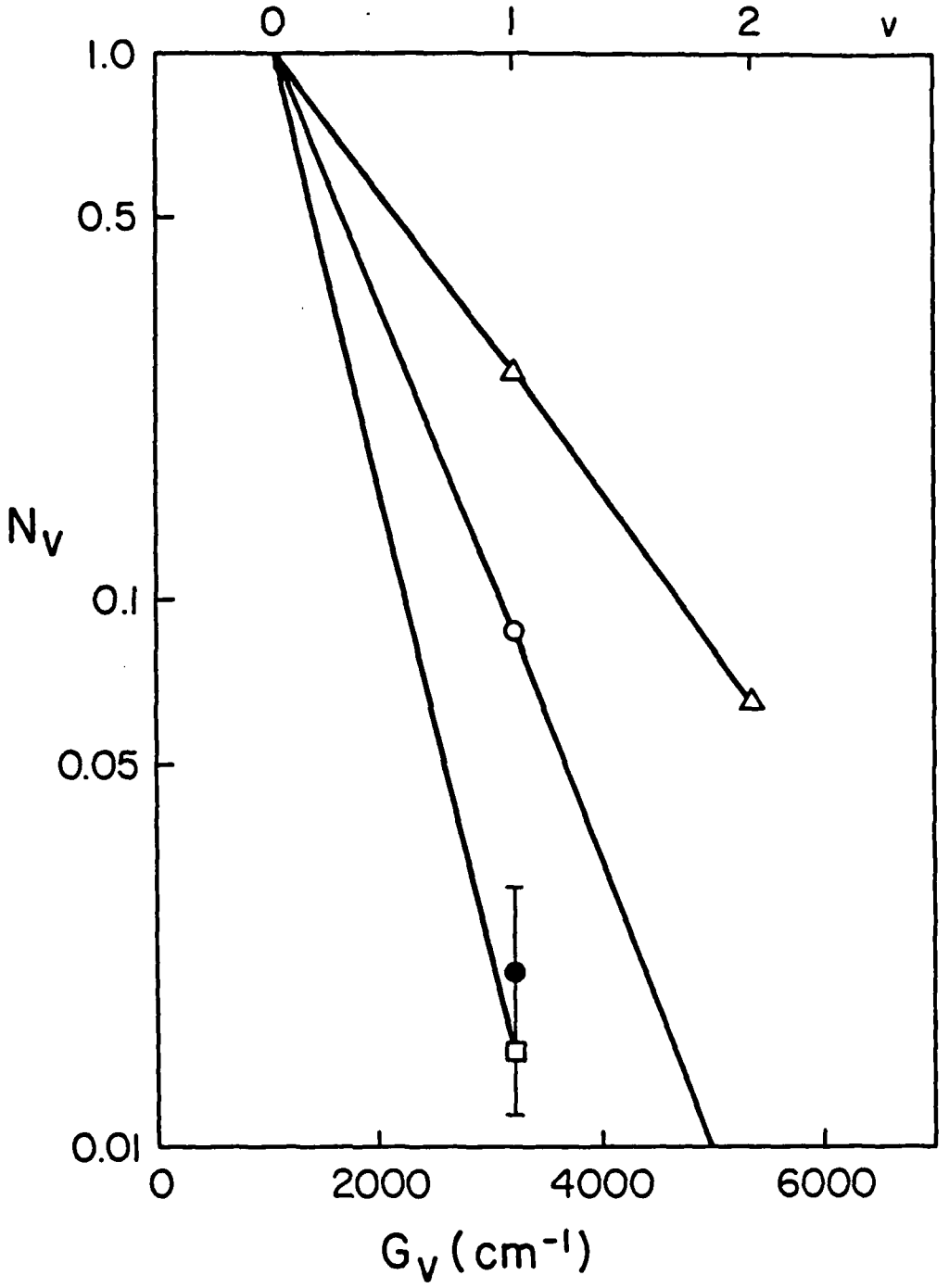

Figure 13

Figure 13. Nascent CO vibrational distribution from the 308 nm photolysis of 3-cyclopentenone. G_v is the vibrational term: (●) experimental data; (△,○,□) calculated by using equation (5.9) with an available energy, E_{av} = 80, 30, and 10 kcal/mol, respectively.

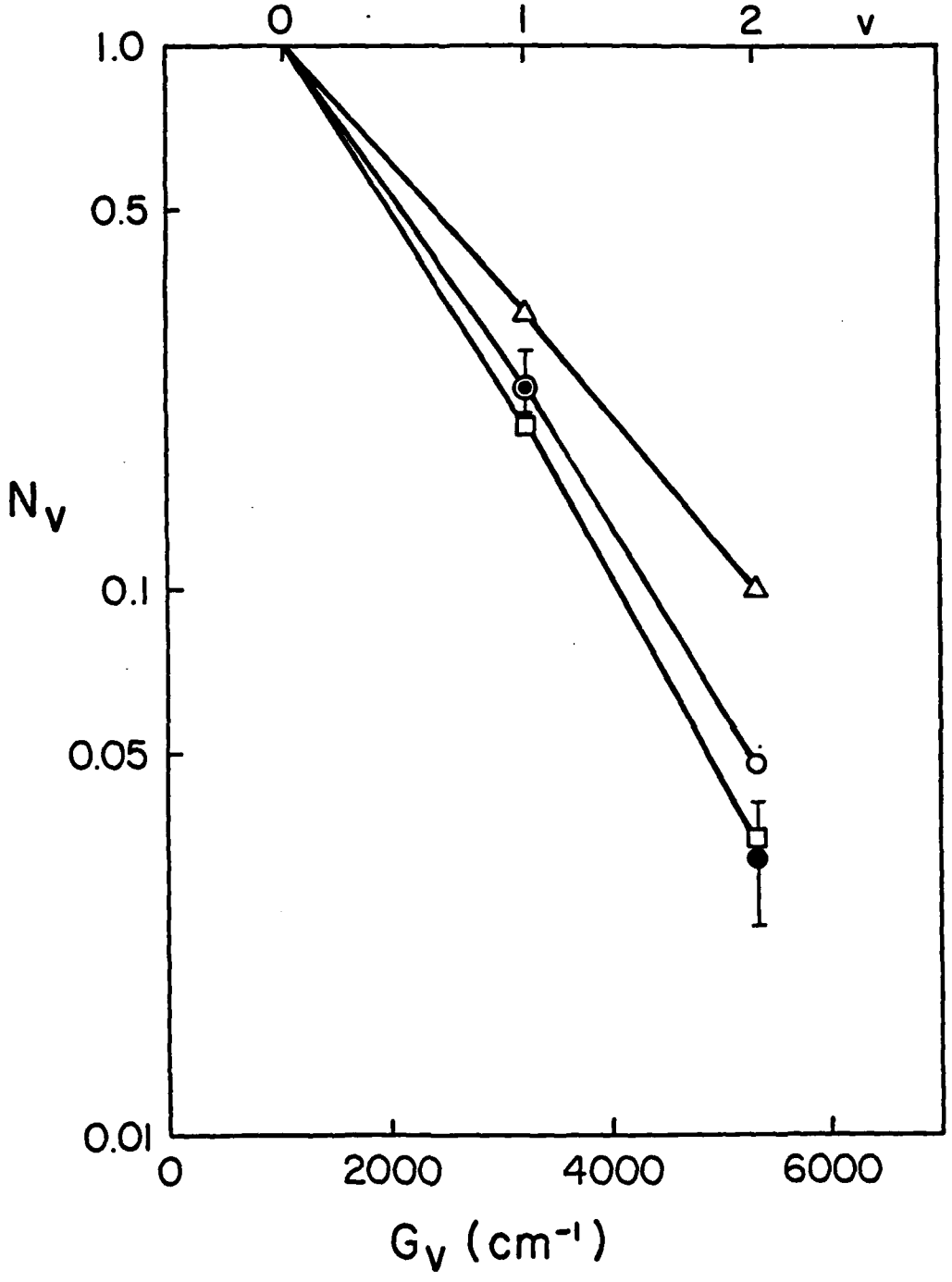

Figure 12

Figure 12. Nascent CO vibrational distribution from the 249 nm photolysis of 3-cyclopentenone. G_v is the vibrational term: (●) experimental data; (Δ,o,□) calculated by using equation (5.9) with an available energy, E_{av}= 100, 70, and 60 kcal/mol, respectively.

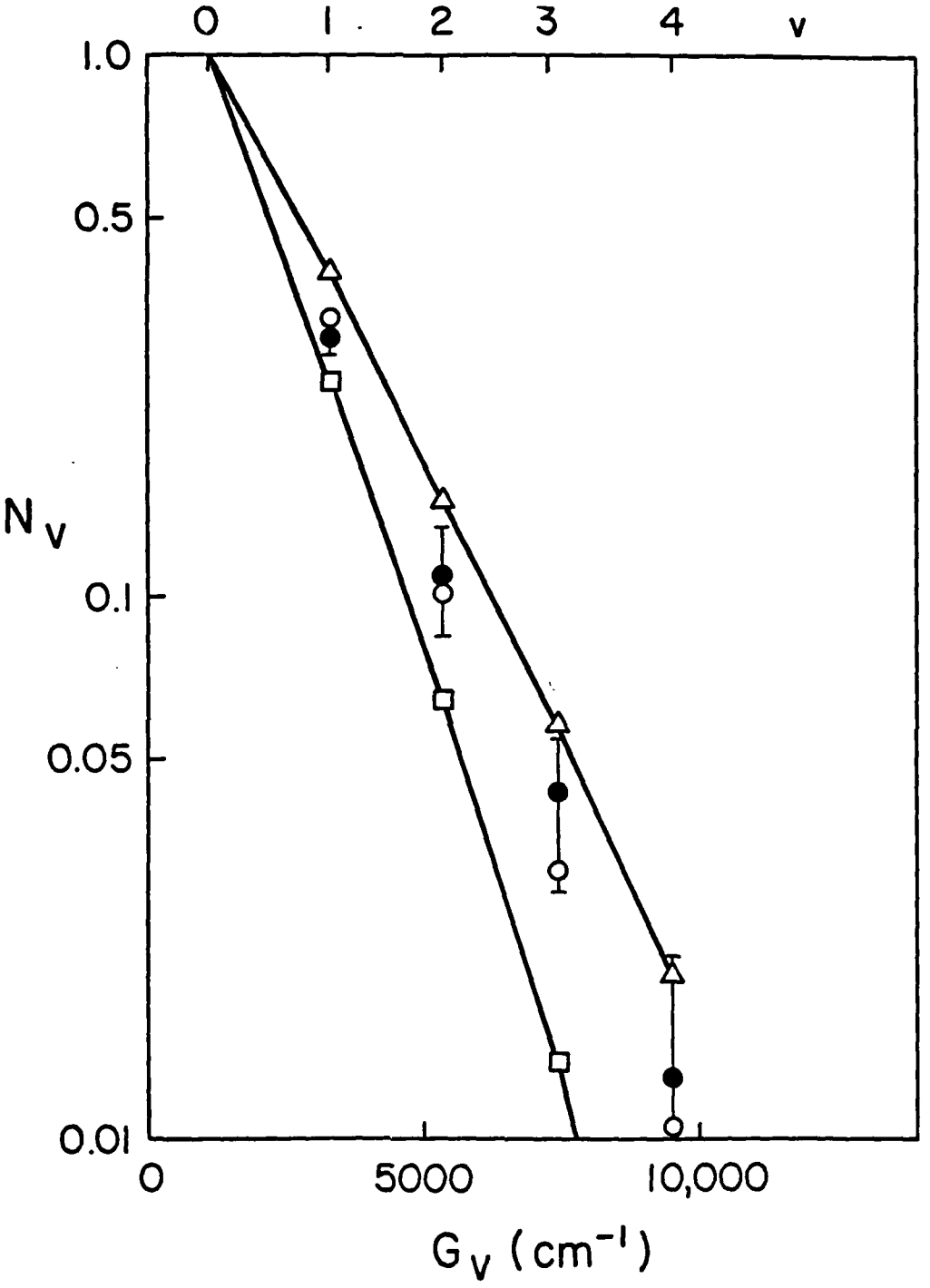

Figure 11

Figure 11. Nascent CO vibrational distribution from the 193 nm photolysis of 3-cyclopentenone. G_v is the CO vibrational term: (●) experimental data; (△,o,□) calculated by using equation (5.9) with an available energy, E_{av} = 130, 100, and 80 kcal/mol, respectively.

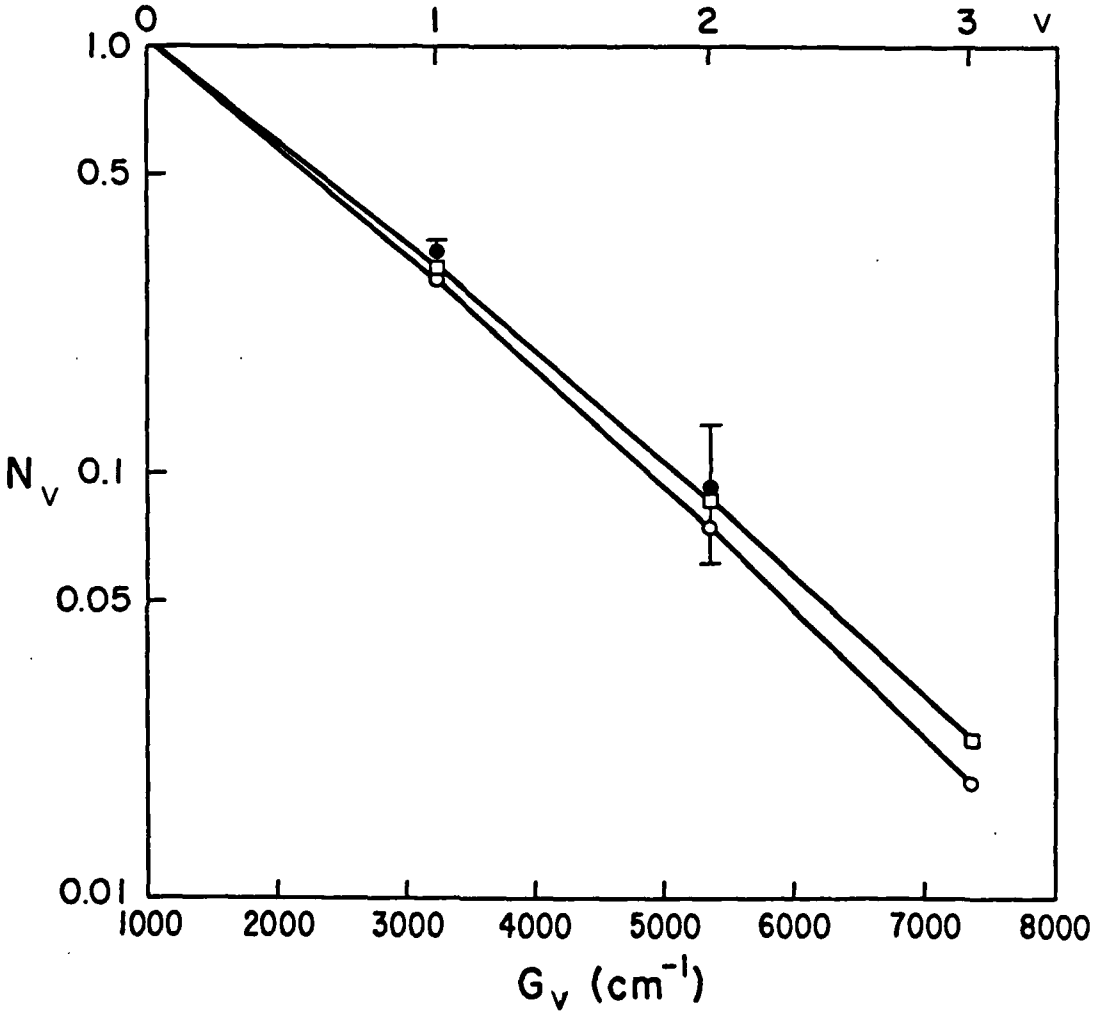
0
1
2
3
v
1.0
0.5
N_v 0.1
0.05
0.01
1000
2000
3000
4000
5000
6000
7000
8000
G_v (cm^{-1})

Figure 15

Figure 16. Nascent CO vibrational distribution from the 249 nm photolysis of 3,5-cycloheptadienone: (●) experimental data; (○,□) calculated using equation (5.9) with an available energy, E_{av} = 100 and 90 kcal/mol, respectively.

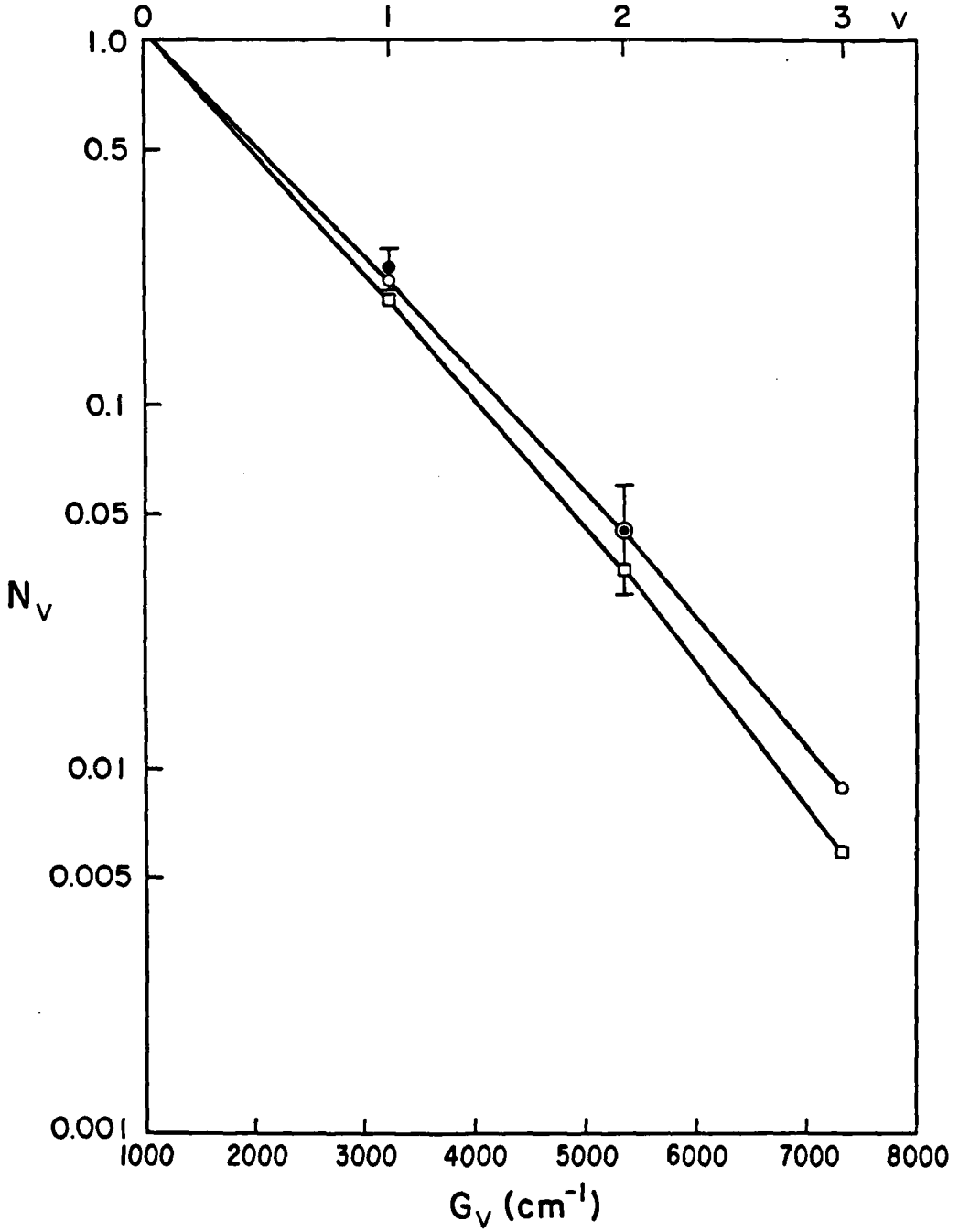
0
1
2
3
V
1.0
0.5
0.1
0.05
0.01
0.005
0.001
N_V
1000
2000
3000
4000
5000
6000
7000
8000
G_V (cm^{-1})

Figure 16

Figure 17. Nascent CO vibrational distribution from the 308 nm photolysis of 3,5-cycloheptadienone: (●) experimental data; (○,□) calculated using equation (5.9) with an available energy, E_{av} = 80 and 70 kcal/mol, respectively.

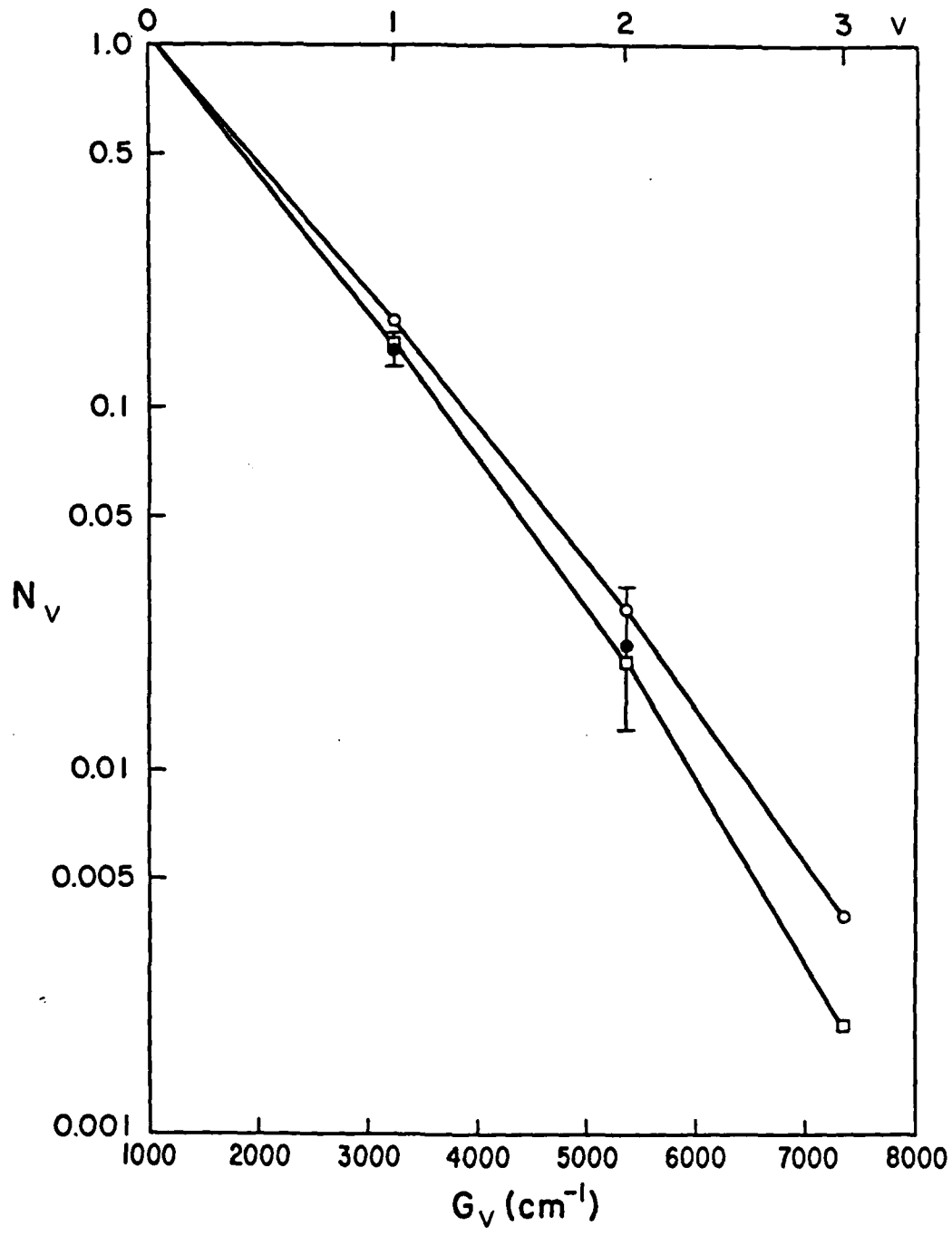
0
1
2
3
V
1.0
0.5
0.1
0.05
0.01
0.005
0.001
N_V
1000
2000
3000
4000
5000
6000
7000
8000
G_V (cm^{-1})

Figure 17

Table 4. Comparison of Results on Energy Disposal to CO in the Photoactivated Fragmentation of 3-Cyclopentenone, 3,5-cycloheptadienone, and Tropone.

	3-Cyclopentenone			3,5-Cycloheptadienone			Tropone		
λ, nm	193	249	308	193	249	308	193	249	308
E_x^a (kcal/mol)	133	99.8	78	132.5	99.3	77.5	-	138	116
E_{nf}^b (kcal/mol)	97	63.8	42	c	c	c	-	67	45
E^d (kcal/mol)	100	60-70	<40	130-140	100	70-80	-	70	55

[a]Reaction Exoergicity; $E_x = h\nu - \Delta H_1^\circ$. [b]Non-Fixed energy of the transition state; $E_{nf} = h\nu - E_a$. [c]No value of E_a for the fragmentation of 3,5-cycloheptadienone has been reported. [d]Energy required to fit experimental CO vibrational energy by using equation (5.9).

dienone, though different electronic transitions are excited by irradiation at 193 and 308 nm, the manner in which energy is partitioned to product vibrations was found to be a consistent and relatively simple function of available energy, showing no discontinuities that might be ascribed to electronic state dependent energy disposal. In the photodissociation of both reactant molecules, ground state products were observed indicating that radiationless transition to the ground state surface occurs prior to fragmentation. Also, fits of the experimental vibrational distributions using equation (5.9) show that the required available energies are in all cases larger than would be anticipated if products were formed on an excited state potential surface. Thus, the photophysics of 3-cyclopentenone and 3,5-cycloheptadienone appear to be at least qualitatively similar and another basis for the observed difference in energy disposal must be considered.

Bernstein and Levine[213] have suggested that a general feature of exoergic reactions is a non-Boltzmann distribution of internal state populations. It might be suggested that the difference observed here is be due to non-statistical energy partitioning among the product modes of 3-cyclopentenone and/or 3,5-cycloheptadienone. Such effects have been previously observed[214] in photofragmentation reactions. The observation in this study that a single statistical energy model fits the 3-cyclopentenone results between 193 and 308 nm and that a single, but different, model fits the 3,5-cycloheptadienone results for the same excitation wavelengths suggests that either non-statistical effects occur to the same extent over this energy range or that

non-statistical effects are not operative in these reactions. Studies of the unimolecular decay of small molecules using trajectory calculations have yielded non-statistical (non-RRKM) lifetime distributions, however, the relative importance of the non-statistical behavior was found to be strongly dependent on the internal energy of the decomposing species.[215]

Differences in the gross shape of the potential surfaces for these reactions may be the cause of differences in the energy disposal dynamics. In the case of 3-cyclopentenone, the ground state potential surface is a type 2 surface (Figure 14) for which the activation barrier has been determined. Only the non-fixed energy of the transition state is available to be statistically distributed. If the dissociation of 3,5-cycloheptadienone occurs on a type 1 surface (Figure 18), the CO product vibrational distribution should be in accord with an energy disposal model which assumes the availability of the full reaction exoergicity. Thus, if the dissociation of 3,5-cycloheptadienone had no potential barrier in excess of the reaction endothermicity, then the same model could be used to explain the results of both reactions. Although no measurements have been reported for the activation barrier for the dissociation of 3,5-cycloheptadienone, it appears that the activation barrier must be significant. If no barrier to decomposition greater than the reaction endothermicity exists, then $E_a = \Delta H_1^\circ \approx 15$ kcal/mol. Assuming an Arrhenius A-factor, $A \gtrsim 10^{13}$ s^{-1}, the lifetime at 300 K would be ≤ 40 ms. 3,5-Cycloheptadienone was found to be stable for several hours at 300 K, therefore, $E_a > \Delta H_1^\circ$. The photochemically and thermally

Figure 18. Schematic potential energy diagram for the dissociation of 3,5-cycloheptadienone. This represents a type 1 surface (see ref. 14).

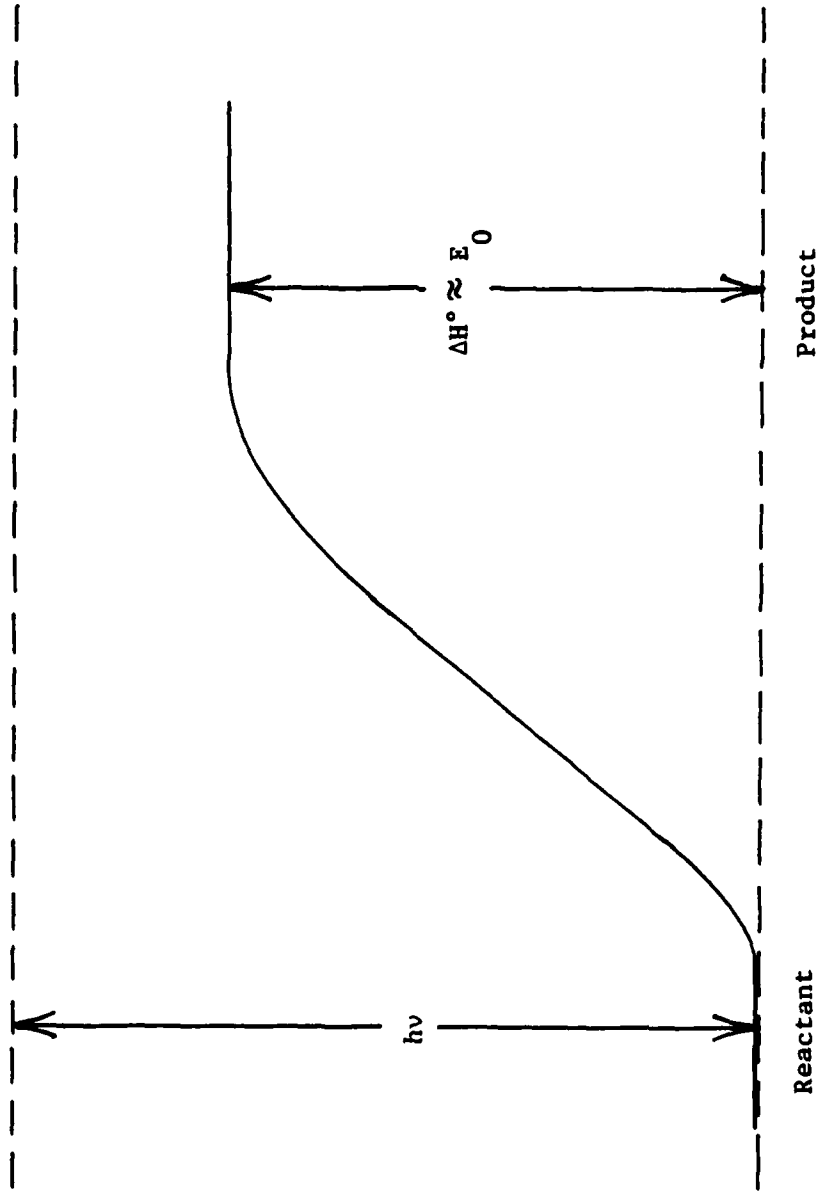

Figure 18

induced cheletropic elimination of SO_2 from sulfones (equations (5.10) and (5.11)), analogs of the photodecarbonylation of 3-cyclopentenone and 3,5-cycloheptadienone have been studied and were found to have comparable barriers to dissociation.[216]

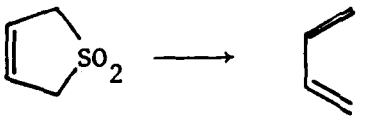

(5.10)

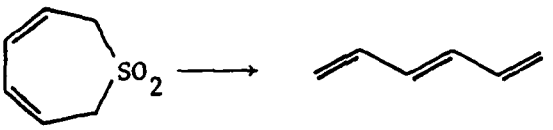

(5.11)

Similarly, diazenes, which are isoelectronic with ketones, also undergo cheletropic eliminations. Diazene XIX undergoes fragmentation significantly faster than diazene XX.[217] These

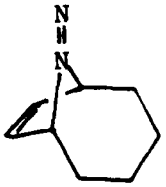

XIX

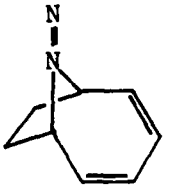

XX

analogies suggest that the activation barrier to the decarbonylation of 3,5-cycloheptadienone is at least as large as the barrier to the decarbonylation of 3-cyclopentenone (51 kcal/mol) and thus the ground state potential surface for 3,5-cycloheptadienone is not a type 1 surface.

If the dissociation of 3,5-cycloheptadienone has an activation barrier, $E_a \geq 51$ kcal/mol, then the non-fixed energy of the transition state available for statistical partitioning at 193, 249, and 308 nm is $\leq$ 96.5, 63.3, and 41.5 kcal/mol, respectively. The CO vibrational distributions resulting from the substitution of these values into equation (5.9) are shown in Figures 15-17 and are substantially colder than those observed experimentally, and lay well below the experimental error limits. Since the exit channels for the photofragmentation of both 3-cyclopentenone and 3,5-cycloheptadienone lay on the ground-state potential surface, the differences in the energy disposal dynamics between the two reactions must arise from the differences in the coupling of the developing products' internal and external degrees of freedom. With 3-cyclopentenone, the non-fixed energy of the transition state is statistically partitioned among the products' vibrational modes and the release of the potential energy, $E_a - \Delta H_1^\circ$, in the exit channel is primarily to the products' relative translational motion. With 3,5-cycloheptadienone, the full reaction exoergicity is statistically partitioned among the products' internal and external degrees of freedom and the developing products' degrees of freedom must be effectively coupled well into the exit channel.

Dynamical effects which couple the developing products' degrees of freedom in qualitatively different ways has a mechanistic origin (by process of elimination). For example, if the photodecarbonylation of both 3-cyclopentenone and 3,5-cycloheptadienone are concerted, then these reactions are subject to selection rules based on the conservation of orbital symmetry.[118,177,179] In accordance

with these orbital symmetry considerations, the allowed ground state (thermal) mode for the dissociation of 3-cyclopentenone is via a linear (least motion) pathway (XXI) while the corresponding allowed dissociation for 3,5-cycloheptadienone is via a non-linear (non-least motion) pathway (XXII).

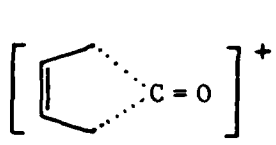

XXI

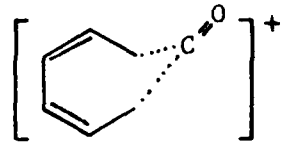

XXII

In the fragmentation of 3-cyclopentenone, where the energy in the reaction coordinate is channeled primarily into the products' (CO and butadiene) translational motion, the internal modes of the developing products are uncoupled from one another in the exit channel. In the case of 3,5-cycloheptadienone, a different situation exists. Here, the reaction coordinate may be considered as some combination of stretching and bending vibrations which correlate with product translational and rotational motion. Any impulsive energy imparted to the CO carbon near the transition state may excite CO rotational and orbital motion to some extent suggesting that on an average, the products formed in the dissociation remain in closer proximity for a longer period of time than in the dissociation of 3-cyclopentenone. Thus, under these conditions, vibration-rotation coupling may provide an effective means of coupling all the products' degrees of freedom well into the exit channel, resulting in complete randomization of the available energy. In the least motion dissociation of 3-cyclopentenone, since product rotational motion is not strongly excited, no

mechanism exists for effectively coupling developing products' degrees of freedom in the exit channel and the relatively rapid, impulsive separation of the products minimizes the time over which coupling could occur.

Vibration-rotation coupling must dominate the dynamics of the non-linear cheletropic dissociation of 3,5-cycloheptadienone well into the exit channel to effectively randomize the complete reaction exoergicity. It is interesting to note that vibration-rotation coupling typically represents only a perturbation on energy levels. Thus, such coupling would seem likely to make available to the developing products' internal modes only a fraction of the potential energy released in the exit channel. The energy made available for partitioning to CO vibration by typical vibration-rotation coupling would be only slightly greater than the transition state's non-fixed energy and significantly less than the full reaction exoergicity. In the present case, vibration-rotation coupling is found to result in strong state mixing and must dominate the dynamics of dissociation.

Preliminary results suggest that the decarbonylation of 3,5-cycloheptadienone occurs via a concerted process.[184] If, however, the concerted pathway does not obtain, a biradical mechanism would be a likely alternative (equation (5.12)). In this case, the

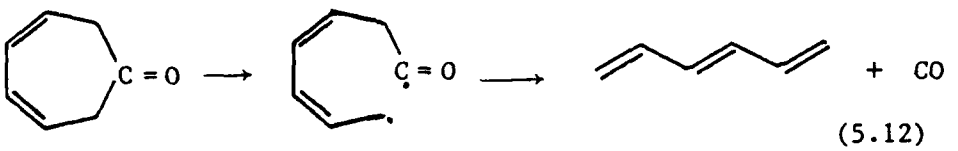

XXIII

(5.12)

REFERENCES

[1]I.W.M. Smith (ed.), Physical Chemistry of Fast Reactions, vol. 2, Plenum Press, New York(1980).

[2]M.G. Evans and M. Polanyi, Trans. Faraday Soc. 1939, 35, 178-185.

[3]J.C. Polanyi, Accts. Chem. Res. 1972, 5, 161-168.

[4]R. Wolfgang, Accts. Chem. Res. 1969, 2, 248-256.

[5]J.M. Farrar and Y.T. Lee, Ann. Rev. Phys. Chem. 1974, 25, 357-385.

[6]C. Maltz, N.D. Weinstein, and D.R. Herschbach, Mol. Phys. 1972, 24, 133.

[7]D.S.Y. Hsu and D.R. Herschbach, Discuss. Faraday Soc. 1973, 55, 116.

[8]S.M. Freund, G.A. Fisk, D.R. Herschbach, and W. Klemperer, J. Chem. Phys. 1971, 54, 2510-18.

[9]Y.B. Band and K.F. Freed, J. Chem. Phys. 1976, 64, 4329-33.

[10]L.C. Lee and D.L. Judge, Can. J. Physics 1973, 51, 378.

[11]G.M. Lawrence, L.C. Klotz, and K.R. Wilson, J. Chem. Phys. 1972, 56, 3534-42.

[12]W.M. Gelbart, Ann. Rev. Phys. Chem. 1977, 28, 323-48.

[13]S.R. Leone, Adv. Chem. Phys. 1982, 50, 255-324.

[14]W. Forst, Theory of Unimolecular Reactions, Academic Press, New York (1973).

[15]P.J. Robinson and K.A. Holbrook, Unimolecular Reactions, Wiley-Interscience, London (1972).

[16]N.B. Slater, Theory of Unimolecular Reactions, Cornell University Press, New York (1959).

[17]G. Wentzel, Z. Physik 1927, 43, 524.

[18]A.S. Davydov, Quantum Mechanics, Pergammon Press, New York (1976), pp. 399-400.

[19]R.S. Berry, Rec. Chem. Prog. 1970, 31, 9-25.

to products, the fragments are vibrationally decoupled from one another. However, in the dissociation of 3,5-cycloheptadienone, the fragments are found to be strongly coupled well into the exit channel. A mechanistically based model has been proposed to account for the differences in the energy disposal dynamics between 3-cyclopentenone and tropone and 3,5-cycloheptadienone.

CHAPTER 6

CONCLUSIONS

The results of this study have shown that energy disposal measurements provide a useful probe of the photofragmentation dynamics of polyatomic molecules. Photofragment infrared fluorescence measurements were used to determine the ro-vibrational energy disposal to the CO product formed upon photolysis of ketene at 193 nm. The nascent CO vibrational distribution can be characterized by a temperature, T_v=3750 K and the rotational excitation in the CO product can be characterized by a temperature of 6700 K, assuming a Boltzmann distribution of the CO rotational states. These results indicate that the photofragmentation of CO at 193 nm proceeds via a non-linear transition state.

Time-resolved laser absorption spectroscopy was used to determine the nascent vibrational distribution of the CO product from the photolysis of 3-cyclopentenone and 3,5-cycloheptadienone at 193, 249, and 308 nm and tropone at 249 and 308 nm. Only the non-fixed energy of the transition state was found to be available to be statistically partitioned among the products' vibrational modes in the photodissociation of 3-cyclopentenone and tropone whereas the full reaction exoergicity was found to be available for statistical partitioning among all the products' degrees of freedom in the photodissociation of 3,5-cycloheptadienone. Thus, in the dissociation of 3-cyclopentenone and tropone, as the transition state is transformed

a transition state that has an energy comparable to C. With the data available, it is not possible to differentiate the two possibilities at this time.

The results of this study demonstrate that energy disposal measurements can provide a useful probe of the photofragmentation dynamics of polyatomic molecules. Such experiments may provide valuable information in characterizing the interaction or coupling of nascent product fragments in the exit channel and near the transition state for dissociation. Significant differences were found in the dissociation dynamics of 3-cyclopentenone, 3,5-cycloheptadienone, and tropone. The mechanistically based models described in this study to account for the differences in the dissociation dynamics is by no means the only ones capable of explaining the results. They are, however, consistent with some of the limited data available and the trends observed in the photochemistry and photophysics of polyatomic molecules. Clearly, further study is required to evaluate the models developed here.

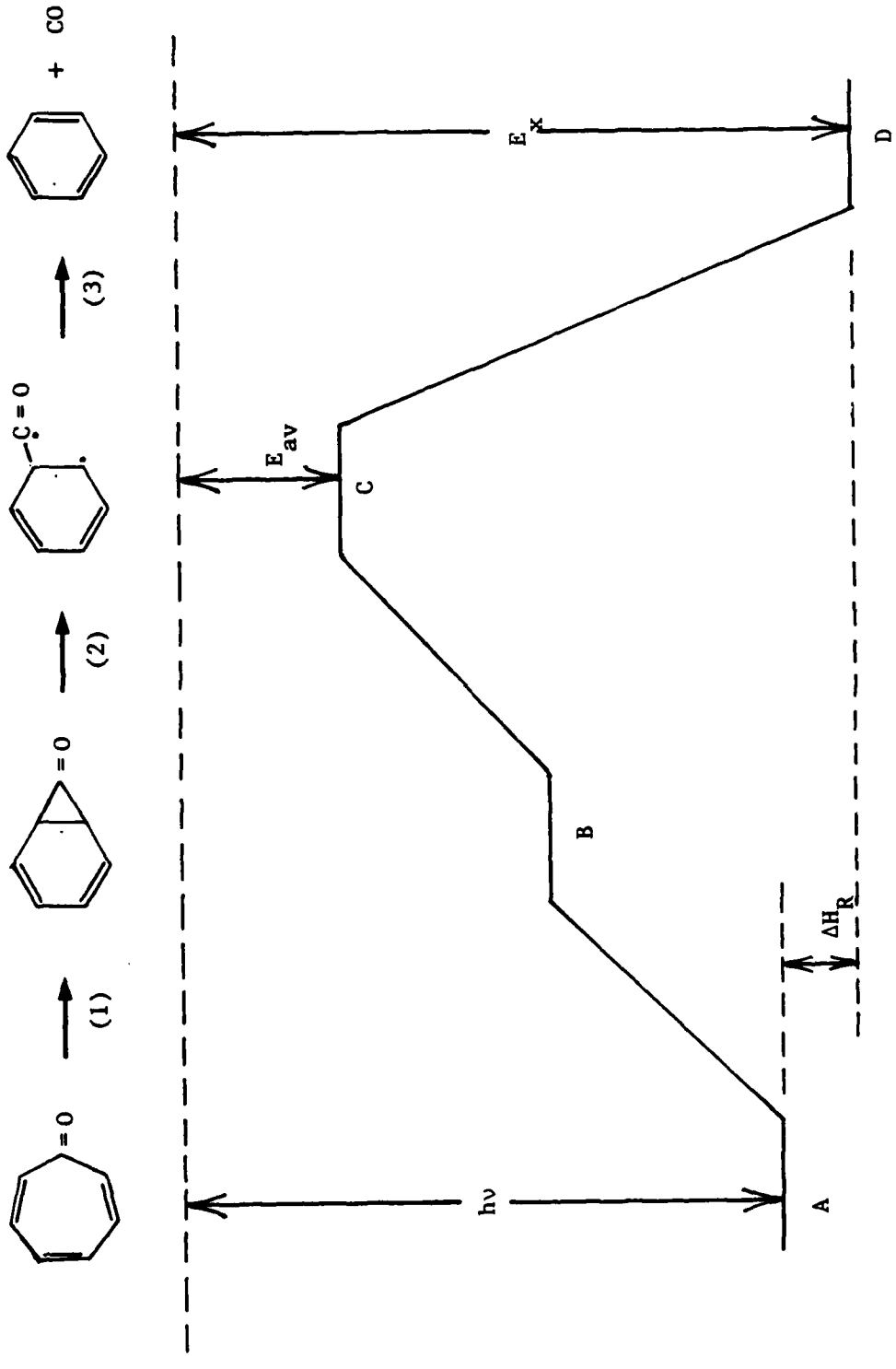

Figure 22

Figure 22. Schematic potential energy diagram for the dissociation of tropone (see text).

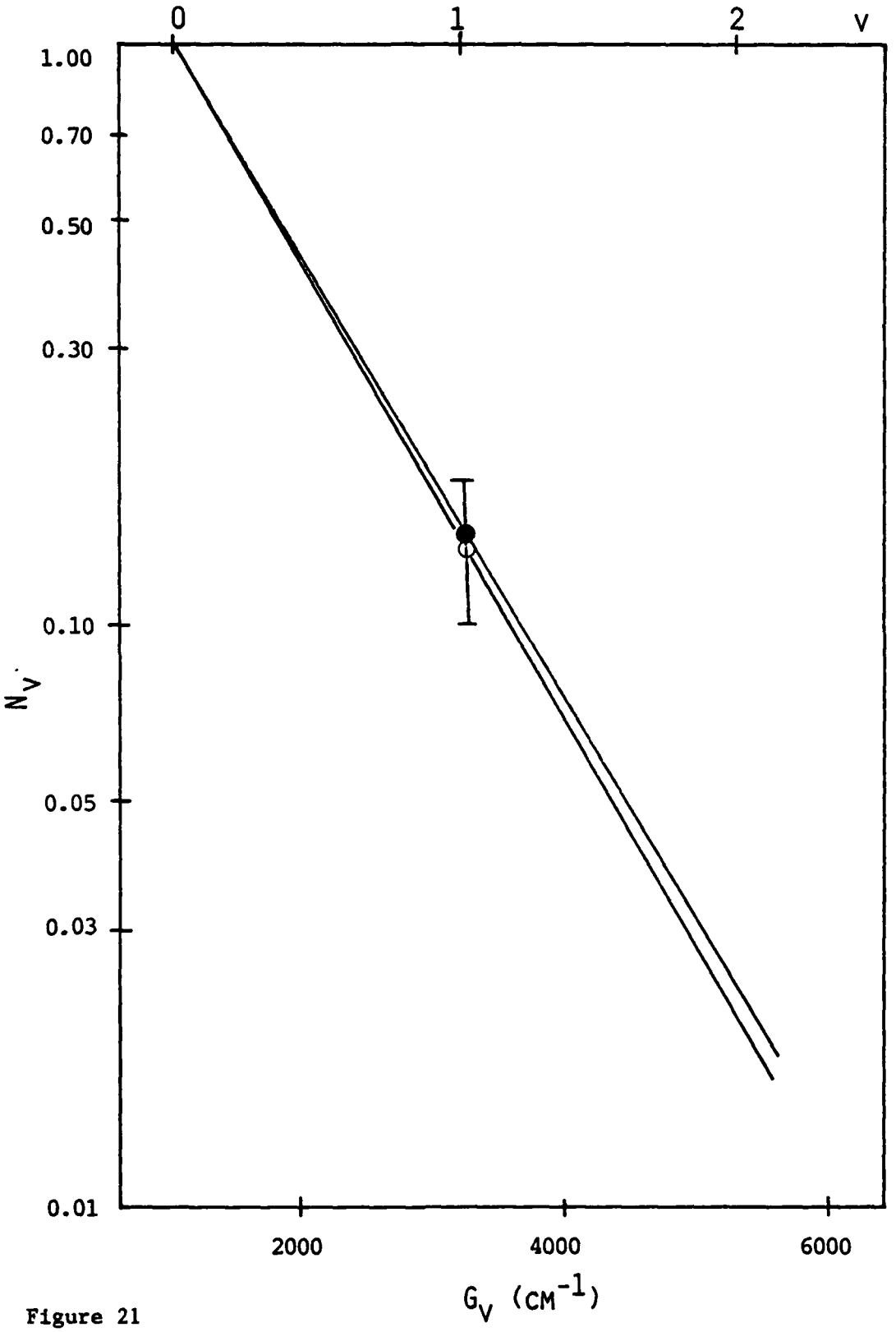

Figure 21

Figure 21. Nascent CO vibrational distribution from the 308 nm photolysis of tropone: (•) experimental data; (○) calculated using equation (5.9) with an available energy, E_{av} = 45 kcal/mol.

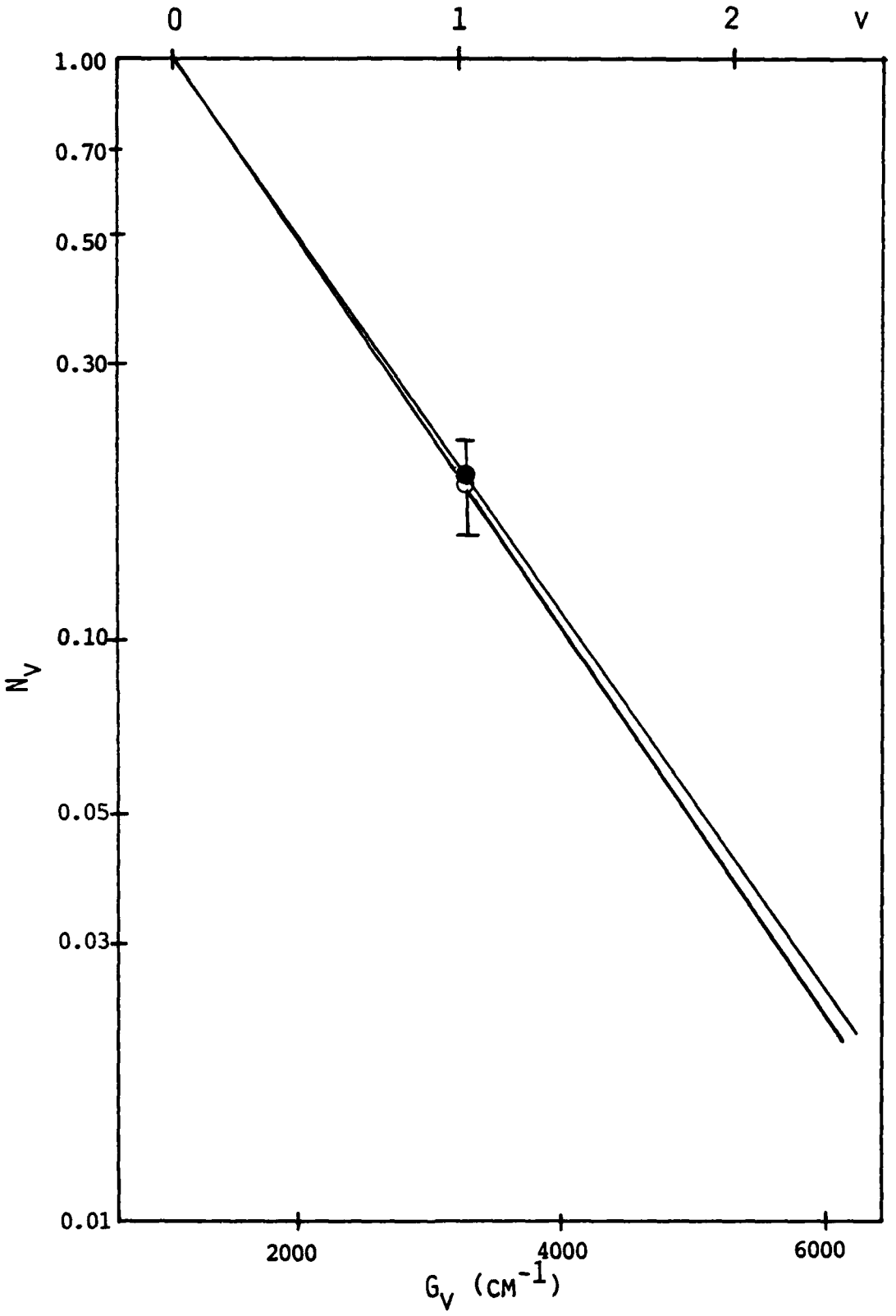

Figure 20

Figure 20. Nascent CO vibrational distribution from the 249 nm photolysis of tropone: (●) experimental data; (○) calculated using equation (5.9) with an available energy, E_{av} = 67 kcal/mol.

observed for 3-cyclopentenone and 3,5-cycloheptadienone. The photochemistry of tropone at 193 nm leading to the production of CO was found to be a two-photon process and further analysis at this wavelength was not made. The plots of the experimentally determined vibrational distributions at 249 and 308 nm show that the nascent CO product formed by the photolysis of tropone is also vibrationally excited (Figures 20 and 21). The experimental vibrational distributions cannot be fit by equation (5.9) if the full reaction exoergicity is used as the available energy. Best fits to the data are obtained when E_{av} = 70 and 55 kcal/mol at 249 and 308 nm, respectively (Figures 20 and 21). Thus some energy much less than the reaction exoergicity is available for partitioning to the developing products' degrees of freedom. These results can be rationalized in terms of the mechanism shown in Figure 22. Using thermochemical estimation methods,[211] $\Delta H(1) \cong +23.6$ kcal/mol, $\Delta H(2) \cong +24$ kcal/mol, $\Delta H(3) \cong -71$ kcal/mol, and $\Delta H_R \cong -23$ kcal/mol. The Arrhenius activation energy has been previously determined to be 54.1 kcal/mol and if only $E_{av}(C)$ (≅67 and 45 kcal/mol at 249 and 308, respectively) is available to be statistically partitioned, then the experimental distribution compares favorably with the distribution predicted by equation (5.9). In this case, the biradical, C, and the transition state may have similar geometries and energies and the CO and benzene products are effectively decoupled from one another after the transition state. The non-fixed energy is thus available for statistical partitioning. However, the results can also be explained if the reaction proceeds directly from B to D (concerted process) with

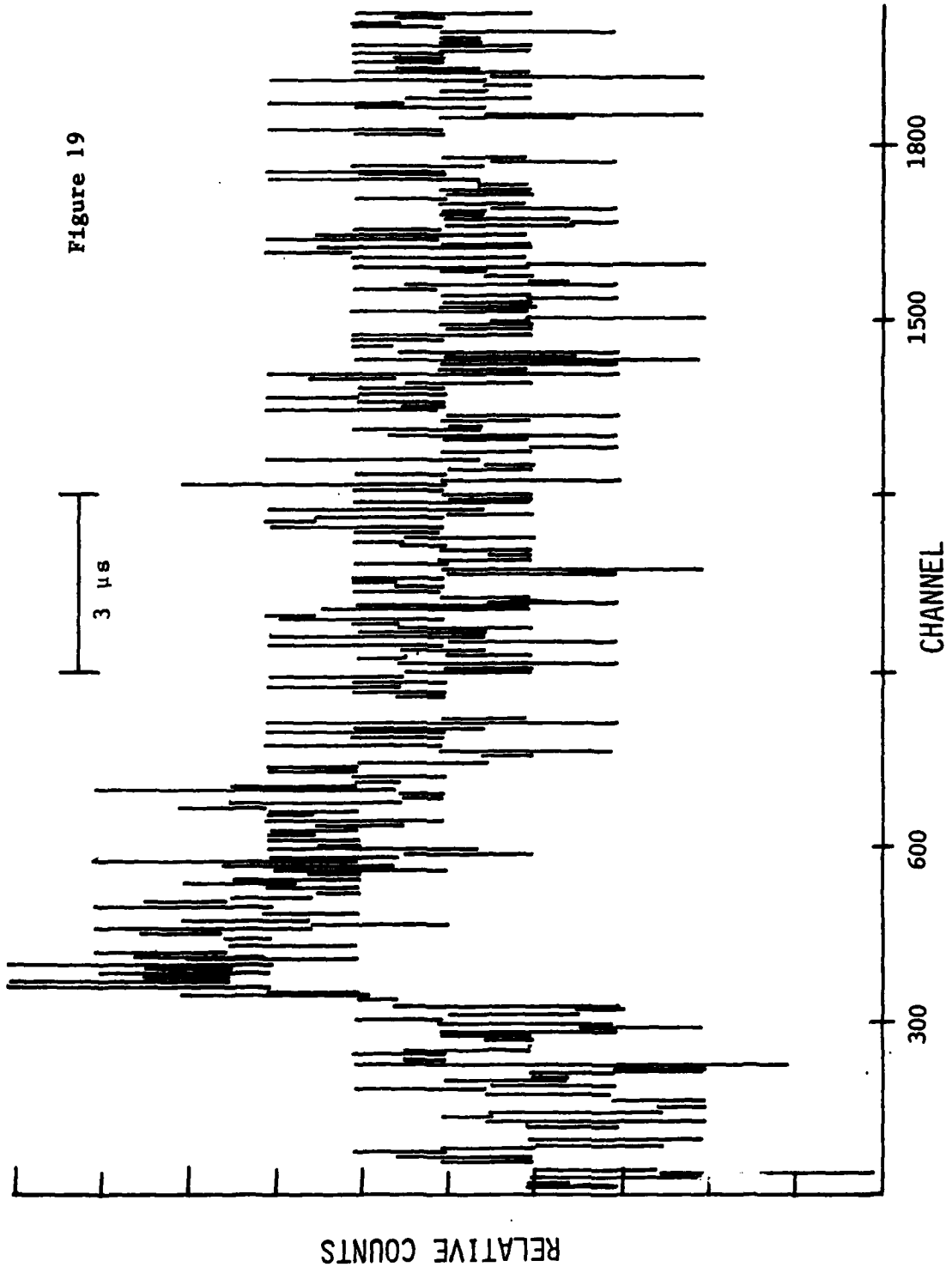

Figure 19

Figure 19. CO transient absorption curve obtained upon the photolysis of 0.15 torr tropone at 249 nm. The $P_{1,0}(9)$ CO laser transition was used as a probe. The reported curve was obtained by averaging 500 KrF* pulses.

experimental results would reflect the dissociation dynamics of the biradical, XXIII. The lifetime of the biradical can be estimated by using quantum RRK theory.[43] For 308 nm excitation of the ketone, the lifetime of XXIII is approximately 10^{-13}-10^{-12} s if the barrier to decomposition is $\sim$3 kcal/mol. If the internal energy of XXIII is randomized within this lifetime, then significant excitation of the biradical's torsional and bending modes can be expected, perhaps leading to the activation of rotational and orbital motion early in the exit channel. Extensive vibration-rotation coupling is again required well into the exit channel to statistically partition the full reaction exoergicity to the developing products' degrees of freedom. Regardless of the mechanisms operative, concerted or biradical, the products must be strongly coupled in the exit channel.

Similar energy disposal studies of tropone may provide valuable insight into the photodissociation of cyclopropanone, a homolog of 3-cyclopentenone and 3,5-cycloheptadienone. The cheletropic elimination of CO from cyclopropanone is an allowed process by orbital symmetry considerations. Cyclopropanone is a highly reactive molecule, and tropone, through its norcaradienone intermediate, provides a convenient means to study the photodecarbonylation of a "substituted" cyclopropanone. From the pressure-dependent rise times of the transient laser absorptions by the nascent CO products, it appears that the CO produced by the photodissociation of tropone is rotationally excited to some extent. The low signal-to-noise ratios of the spectra (Figure 19) prevent effective comparison with those

[20]M.J. Berry, J. Chem. Phys. 1974, 61, 3114-43.

[21]M.J. Berry, Chem. Phys. Lett. 1974, 27, 73-77.

[22]M.J. Berry, Chem. Phys. Lett. 1974, 29, 329.

[23]L.C. Lee and D.L. Judge, Can. J. Phys. 1973, 51, 378.

[24]Y.B. Band and K. F. Freed, J. Chem. Phys. 1975, 63, 3382-97.

[25]K.E. Holdy, L.C. Klotz, and K.R. Wilson, J. Chem. Phys. 1970, 52, 4588-99.

[26]S.J. Riley and K.R. Wilson, Chem. Soc. Faraday Discuss. 1972, 53, 132-46.

[27]R.D. Levine and R.B. Bernstein, Chem. Phys. Lett. 1972, 15, 1-6.

[28]G. Karl, P. Kruus, and J.C. Polanyi, J. Chem. Phys. 1967, 46, 224-43.

[29]M.A. Gonzalez, G. Karl, and P.J.S. Watson, J. Chem. Phys. 1972, 57, 4054-55.

[30]N.B. Slater, Proc. Camb. Phil. Soc. 1939, 35, 56.

[31]N.B. Slater, Theory of Unimolecular Reactions, Cornell Univ. Press, New York (1959),

[32]G.L. Pratt, Gas Kinetics, John Wiley and Sons, Ltd., London (1969), pp. 116-49.

[33]P.J. Robinson and K.A. Holbrook, Unimolecular Reactions, Wiley-Interscience, London (1972), pp. 28-51.

[34]W. Forst, Theory of Unimolecular Reactions, Academic Press, New York (1973), p. 14.

[35]E.K. Gill and K.J. Laidler, Proc. Roy. Soc. (A) 1959, 250, 121.

[36]K.A. Holbrook and A.R.W. Marsh, Trans. Faraday Soc. 1967, 63, 643.

[37]J.C. Light, J. Chem. Phys. 1964, 40, 3221-29.

[38]J.C. Light, Chem. Soc. Faraday Discuss. 1967, 44, 14-29.

[39]F.A. Wolf, J. Chem. Phys. 1966, 44, 1619-28.

[40]P. Pechukas and J.C. Light, J. Chem. Phys. 1965, 42, 3281-91.

[41]P. Pechukas, J.C. Light and C. Rankin, J. Chem. Phys. 1966, 44,

794-805.

[42]J.C. Light and J. Lin, J. Chem. Phys. 1965, 43, 3209-19.

[43]P.J. Robinson and K.A. Holbrook, Unimolecular Reactions, Wiley-Interscience, London (1972), pp. 15-28 and 52-108.

[44]F.A. Lindemann, Trans. Faraday Soc. 1922, 17, 598.

[45]B.S. Rabinovitch and K.W. Michel, J. Amer. Chem. Soc. 1959, 81, 5065.

[46]C.N. Hinshelwood, Proc. Roy. Soc. (A) 1922, 113, 230.

[47]O.K. Rice and H.C. Ramsperger, J. Amer. Chem. Soc. 1927, 49, 1617.

[48]O.K. Rice and H.C. Ramsperger, J. Amer. Chem. Soc. 1928, 50, 617.

[49]L.S. Kassel, J. Phys. Chem. 1928, 32, 225.

[50]L.S. Kassel, J. Phys. Chem. 1928, 32, 1065.

[51]R.A. Marcus and O.K. Rice, J. Phys. and Colloid Chem. 1951, 55, 894.

[52]R.A. Marcus, J. Chem. Phys. 1952, 20, 359.

[53]B.S. Rabinovitch and D.W. Setser, Adv. Photochem. 1964, 3, 1-82.

[54]J.W. Moore and R.G. Pearson, Kinetics and Mechanism, Wiley-Interscience, New York (1981), pp. 192-233.

[55]H.O. Pritchard, R.G. Sowden, and A.F. Trotman-Dickenson, Proc. Roy. Soc. A 1953, 217, 563.

[56]N.B. Slater, Proc. Roy. Soc. A 1953, 218, 224.

[57]G.M. Weider and R.A. Marcus, J. Chem. Phys. 1962, 37, 1835.

[58]M.C. Lin and K.J. Laidler, Trans. Faraday Soc. 1968, 64, 927.

[59]C.S. Elliott and H.M. Frey, Trans. Faraday Soc. 1962, 62, 895; M.C. Lin and K.J. Laidler, Trans. Faraday Soc. 1964, 64, 95.

[60]F.W. Scheider and B.S. Rabinovitch, J. Amer. Chem. Soc. 1962, 84, 4215; F.J. Fletcher, B.S. Rabinovitch, K.W. Watkins, and D.J. Locker, J. Chem. Phys. 1966, 70, 2823.

[61]R.L. Johnson and D.W. Setser, J. Phys. Chem. 1967, 71, 4366; K.A. Holbrook and A.R.W. March, Trans. Faraday Soc. 1969, 65, 441.

[62]J.N. Butler and G.B. Kistiakowsky, J. Amer. Chem. Soc. 1960, 82,

759.

[63]J.D. Rynbrandt and B.S. Rabinovitch, J. Phys. Chem. 1970, 74, 4175; 1971, 75, 2164.

[64]K.W. Hicks, M.L. Lesiecki, S.M. Riseman, and W.A. Guillory, J. Phys. Chem. 1979, 83, 1936.

[65]K.V. Reddy and M.J. Berry, Chem. Phys. Lett. 1979, 66, 223.

[66]M.D. Moser and E. Weitz, Chem. Phys. Lett. 1981, 82, 285-91.

[67]A.J. Grimley and P.L. Houston, J. Chem. Phys. 1980, 72, 1471.

[68] R.N. Rosenfeld and B. Weiner, J. Amer. Chem. Soc. 1983, 105, 3485-88.

[69]S.L. Baughcum and S.R. Leone, J. Chem. Phys. 1980, 72, 6531-45.

[70]G.S. Ondrey and R. Bersohn, J. Chem. Phys. 1983, 79, 175-78.

[71]G.S. Ondrey and R. Bersohn, J. Chem. Phys. 1983, 79, 179-84.

[72]A.D. Wilson and R.D. Levine, Mol. Phys. 1974, 27, 1197.

[73]R. Lu, J.B. Halpern, and W.M. Jackson, J. Phys. Chem. 1984, 88, 3419-25.

[74]P.L. Houston and C.B. Moore, J. Chem. Phys. 1976, 65, 757-70.

[75]P. Ho and A.V. Smith, Chem. Phys. Lett. 1982, 90, 407.

[76]G.T. Fugimoto, M.E. Ulmstead, and M.C. Lin, Chem. Phys. 1982, 65, 197-203.

[77]T.R. Fletcher and R.N. Rosenfeld, J. Amer. Chem. Soc. 1983, 105, 6358-59.

[78]J. Husain, J.R. Wiesenfeld, and R.N. Zare, J. Chem. Phys. 1980, 72, 2479-83.

[79]H. Reisler, F. Konig, A.M. Renlund, and C. Wittig, J. Chem. Phys. 1982, 76, 997-1006.

[80]A.J. Grimley and J.C. Stephenson, J. Chem. Phys. 1981, 74, 447-52.

[81]J.C. Stephenson, S.E. Bialkowski, and D.S. King, J. Chem. Phys. 1980, 72, 1161-69.

[82]D.G. Leopold and V. Vaida, J. Amer. Chem. Soc. 1983, 105, 6809-11.

[83]R.G.W. Norrish and J.G.A. Griffiths, J. Chem. Soc. 1928, 2829-40.

[84]F.W. Kirkbride and R.G.W. Norrish, Trans. Faraday Soc. 1931, 27, 404-09.

[85]R.G.W. Norrish and F.W. Kirkbride, J. Chem. Soc. 1932, 1518-30.

[86]H.G. Crone and R.G.W. Norrish, Nature 1933, 132, 241.

[87]R.G.W. Norrish, Trans. Faraday Soc. 1934, 30, 103-20.

[88]R.G.W. Norrish and M.E.S. Appleyard, J. Chem. Soc. 1934, 874-81.

[89]J.G. Calvert and J.N. Pitts, Jr., Photochemistry, John Wiley, New York(1966).

[90]J.C. Dalton and N.J. Turro, Ann. Rev. Phys. Chem. 1970, 31, 499.

[91]E.K.C. Lee and R.S. Lewis, Adv. Photochem. 1980, 12, 1-95.

[92]N.J. Turro, Techniques of Organic Chemistry 1969, 12, 133-296.

[93]K. Schaffner and O. Jeger, Tetrahedron 1974, 30, 1891-1902.

[94]R.B. Cundall and A.J. Davies, Prog. React. Kin. 1967, 4, 149-213.

[95]D.S. Weiss, Org. Photochem. 1981, 5, 347-420 and references cited therein.

[96]O.D. Saltmarsh and R.G.W. Norrish, J. Chem. Soc. 1935, 455-9.

[97]J.C. Dalton, D.M. Pond, D.S. Weiss, F.D. Lewis, and N.J. Turro, J. Amer. Chem. Soc. 1970, 92, 2564.

[98]D.S. Weiss, N.J. Turro, and J.C. Dalton, Mol. Photochem. 1970, 2, 91.

[99]J.A. Baltrop and J.C. Coyle, Chem. Commun. 1969, 1081.

[100]R.G.W. Norrish, Trans. Faraday Soc. 1939, 33, 1521.

[101]P.J. Wagner, Accts. Chem. Res. 1971, 4, 1681.

[102]P. Ausloos and E. Murad, J. Amer. Chem. Soc. 1958, 80, 5929.

[103]R. Srinivasan, J. Amer. Chem. Soc. 1959, 81, 1546-49.

[104]G.R. McMillan, J.G. Calvert, and J.N. Pitts, Jr., J. Amer. Chem. Soc. 1964, 86, 3602.

[105]W. Davis, Jr. and W.A. Noyes, Jr., J. Amer. Chem. Soc. 1947, 69,

5061-65.

[106]G.R. McMillan, J.G. Calvert, and J.N. Pitts, Jr., J. Amer. Chem. Soc. 1964, 84, 3602.

[107]P. Borrell and R.G.W. Norrish, Proc. Roy. Soc. A 1955, 153.

[108]T.J. Dougherty, J. Amer. Chem. Soc. 1965, 87, 4011.

[109]P.J. Wagner and G.S. Hammond, J. Amer. Chem. Soc. 1965, 87, 4009.

[110]P.J. Wagner and G.S. Hammond, J. Amer. Chem. Soc. 1966, 88, 1245.

[111]D.R. Coulson and N.C. Yang, J. Amer. Chem. Soc. 1966, 88, 4511.

[112]P.J. Wagner, Tet. Lett. 1968, 5385.

[113]C.H. Bibart, M.G. Rockley, and F.S. Wettack, J. Amer. Chem. Soc. 1969, 91, 2802.

[114]N.C. Yang and S.P. Elliott, J. Amer. Chem. Soc. 1968, 90, 4194-95.

[115]C.H. Bamford and R.G.W. Norrish, J. Chem. Soc. 1938, 1521-31.

[116]A. Zahra and W.A. Noyes, Jr., J. Phys. Chem. 1965, 69, 943.

[117]S.J. Rhoads, Molecular Rearrangements, vol. 1, P deMayo (ed.), Interscience, New York(1963).

[118]R.B. Woodward and R. Hoffmann, The Conservation of Orbital Symmetry, Academic Press, New York(1970); R.B. Woodward and R. Hoffmann, Ange. Chem. Int. Ed. 1969, 8, 781-932.

[119]M.P. Cava, R.H. Schlessinger, and J.P. VanMeter, J. Amer. Chem. Soc. 1964, 86, 3173-75.

[120]J. Saltiel and L. Metts, J. Amer. Chem. Soc. 1967, 89, 2232-34.

[121]W.L. Mock, J. Amer. Chem. Soc. 1966, 88, 2857-58.

[122]S.D. McGregor and D.M. Lemal, J. Amer. Chem. Soc. 1966, 88, 2858-60.

[123]R.J. Crawford and A. Mishra, J. Amer. Chem. Soc. 1966, 88, 3963-69.

[124]S. Seltzer, J. Amer. Chem. Soc. 1961, 83, 2625-29.

[125]R. Moore, A. Mishra, and R.J. Crawford, Can. J. Chem. 1968, 46, 3305-13.

[126]R.G. Bergman and W.L. Carter, J. Amer. Chem. Soc. 1969, 91, 7411-25.

[127]D.C. Duan and P.B. Dervan, J. Org. Chem. 1983, 48, 970-76.

[128]J.A. Berson, S.S. Olin, E.W. Petrillo, Jr., and P. Bickhart, Tetrahedron 1974, 30, 1639-49.

[129]P.B. Dervan and T. Uyehara, J. Amer. Chem. Soc. 1976, 98, 2003-05.

[130]P.B. Dervan and T. Uyehara, J. Amer. Chem. Soc. 1976, 98, 1262-64.

[131]J.E. Starr and R.H. Eastman, J. Org. Chem. 1966, 31, 1393-1402.

[132]J.E. Baldwin, Can. J. Chem. 1966, 44, 2051-56.

[133]G. Quinkert, Ange. Chem. Int. Ed. Engl. 1971, 10, 194-96.

[134]L.D. Hess and J.N. Pitts, J. Amer. Chem. Soc. 1967, 89, 1973-79.

[135]H.A.J. Carless and E.K.C. Lee, J. Amer. Chem. Soc. 1970, 92, 4482; H.A.J. Carless and E.K.C. Lee, J. Amer. Chem. Soc. 1970, 92, 6683-85; H.A.J. Carless, J. Metcalfe, and E.K.C. Lee, J. Amer. Chem. Soc. 1972, 94, 7221-35; J. Metcalfe, H.A.J. Carless, and E.K.C. Lee, J. Amer. Chem. Soc. 1972, 94, 7235-41.

[136]S.H. Bauer, J. Amer. Chem. Soc. 1969, 91, 3688-89.

[137]K.K. Shen and R.G. Bergman, J. Amer. Chem. Soc. 1977, 99, 1655-57.

[138]G.B. Kistiakowsky and T.A. Butler, J. Phys. Chem. 1968, 72, 3952-58.

[139]V. Zabransky and R.W. Carr, Jr., J. Phys. Chem. 1975, 79, 1618-22.

[140]R.N. Dixon and G.H. Kirby, Trans. Faraday Soc. 1966, 62, 1406.

[141]C.E. Dykstra and H.F. Schaefer, III, J. Amer. Chem. Soc. 1976, 98, 2689-95

[142]H. Basch, Theor. Chim. Acta 1978, 151-60.

[143]P. Pendergast and W.H. Fink, J. Amer. Chem. Soc. 1976, 98, 648-55.

[144]J.E. Del Bene, J. Amer. Chem. Soc. 1972, 94, 3713-18.

[145]D. Feldmann, K. Meier, H. Zacharias, and K.H. Welge, Chem. Phys. Lett. 1978, 59, 171-77.

[146]G.T. Fujimoto, M.E. Ulmstead, and M.C. Lin, Chem. Phys. 1982, 65, 197-203.

[147]R.B.W. Norrish, H.G. Crone, and O.D. Saltmarsh, J. Chem. Soc. 1933, 1533.

[148]A.N. Strachan and D.E. Thornton, Can. J. Chem. 1968, 46, 2353-60.

[149]R.K. Lengel and R.N. Zare, J. Amer. Chem. Soc. 1978, 100, 7495-99 and references cited therein.

[150]C.D. Hayden, D.M. Neumark, K. Shobatake, R.K. Sparks, and Y.T. Lee, J. Chem. Phys. 1982, 76, 3607-13.

[151]G.A. Taylor and G.B. Porter, J. Chem. Phys. 1962, 36, 1353-56.

[152]G.B. Porter and B.T. Connelly, J. Chem. Phys. 1960, 33, 81-85.

[153]P.G. Bowers, J. Chem. Soc. A 1967, 466-69.

[154]R.L. Russell and F.S. Rowland, J. Amer. Chem. Soc. 1970, 92, 7508-10.

[155]K. Tanaka and M. Yoshimine, J. Amer. Chem. Soc. 1980, 102, 7655-62.

[156]W.J. Bouma, R.H. Nobles, L. Radom, and C.E. Woodward, J. Org. Chem. 1982, 47, 1869-75.

[157]M.L. Halberstadt and J.R. McNesby, J. Amer. Chem. Soc. 1967, 89, 4317.

[158]R.W. Carr, Jr., T.W. Elder, and M.G. Topor, J. Chem. Phys. 1970, 53, 4716.

[159]P.C. Engleking, P.R. Corderman, J.J. Wendloski, G.B. Ellison, S.V. O'Neil, and W.C. Linebarger, J. Chem. Phys. 1981, 74, 5460.

[160]D.G. Leopold, K.K. Murray, and W.C. Linebarger, J. Chem. Phys. 1984, 81, 1048-50.

[161]R.L. Nuttall, A.H. Laufer, and M.V. Kilday, J. Chem. Thermodynamics, 1971, 3, 167-74.

[162]These results have been previously published. See R.N. Rosenfeld and B.I. Sonobe, J. Amer. Chem. Soc. 1983, 105, 1061-62; B.I. Sonobe and R.N. Rosenfeld, J. Amer. Chem. Soc. 1983, 7528-30.

[163]G. Herzberg, Molecular Spectra and Structure: I. Spectra of Diatomic Molecules, Van Nostrand-Reinhold, New York (1950), p. 518; H. Okabe, Photochemistry of Small Molecules, Wiley-Interscience, New York (1978), p. 194.

[164]G.W. Flynn, J. Mol. Structure 1980, 59, 197-205; R.E. McNair, S.F. Flughum, G.W. Flynn, M.S. Feld, and B.T. Feldman, Chem. Phys. Lett. 1977, 48, 241-44.

[165]J.W. Rabalais, J.M. McDonald, V. Scherr, and S.P. McGlynn, Chem.

Rev. 1971, 71, 73-108.

[166]J.W. Simons and R. Curry, Chem. Phys. Lett. 1976, 38, 171.

[167]H.S. Heaps and G. Herzberg, Z. Physik 1952, 133, 48-64.

[168]L.A. Young and W.J. Eachus, J. Chem. Phys. 1966, 44, 4195-4206.

[169]R. Herman and R.F. Wallis, J. Chem. Phys. 1955, 23, 637-46.

[170]R.A. Toth, R.H. Hunt, and E.K. Plyler, J. Mol. Spectroscopy 1969, 32, 85-96.

[171]L.A. Young, AVCO-Everett Research Laboratory Report, AMP 188, 1966.

[172]The listing for the computer program used to perform these calculations can be found in the Appendix.

[173]S. Yamabe and K. Morokuma, J. Amer. Chem. Soc. 1978, 100, 7551-56.

[174]R.H. Eastman, J.E. Starr, R. St. Martin, and M.K. Sakata, J. Org. Chem. 1963, 28, 2162-63.

[175]K. Nakamura and S. Koda, Bull. Chem. Soc. Jap. 1978, 51, 1665-70.

[176]W.R. Dolbier, Jr. and H.M. Frey, J. Chem. Soc. Perkin Trans. II 1974, 14, 1674-76.

[177]T.R. Darling, J. Pouliquen, and N.J. Turro, J. Amer. Chem. Soc. 1974, 96, 1247-48.

[178]K. Nakamura and S. Koda, Int. J. Chem. Kinet. 1977, 9, 67.

[179]D.M. Lemal and S.D. McGregor, J. Amer. Chem. Soc. 1966,88, 1335-36.

[180]O.L. Chapman and G.W. Borden, J. Org. Chem. 1961, 26, 4185-86.

[181]O.L. Chapman, D.J. Pastos, G.W. Borden, and A.A. Griswold, J. Amer. Chem. Soc. 1962, 84, 1220-24.

[182]L.A. Paquette, R.F. Eizember, and O. Cox, J. Amer. Chem. Soc. 1968, 90, 5153-59.

[183]D.I. Schuster, B.R. Sckolnick, and F.-T. Lee, J. Amer. Chem. soc. 1968, 90, 1300-07; J. Erikson, K. Krogh-Jesperson, M.A. Ratner, and D.I. Schuster, J. Amer. Chem. Soc. 1975, 97, 5596.

[184]D.I. Schuster and L. Wang, J. Amer. Chem. Soc. 1983, 105, 2900-01.

[185]W.L. Mock, J. Amer. Chem. Soc. 1969, 91, 5692.

[186]D.I. Schuster and J. Erikson, J. Org. Chem. 1979, 44, 4254-65.

[187]K. Freed, Top. Appl. Phys. 1976, 15, 23.

[188]T. Mukai, T. Nakazawa, and T. Shishido, Tet. Lett. 1967, 26, 2465-69.

[189]T. Mukai, T. Sato, M. Takahashi, and H. Mikuni, Bull. Chem. Soc. Jap. 1968, 41, 2819.

[190]A. Amano, T. Mukai, T. Nakazawa, and K. Okayama, Bull. Chem. Soc. Jap. 1976, 49, 1671-75.

[191]T. Tezuka, Y. Akasaki, and T. Mukai, Tet. Lett. 1967, 5003-03.

[192]A.S. Kende, J. Amer. Chem. Soc. 1966, 88, 5026.

[193]A.S. Kende and J.E. Lancaster, J. Amer. Chem. Soc. 1967, 89, 5283-84.

[194]T. Tezuka, Y. Akasaki, and T. Mukai, Tet. Lett. 1967, 1397-1402.

[195]M. Berger. I.L. Goldblatt, and C. Steel, J. Amer. Chem. Soc. 1973, 95 1717-25.

[196]K.N. Klump and J.P. Cheswick, J. Amer. Chem. Soc. 1963, 85, 130.

[197]T. Mukai, H. Kubata, and T. Toda, Tet. Lett. 1967, 3581-85.

[198]M.J. Goldstin and A.H. Givertz, Tet. Lett. 1965, 4417.

[199]M. Korach, D.R. Nielsen, and W.H. Rideout, J. Amer. Chem. Soc. 1960, 82, 4328-30.

[200]D.L. Whalen and A.M. Ross, J. Amer. Chem. Soc. 1974, 96, 3678-79.

[201]M. Suzuki, Y. Oda, and R. Noyori, J. Amer. Chem. Soc. 1979, 101, 1623-25.

[202]D.I. Schuster and B.R. Sckolnick, Org. Photochem. Syn. 1966, 1, 28-30; D.I. Schuster, J.M. Palmer, and S.C. Dickerman, J. Org. Chem. 1966, 31, 4281-82.

[203]P. Radlick, J. Org. Chem. 1964, 29, 960.

[204]I.M. Takakis and W.C. Agosta, J. Org. Chem. 1978, 43, 1952-56.

[205]N. Djeu, Appl. Phys. Lett. 1973, 23, 309-10.

[206]The 3-cyclopentenone and 3,5-cycloheptadienone results have been previously reported. For 3-cyclopentenone, see B.I. Sonobe, T.R. Fletcher, and R.N. Rosenfeld, Chem. Phys. Lett. 1984, 105, 322-26 and B.I. Sonobe, T.R. Fletcher, and R.N. Rosenfeld, J. Amer. Chem. Soc.

1984, 106, 4352-56. For 3,5-cycloheptadienone, see B.I. Sonobe, T.R. Fletcher, and R.N. Rosenfeld, J. Amer. Chem. Soc. 1984, 106, 5800-05.

[207]D.J. Bogan and D.W. Setser, J. Chem. Phys. 1976, 64, 586-602.

[208]J. Jortner, S.A. Rice, R.M. Hochstrasser, Adv. Photochem. 1969, 7, 149.

[209]J.L. Kinsey, J. Chem. Phys. 1971, 54, 1206-17.

[210]G.Z. Whitten and B.S. Rabinovitch, J. Chem. Phys. 1964, 41, 1883.

[211]S.W. Benson, Thermochemical Kinetics, 2nd Ed., Wiley, New York, 1974.

[212]F. Huisken, D. Krajnovich, Z. Zhang, Y.R. Shen, and Y.T. Lee, J. Chem. Phys. 1983, 78, 3806-15.

[213]R.B. Bernstein and R.D. Levine, Adv. At. Mol. Phys. 1975, 11, 215-97.

[214]D. Coulter, D. Dows, H. Reisler, C. Wittig, C. Chem. Phys. 1978, 32, 429; G. Ondrey, N. van Veen, and R. Bersohn, J. Chem. Phys. 1983, 78, 3732.

[215]G.H. Kwei, B.P. Goffard, and S.F. Sun, J. Chem. Phys. 1973, 58, 1722.

[216]W.L. Mock in Pericyclic Reactions, A.P. Marchand and R.E. Lehrs, Eds., Academic Press, New York, 1977, vol. 2, p. 141.

[217]A.G. Anastassiou and H. Yamamoto, J. Chem. Soc. Chem. Commun. 1973, 840.

[218]G. Hancock, B.A. Ridley, and I.W.M. Smith, J. Chem. Soc. Faraday Trans. II 1973, 68, 2117-26; N. Djeu and S.K. Searles, J. Chem. Phys. 1973, 4681.

[219]K.P. Huber and G. Herzberg, Constants of Diatomic Molecules, van Nostrand Reinhold Co., New York, 1979, pp. 158-66.

[220]G. Herzberg, Spectra of Diatomic Molecules, van Nostrand Reinhold Co., New York, 1950, p. 522.

APPENDIX

ROTATIONAL TEMPERATURE DETERMINATION

The computer listing at the end of this appendix was used to evaluate the expression (see Chapter 4),

$$I_{CGF}/I_o = \sum_v \sum_{J'} I_{CGF}(v,J') / \sum_v \sum_{J'} I_o(v,J') \qquad (A.1)$$

where the resulting degree of attenuation used is,

$$1 - I_{CGF}/I_o \qquad (A.2)$$

with,

$$I_o(v,J') = I_o D_v(T_v) D_r(T_v,T_r) A_v F_v(J',J'') \qquad (A.3)$$

and,

$$I_{CGF}(v,J') = I_o(v,J') 10^{-kpl} \qquad (A.4)$$

The fluorescence intensity, I_o, is determined in the first subroutine in the program by,

$$I_o = \left(\frac{E_p}{hc/\lambda} - \frac{E_p}{hc/\lambda} e^{-\varepsilon c l} \right) \Phi\omega \qquad (A.5)$$

where,

E_p = energy of the laser pulse

h = Planck's constant

c = speed of light

λ = photolyzing wavelength

ε = molar absorption coefficient at λ

l = cell length

Φ = quantum yield

ω = fraction of the product ir fluorescence viewed by the detector

The Einstein coefficients for spontaneous emission, A_v, are calculated in the second subroutine and are in good agreement with previous calculations.[218] The spontaneous emission coefficients were determined using,

$$A_{v'v''} \sim \nu_{v'v''} C^2_{v'v''} \qquad (A.6)$$

where $\nu_{v'v''}$ is the energy of the transition from v' to v'' in cm^{-1} and,[167]

$$C^2_{v'v''} = \frac{[1-(2v''+1)\chi_e][(1-(2v'+1)\chi_e]\chi_e^{v'-v''}v'!}{[1-(v''+1)\chi_e][1-v''+2]\ldots[1-v'\chi_e]v''!} \qquad (A.7)$$

The values for $\nu_{v'v''}$ were calculated using,

$$\nu_{v'v''} = G(v') - G(v'') \qquad (A.8)$$

where,

$$G(v) = \omega_e(v+\tfrac{1}{2}) - \chi_e\omega_e(v+\tfrac{1}{2})^2 + \chi_e y_e(v+\tfrac{1}{2})^3 \qquad (A.9)$$

The values for ω_e and $\chi_e\omega_e$ were obtained from Huber and Herzberg[219] and $\chi_e y_e$ was obtained from Herzberg.[220]

Corrections for the influence of vibration-rotation interactions in the vibrational transitions are contained in the Herman-Wallis F-factors.[169] The F-factor were derived from,

$$F_v^{v+1}(m) = 1 + C_v m + D_v m \qquad (A.10)$$

where $F_v^{v+1}(m)$ is the F-factor for the transition from v+1 to v and,

$$m \begin{cases} = J+1, & \text{R-branch} \\ = -J, & \text{P-branch} \end{cases}$$

The values for C_v and D_v were given by Toth and co-workers.[170]

The Boltzmann distributions for vibration and rotation were determined by,

$$D_v(v) = e^{-G(v)hc/kT} \qquad \text{(vibration)} \qquad (A.11)$$

and,

$$D_r(v,J) = (2J+1)e^{-F(v,J)hc/kT} \quad \text{(rotation)} \quad \text{(A.12)}$$

Here, k is Boltzmann's constant and F(v,J) is the rotational energy level within a vibrational level given by,

$$F(v,J) = B_v J(J+1) \quad \text{(A.13)}$$

where,

$$B_v = B_e - \alpha_e(v+\tfrac{1}{2}) \quad \text{(A.14)}$$

The values for B_e and α_e can be found in Herzberg.[220] The energy of a given rotational-vibrational level is then,

$$T_v(v,J) = G(v) + F(v,J) \quad \text{(A.15)}$$

The following program is written in BASIC and is designed to be run on the Commodore 8032 microcomputer.

```
10 REM THIS PROGRAM CALCULATES THE PERCENT ATTENUATION OF THE IR FLUORESCENCE
20 REM OF CO THROUGH A COLD GAS FILTER.  GIVEN THE ROTATIONAL AND VIBRATIONAL
30 REM TEMPERATURES AND THE ROTATIONAL AND VIBRATIONAL LIMITS, THE ATTENUATION
40 REM IS CALCULATED.
70 DIM G(12),C2(12),EA(12),F(12,115),T(12,115),DV(12),DR(12,115),HR(115)
80 DIM HP(115)
90 PRINT "WHAT IS THE COMPOUND BEING PHOTOLYZED?  (NAME OR FORMULA)"
95 INPUT N$
100 PRINT "VIBRATIONAL TEMPERATURE (IN K)?"
105 INPUT VT
110 PRINT "ROTATIONAL TEMPERATURE (IN K)?"
115 INPUT RT
120 PRINT "WAVELENGTH OF LASER RADIATION (IN NM)?"
125 INPUT WL
130 PRINT "LASER ENERGY PER PULSE REACHING THE CELL (IN MJ)?"
135 INPUT E1
140 PRINT "PRESSURE OF THE GAS IN THE CELL (IN TORRS)?"
145 INPUT P1
150 PRINT "DISTANCE FROM THE CELL FRONT TO AREA UNDER THE DETECTOR (IN CM)?"
160 INPUT D1
165 PRINT "ABSORPTION COEFFICIENT OF THE GAS (IN L/MOL-CM)?"
170 INPUT AG
175 PRINT "DISTANCE IN THE CELL OBSERVED BY THE DETECTOR (IN CM)?"
180 INPUT D2
185 PRINT "FRACTION OF EMITTING SPECIES REACHING THE DETECTOR (RESULTING ";
190 PRINT "FROM ISOTROPIC";PRINT " RADIATION)?"
195 INPUT F1
200 PRINT "VIBRATIONAL LEVEL? (LIMIT 11)
205 INPUT VI
210 PRINT "ROTATIONAL LEVEL? (LIMIT 114)
215 INPUT RO
220 PRINT "PRESSURE OF CO IN THE COLD GAS FILTER (IN TORRS)?"
225 INPUT P2
230 PRINT "LENGTH OF THE COLD GAS FILTER (IN CM)?"
235 INPUT D3
310 OPEN 4,4:CMD4
340 PRINT "THE COMPOUND BEING PHOTOLYZED IS ";N$
360 PRINT "THE LASER WAVELENGTH IS ";WL;" NM"
365 PRINT "THE LASER ENERGY REACHING THE CELL IS ";E1;" MJ"
370 PRINT "THE CELL PRESSURE IS ";P1;" TORRS"
375 PRINT "THE DISTANCE FROM THE CELL WINDOW TO THE AREA UNDER THE DETECTOR";
380 PRINT "IS ";D1;" CM"
385 PRINT "THE ABSORPTION COEFFICIENT OF THE GAS IS ";AG;" LITERS/MOLE-CM"
390 PRINT "THE DISTANCE OBSERVED BY THE DETECTOR IS ";D2;" CM"
395 PRINT "THE FRACTION OF IR PHOTONS REACHING THE DETECTOR IS ";F1
410 PRINT "THE PRESSURE OF THE COLD GAS FILTER IS ";P2;" TORRS"
450 GOSUB 1000
460 GOSUB 2000
470 GOSUB 3000
480 GOSUB 3500
485 GOSUB 4000
490 GOSUB 4500
```

```
500 PRINT"OTHER ROTATIONAL AND VIBRATIONAL TEMPERATURES EVALUATED?"
510 PRINT "YES = 1; NO = 0.  TO CHANGE OTHER PARAMETERS PRESS 2."
515 INPUT YN
520 IF YN=1  THEN 550
525 IF YN=0  THEN 605
530 IF YN=2 THEN 600
550 PRINT"VIBRATIONAL TEMPERATURE (IN K)"
555 INPUT VT
560 PRINT"ROTATIONAL TEMPERATURE (IN K)"
565 INPUT RT
570 PRINT"VIBRATIONAL LEVEL? (LIMIT 11)"
575 INPUT VI
580 PRINT"ROTATIONAL LEVEL? (LIMIT 114)"
585 INPUT RO
586 OPEN 4,4:CMD4
590 GOTO 485
600 GOTO 90
605 END
1000 REM SUBROUTINE TO CALCULATE THE AMOUNT OF CO PRODUCED
1020 REM N1 IS THE NUMBER OF PHOTONS REACHING THE CELL PER PULSE
1025 N1 = E1*(1E-3)*(5.0348E22)*WL*(1E-7)
1030 REM C1 IS THE CONCENTRATION OF THE GAS IN THE CELL (MOLES/LITER)
1035 C1 = (1/22.414)*(P1/760)*(273/298)
1040 REM N2 IS THE NUMBER OF PHOTONS REACHING THE AREA UNDER THE DETECTOR
1045 N2 = N1*(10↑(-AG*C1*D1))
1050 REM E2 IS THE NUMBER OF CO MOLECULES PRODUCED
1055 E2 = N2 - (N2*(10↑(-AG*C1*D2)))
1060 REM E3 IS THE CO VIEWED BY THE DETECTOR
1065 E3 = F1*E2
1100 PRINT "THE NUMBER OF PHOTONS REACHING THE CELL IS ";N1
1105 PRINT "THE NUMBER OF PHOTONS IN VIEW OF THE DETECTOR IS ";N2
1115 PRINT "THE CELL CONCENTRATION IS ";C1;" MOLES/LITER"
1120 PRINT "THE NUMBER OF CO PRODUCED IN VIEW OF THE DETECTOR IS ";E2
1125 PRINT "THE NUMBER OF CO THAT CAN BE DETECTED IS ";E3
1150 RETURN
2000 REM SUBROUTINE TO CALCULATE THE EINSTEIN COEFFICIENTS FOR CO
2005 REM FROM HUBER & HERZBERG:  CONSTANTS OF DIATOMIC MOLECULES
2010 LET XE = .00612417   : LET WE = 2169.81358
2015 LET XY = .0308       : LET WX = 13.28831
2020 REM G(V) IS THE VIBRATIONAL ENERGY LEVELS
2025 FOR V=0 TO (VI+1)
2030 REM FROM HEAPS & HERZBERG:  ZEIT FUR PHYSIK 1952. 133. 48-64
2035 G(V) = (WE*(V+.5))-(WX*((V+.5)↑2))+(XY*((V+.5)↑3))
2055 NEXT V
2065 FOR V=1 TO VI+1
2070 V1=V-1
2075 C2(V) = ((1-(2*V1+1)*XE)*(1-(2*V+1)*XE)*XE*V)/(1-(V1+1)*XE)
2080 NEXT V
2085 LET K = (33.365)/(C2(1)*(G(1)-G(0)))
2090 FOR V=1 TO VI+1
2095 TE = G(V) - G(V-1)
```

```
2105 EA(V) = K*C2(V)*TE
2115 NEXT V
2125 RETURN
3000 REM SUBROUTINE TO CALCULATE THE ENERGY LEVELS
3010 LET BE = 1.9313 :  LET AE = .01748
3015 FOR V=0 TO VI + 1
3020 FOR J=0 TO RO + 1
3035 B = BE - AE*(V+.5)
3040 F(V,J) = B*J*(J+1)
3050 T(V,J) = G(V) + F(V,J)
3055 NEXT J
3060 NEXT V
3065 RETURN
3500 REM SUBROUTINE TO CALCULATE THE HERMAN-WALLIS FACTORS
3505 REM FROM TOTH, HUNT & PLYLER, J MOLECULAR SPEC L969, 32, 85-96
3510 FOR J=0 TO RO
3520 IF J=0 THEN 3540
3530 HR(J) = 1 + (-2.8E-4)*J + (7.5E-6)*((J+1)↑2)
3540 HP(J) = 1 + (-2.8E-4)*(-(J+1)) + (7.5E-6)*((J+1)↑2)
3550 NEXT J
3560 RETURN
4000 REM SUBROUTINE TO CALCULATE BOLTZMANN VIB AND ROT DISTRIBUTIONS
4010 PRINT
4020 LET SV=0:  LET SR=0
4030 FOR V=0 TO VI+1
4040 DV(V) = EXP(-G(V)/(.6952*VT))
4050 FOR J=0 TO RO+1
4060 DR(V,J) = (2*J+1)*EXP(-F(V,J)/(.6952*RT))
4070 LET SR = SR + DR(V,J)
4080 NEXT J
4090 SV = SV + DV(V)
4100 NEXT V
4110 RETURN
4500 REM SUBROUTINE TO CALCULATE THE % ATTENUATION
4510 LET TP=0: LET AP=0: LET AR=0: LET TR=0: LET AT=0: LET TT=0
4520 FOR V=1 TO VI
4530 FOR J=0 TO RO
4540 Z = T(V,J) - T((V-1),(J+1))
4550 IF V=1 THEN 4580
4560 AC=0
4570 GOTO 4590
4580 GOSUB 5000
4590 WP=E3*(DV(V)/SV)*(DR(V,J)/SR)*HP(J)*EA(V)*(10↑(-AC*P2*D3))
4600 XP=(E3*(DV(V)/SV)*(DR(V,J)/SR)*HP(J)*EA(V)) - WP
4610 IF J=0 THEN 4700
4620 Z = T(V,J) - T((V-1),(J-1))
4630 IF V=1 THEN 4660
4640 AC=0
4650 GOTO 4670
4660 GOSUB 5000
4670 WR=E3*(DV(V)/SV)*(DR(V,J)/SR)*HR(J)*EA(V)*(10↑(-AC*P2*D3))
4680 XR=(E3*(DV(V)/SV)*(DR(V,J)/SR)*HR(J)*EA(V)) - WR
4690 GOTO 4710
```

```
4700 WR=0:XR=0
4710 LET TR = TR + WR
4720 LET AR = AR + XR
4730 LET TP = TP + WP
4740 LET AP = AP + XP
4750 NEXT J
4760 NEXT V
4770 AT = AT + AR + AP
4780 TT = TT + TR + TP
4790 TD = AT + TT
4800 PRINT
4810 PRINT "THE PERCENT ATTENUATION AT A VIBRATIONAL TEMPERATURE OF";VT;
4820 PRINT "K AND A ROTATIONAL":PRINT"TEMPERATURE OF ";RT;"K IS ";(AT/TD)*100;
4830 PRINT "PERCENT.  THE VIBRATIONAL LIMIT WAS";VI;".";
4840 PRINT "   THE ROTATIONAL LIMIT WAS ";RO;"."
4850 PRINT
4860 PRINT#4:CLOSE4
4870 RETURN
5000 REM SUBROUTINE TO DETERMINE THE ABSORPTION COEFFICIENTS
5010 IF Z<1987 THEN 5200
5012 IF Z>=1975 AND Z<L987 THEN 5205
5013 IF Z>=1987 AND Z<2000 THEN 5207
5015 IF Z>=2000 AND Z<2018 THEN 5210
5020 IF Z>=2018 AND Z<2031 THEN 5220
5025 IF Z>=2031 AND Z<2043 THEN 5230
5030 IF Z>=2043 AND Z<2056 THEN 5240
5035 IF Z>=2056 AND Z<2068 THEN 5250
5040 IF Z>=2068 AND Z<2081 THEN 5260
5045 IF Z>=2081 AND Z<2093 THEN 5270
5050 IF Z>=2093 AND Z<2106 THEN 5280
5055 IF Z>=2106 AND Z<2118 THEN 5290
5060 IF Z>=2118 AND Z<2131 THEN 5300
5065 IF Z>=2131 AND Z<2143 THEN 5310
5070 IF Z>=2143 AND Z<2156 THEN 5320
5075 IF Z>=2156 AND Z<2168 THEN 5330
5080 IF Z>=2168 AND Z<2181 THEN 5340
5085 IF Z>=2181 AND Z<2193 THEN 5350
5090 IF Z>=2193 AND Z<2206 THEN 5360
5095 IF Z>=2206 AND Z<2218 THEN 5370
5100 IF Z>=2218 AND Z<2231 THEN 5380
5105 IF Z>=2231 AND Z<2243 THEN 5390
5110 IF Z>=2243 AND Z<2256 THEN 5400
5120 IF Z>2256 THEN 5200
5200 AC=0         : RETURN
5205 AC=1.1E-4    : RETURN
5207 AC=6.5E-4    : RETURN
5210 AC=2.73E-3   : RETURN
5220 AC=3.73E-3   : RETURN
5230 AC=3.49E-2   : RETURN
5240 AC=1.06E-1   : RETURN
```

```
5250 AC=2.73E-1 : RETURN
5260 AC=6.33E-1 : RETURN
5270 AC=1.31    : RETURN
5280 AC=1.96    : RETURN
5290 AC=2.51    : RETURN
5300 AC=2.29    : RETURN
5310 AC=1.10    : RETURN
5320 AC=9.27E-1 : RETURN
5330 AC=2.51    : RETURN
5340 AC=3.16    : RETURN
5350 AC=2.62    : RETURN
5360 AC=1.53    : RETURN
5370 AC=5.23E-1 : RETURN
5380 AC=1.53E-1 : RETURN
5390 AC=2.18E-2 : RETURN
5400 AC=1.85E-3 : RETURN
5410 REM THE ABSORPTION COEFFICIENTS WERE DETERMINED BY SCALING THE ABS COEFF
5420 REM OBTAINED FROM THE ABS SPECTRA CALCULATED BY YOUNG, AVCO EVERETT LAB
5430 REM RESEARCH REPORT AMP188, MAY 196E WITH THE P(9) LINE OF THE 1-0 TRANS
5440 REM FROM OUR CO LASER
```

VITA

Blake Isamu Sonobe was born on January 17, 1948 in Honolulu, Hawaii. His parents, Stanley and Elaine Sonobe, currently reside in Belmont, CA. He graduated from Samuel F. B. Morse Senior High School, San Diego, CA in 1966 and attended the United States Air Force Academy where he graduated in 1970 with a Bachelor of Science degree in Chemistry. Mr. Sonobe was commissioned an officer in the United States Air Force upon graduation and was assigned to Eglin Air Force Base where he served as a development engineer, chemist, and chief of the Explosive Dynamics Testing Laboratory in the development of non-nuclear munitions.

Mr. Sonobe attended Texas AM University where he worked under Dr. Rand L. Watson while completing the requirements for a Master of Science degree in chemistry. Upon completion of his studies at Texas AM, he was assigned to the United States Air Force Academy as an instructor in chemistry. In 1981, he moved to Davis, CA to attend the University of California at Davis. During his degree program under the direction of Professor Robert N. Rosenfeld, Mr. Sonobe was supported by the Air Force Institute of Technology.

Mr. Sonobe resides at 6441 Dewsbury Drive, Colorado Springs, CO with his wife Janie and their four children, Abigail, Bethany, Rebecca, and Nathanael. He is assigned as an instructor in the Department of Chemistry at the Air Force Academy.

END

FILMED

10-85

DTIC